

OAK RIDGE NATIONAL LABORATORY

operated by
UNION CARBIDE CORPORATION
for the
U.S. ATOMIC ENERGY COMMISSION



ORNL - TM - 2628

COPY NO. - 140

DATE -



3 4456 0360005 7

EVALUATION OF VARIOUS METHODS OF FISSION PRODUCT AEROSOL SIMULATION

B. F. Roberts, S. H. Freid, G. W. Parker
L. F. Parsly, and T. H. Row

NOTICE This document contains information of a preliminary nature and was prepared primarily for internal use at the Oak Ridge National Laboratory. It is subject to revision or correction and therefore does not represent a final report.

LEGAL NOTICE

This report was prepared as an account of Government sponsored work. Neither the United States, nor the Commission, nor any person acting on behalf of the Commission:

A. Makes any warranty or representation, expressed or implied, with respect to the accuracy, completeness, or usefulness of the information contained in this report, or that the use of any information, apparatus, method, or process disclosed in this report may not infringe privately owned rights; or

B. Assumes any liabilities with respect to the use of, or for damages resulting from the use of any information, apparatus, method, or process disclosed in this report.

As used in the above, "person acting on behalf of the Commission" includes any employee or contractor of the Commission, or employee of such contractor, to the extent that such employee or contractor of the Commission, or employee of such contractor prepares, disseminates, or provides access to, any information pursuant to his employment or contract with the Commission, or his employment with such contractor.

ORNL-TM-2628

Contract No. W-7405-eng-26

REACTOR CHEMISTRY DIVISION

EVALUATION OF VARIOUS METHODS OF FISSION PRODUCT
AEROSOL SIMULATION

B. F. Roberts, S. H. Freid, G. W. Parker
L. F. Parsly, and T. H. Row

SEPTEMBER 1969

OAK RIDGE NATIONAL LABORATORY
Oak Ridge, Tennessee
operated by
UNION CARBIDE CORPORATION
for the
U.S. ATOMIC ENERGY COMMISSION



3 4456 0360005 7



CONTENTS

	<u>Page</u>
ABSTRACT	1
1.0 INTRODUCTION	2
1.1 Reasons for Use of Simulants	2
1.2 Methods of Simulation	3
1.3 Isotopes to be Studied	3
1.4 Sampling Techniques	4
1.5 Purpose of Present Validation Studies	4
1.6 Validation Experiments	4
2.0 USE OF IMPREGNATED FUELS	5
2.1 Introduction	5
2.2 Fuel Preparation for the CMF	6
2.3 Behavior of Pellet Type Simulant in the Containment Mockup Facility (CMF)	7
2.4 Evaluation of the Pellet-Type Simulant in the CMF	22
2.5 Fuel Preparation for the Nuclear Safety Pilot Plant	22
2.6 Simulant Evaluation Experiments in the NSPP	24
3.0 CSE SIMULANT TESTS OUT-OF-PILE	32
3.1 Introduction	32
3.2 Description of Simulant Vaporizer Unit	33
3.3 Fuel Preparation	36
3.4 Behavior of Simulants in the CMF	41
3.5 Behavior of Simulants in the CRI	47
3.6 Evaluation of CSE-Type Simulant	64
4.0 CSE SIMULANT TESTS IN-PILE	66
4.1 Introduction	66
4.2 Experimental Facilities	67
4.3 Experimental Procedure	72
4.4 Experimental Results	76
4.5 Evaluation	84

	<u>Page</u>
5.0 MEASUREMENT OF AEROSOLS WITH PORTABLE SAMPLER . . .	88
5.1 Introduction	88
5.2 Description of Sampler	88
5.3 Aerosol Measurements at Various Facilities . . .	93
5.4 Conclusions	103
6.0 GENERAL EVALUATION OF THE RESULTS OF SIMULANT VALIDATION EXPERIMENTS	104
6.1 Criteria of Validation Experiments	104
6.2 Relative Significance of Various Types of Data	104
6.3 Limitations of Validation Experiments	105
6.4 Fuel Compact Method of Simulant Generation	106
6.5 Vaporized Simulant Method of Simulant Generation: Out-of-Pile Studies	106
6.6 Vaporized Simulant Method of Simulant Generation: In-Pile Studies	108
7.0 CONCLUSIONS AND RECOMMENDATIONS	110
REFERENCES	111

EVALUATION OF VARIOUS METHODS OF FISSION PRODUCT
AEROSOL SIMULATION

B. F. Roberts, S. H. Freid, G. W. Parker,
L. F. Parsly, and T. H. Row

ABSTRACT

Although the use of simulated fission products is desirable in certain experiments of the Nuclear Safety Program, such use is justified only if the simulants behave like real fission products under similar conditions. This report describes the work done in the major nuclear safety facilities at ORNL to evaluate simulants and determine whether their use is justified. Direct comparison of simulated and real fission product aerosols has been performed in the Containment Mockup Facility (CMF), the Nuclear Safety Pilot Plant (NSPP), the Containment Research Installation (CRI), and the In-Pile Installation (IPI). The results of these studies suggest that the mechanisms controlling the release, transport, and aging behavior of simulated or real fission product aerosols is governed more by the conditions of the experiment than by the nature of the aerosol. Thus variation between duplicate experiments is greater than between simulated and real fission products. Accordingly, the use of simulants in certain experiments of the Nuclear Safety Program appears to produce valid and realistic results.

1.0 INTRODUCTION

1.1 Reasons for Use of Simulants

In the case of a reactor accident, fission products may be released from the fuel and from the primary reactor chamber and be transported to the large surrounding vessel designed to contain them. A major objective of the Nuclear Safety Program is to study the release, transport, and deposition behavior of fission products under reactor accident conditions. Since the physical size of the experimental facility and the concentration of fission products may influence the experimental results, large scale engineering tests using highly irradiated fuel are required in order to evaluate both theory and small-scale tests.

When a large-scale experimental program requires repetitive tests involving large masses of fission-product aerosol, use of irradiated fuel to obtain the aerosol is impractical¹ because the fuel specimen would be too large and the intense radioactivity would pose inordinate shielding and decontamination problems. Therefore it is desirable to use a simulated fission-product aerosol. Such an aerosol may be composed of inactive isotopes of the pertinent fission products and traced with small amounts of suitable radioactive isotopes.

Studies which utilize simulated fission-product aerosols are applicable to the Nuclear Safety Program only if the behavior of the simulant aerosol is similar to that of a real fission-product aerosol under similar conditions. The similarity must exist for both the composition of the aerosol entering the containment vessel and for the aging behavior of the aerosol while it is in the vessel. In order to determine the applicability of utilizing simulants several experimental programs have been performed. Hilliard, Coleman, and McCormack² have recently reported the results of

experiments in the Aerosol Development Facility (ADF) at the Pacific Northwest Laboratory (PNL), and this report summarizes the several programs performed at Oak Ridge National Laboratory (ORNL).

1.2 Methods of Simulation

Simulant aerosols are usually generated by one of two methods. In the first method inactive isotopes and tracers are mixed with UO_2 and then clad. The fuel compact is then melted to release the simulant aerosol. In the second method the inactive isotopes and tracers are vaporized in a separate furnace and the vapors are passed into a second furnace where they are mixed with those of molten UO_2 and cladding material. Although the first method appears simpler and more direct, the second method has been considered more practical for large-scale experiments such as the Containment Systems Experiment (CSE) at PNL. The ORNL work described in this report utilized both methods but the second method was emphasized because of the importance of the CSE in the Nuclear Safety Program.

1.3 Isotopes to be Studied

Aerosol studies in nuclear safety are generally directed toward determining the amount of fission products which could be released from the containment vessel under reactor accident conditions. This amount is largely determined by the gasborne concentration of the individual fission products. The situation is further simplified because only certain chemical elements are highly significant from a safety standpoint. Thus, iodine and to a much lesser extent cesium, tellurium, and ruthenium are the fission products which are generally emphasized.

1.4 Sampling Techniques

Since fission-product iodine can exist in various forms and can change form while inside a containment vessel,³ much effort has been devoted to the study of iodine^{4,5} and the development of iodine characterization devices.^{6,7} Iodine aerosols are generally divided into three species: particulate iodine is generally defined as that which is associated with particles. Molecular iodine is that which readily reacts with metallic surfaces. Silver is the best surface for this purpose. Organic iodine is a mixture of alkyl iodide which can only be conveniently trapped by charcoal. Until recently the most widely used iodine characterization device has been the May pack.⁶ This device generally consists of first a high efficiency filter to trap particulate iodine, then a series of silver screens to adsorb the molecular iodine, and finally charcoal-impregnated filter papers and charcoal beds to trap the organic iodine. Because this device does not clearly distinguish between particulate and molecular iodine, the honeycomb sampler⁷ has recently been developed. This device consists of first a silver-plated honeycomb to provide adequate surface to trap the molecular iodine, then a high efficiency filter to trap the particulate iodine, and finally charcoal beds to trap the organic iodine.

1.5 Purpose of Present Validation Studies

The purpose of the present validation studies is to compare the behavior of real fission products with simulated ones and to ascertain the validity of the various methods of simulation.

1.6 Validation Experiments

The experimental results to be examined will consist of groups of experiments which used impregnated fuels, real fission products, and CSE simulants. For purposes of comparison the results will be subdivided according to the experimental facility in which they were obtained: the CMF, the CRI, the NSPP, and the in-pile facility in the ORR.

2.0 USE OF IMPREGNATED FUELS

2.1 Introduction

The simulation of radiogenic fission products in metallic fuels was first utilized by ANL in connection with developmental studies of recycle fuels in the breeder reactor program. Their objectives were satisfied with the addition of a few readily alloyed metals such as palladium, ruthenium, rhodium, tin, antimony, etc. The alloying process leads to a homogeneous metallic fuel almost undistinguishable from irradiated uranium, thus the objective is accomplished.

The manufacture of sintered-high density UO_2 , however, does not permit dilution with most of the fission product elements, especially the volatile ones of interest to nuclear safety work and therefore other means of impregnating or simulating fuels had to be devised.

Simulation of fission product iodine in UO_2 aerosols has been accomplished in different ways. Parker et al.⁸ released molecular iodine in a UO_2 melting experiment by sealing ^{127}I carrier and ^{131}I in a small quartz capillary tube that was arranged in the fuel-melting furnace to melt after the stainless steel cladding. Parsly et al. mixed Na^{127}I containing ^{131}I with UO_2 powder and packed the mixture in the core of EGCR-type UO_2 pellets. Methods of incorporating other fission product simulants in UO_2 fuels were discussed by Rodgers⁹ and by Barton et al,¹⁰ who considered the possibility of using completely inactive simulants and determining their distribution in simulated-accident experiments by activation analysis. While this technique offers promise of possessing the requisite

sensitivity, the great expense of activation analysis, and the problem of avoiding sample contamination has discouraged pursuit of this approach. The preferred method, at present, is to incorporate in the fuel the amount of inactive fission product element corresponding to the desired burnup, blended with just enough radioactive tracer to facilitate analysis. This approach was applied in the first attempt to simulate fission products other than iodine in experiments in the Containment Mockup Facility (CMF).

2.2 Fuel Preparation for the CMF

Pellets were fabricated containing the following concentrations of fission product elements (in milligrams of element per 100 g of UO_2 , corresponding to equivalent concentrations for 10,000 Mwd/ton burnup):

<u>Element</u>	<u>Quantity (mg)</u>	<u>Tracer Isotope Added or Induced</u>
Iodine	7.2	8d I^{131} -added
Tellurium	14.7	30d Te^{133} -induced
Ruthenium	51.3	42d Ru^{103} -induced
Strontium	40	30y Sr^{90} -added
Cesium	96	23y Cs^{134} -induced
Molybdenum	94	67hr Mo^{99} -induced
Barium	36	12d Ba^{140} -added

A slurry of Cs_2CO_3 and $SrCO_3$ was prepared, and iodine was added as HI. Millicurie amounts of $^{131}CsCl$, $^{90}SrCl_2$, and $Na^{131}I$ were added to the slurry, which was evaporated to dryness with a heat lamp and mixed with 100 g of depleted UO_2 of selected grain size (100% 11 μ particle diameter). To this mixture, the above-listed quantities of ruthenium, tellurium, and molybdenum were added as the powdered metals after irradiating them in the ORR for about three days at a flux of 3×10^{14} and allowing a week or more for decay of the shorter lived activities. The mixture was tumbled in

a screw-cap glass bottle to which several 5/8-in. diameter stainless steel balls were added. Two 10-g portions of the resulting mixture were formed into 1 cm diameter pellets by cold pressing in a hydraulic press to a maximum total pressure of 15,000 lb. The die pieces were coated with stearic acid to minimize sticking. The pellets were transferred directly from the die into a stainless steel can and sealed with a press-fit lid. The pellet density achieved was only about 70%.

2.3 Behavior of Pellet-Type Simulant in the Containment Mock-up Facility (CMF)

Nuclear Safety Program Progress Reports^{8,10,11} contain more detailed information on the conduct of the fuel melting experiments in CMF. An earlier series of release tests were conducted in a vertical furnace tube at atmospheric pressure in ambient air. Later a revised furnace design (Fig. 2.3.1) was used to permit the use of steam as well as the addition of extra pressure.

The jacketed furnace arrangement developed for use with the Containment Research Installation (CRI) was used in the later experiment and was coupled with the CMF containment tank. Prior to heating the fuel specimen, the CMF tank was brought up to a pressure of 15 psig with steam, and then the pressure was increased to 29.5 psig by adding air. Heaters on the tank helped to hold the pressure nearly constant during the melting operation.

The melting procedure usually followed a preheat in air. When the temperature approached the approximate melting point of the metal cladding, the air flow over the sample was adjusted to 1.36 liters/min measured at 25°C and 30 psig. An equal volume of steam at the same temperature and pressure was mixed with the air at this time and flow was continued until the specimen melted. The specimen was cooled by the air flow but remained at a temperature of 1000°C or higher

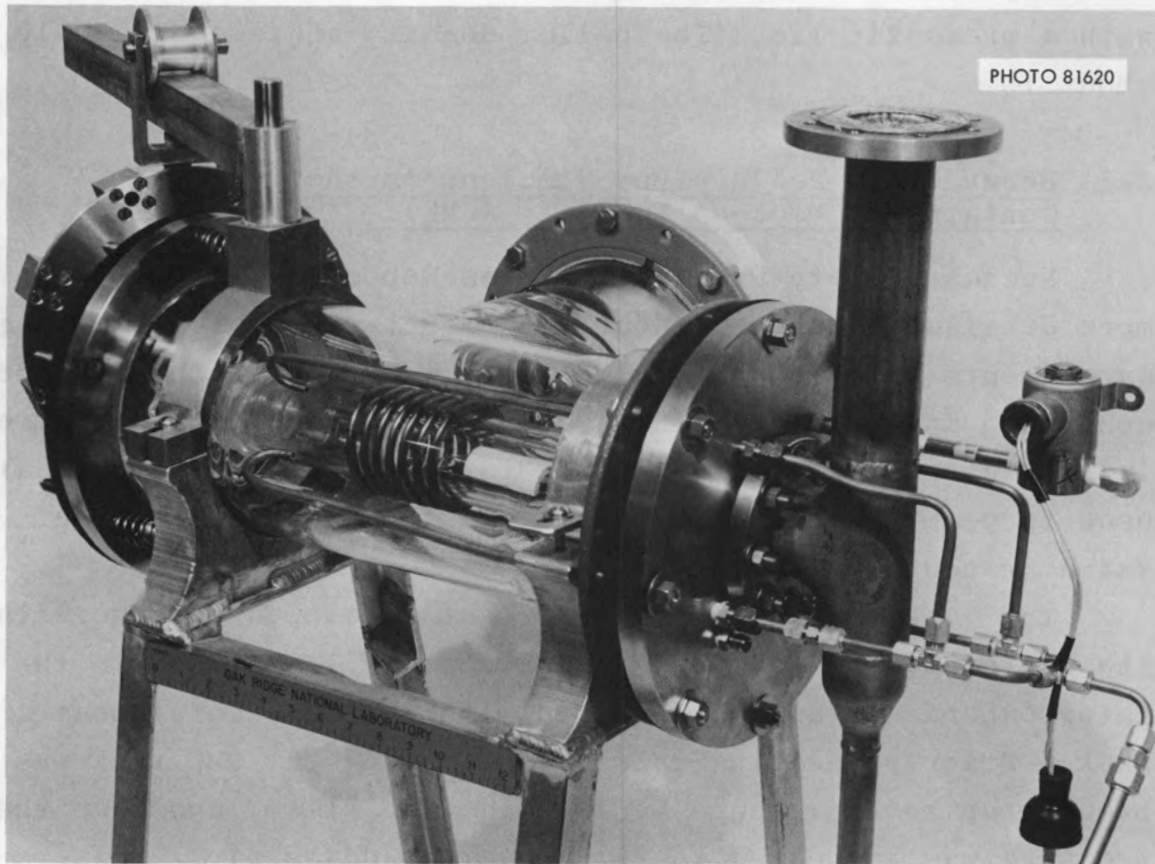


Fig. 2.3.1 Pressurized Induction-Heating Furnace for Containment Research Installation.

for about 10 min. The tank fan was started 1.5 min after the specimen melted and it operated for 1/2 min. Approximately 5 minutes after the sample melted, the air flow was shut off, the main valve at the bottom of the containment tank was closed, and the furnace pressure reduced to 1 atm. Heating of the containment tank was also discontinued at this time to allow the pressure of the tank to decrease slowly until it reached 11.5 psig, three hr after completion of fuel melting. Enough air was then added to the tank to bring the pressure back to 15 psig, and the fan was operated for another 1/2 minute to mix the contents of the tank. Depressurization of the tank started at this time and was completed about 4 hours after the fuel melted.

The conditions existing in the containment tank during all the experiments listed below in Table 2.3.1 were nearly the same, except for the aging times which are somewhat different. However, it is felt that the comparisons will be valid.

2.3.1 Runs 995H and 996H

The type fuel and its cladding for these two runs, as well as additional information, can be found in Table 2.3.1.

The conditions used in 996H were quite close to those prevailing in 995H. The total pressure was about 29 psig. Heating of the fuel was started with a mixture of steam and air flowing through the pressurized tube, but steam flow was discontinued before the fuel reached an estimated temperature of 2200°C because of excess condensation and water accumulation. Dry air flow continued during the balance of the heating period (10 min total) and for 20 min thereafter. During most of the 20 min cooling period, burning of the specimen was observed at irregular intervals as is usual with Zircaloy clad UO₂ specimens melted and cooled in air.

Table 2.3.1 Experimental Conditions for Runs 990S, 991S, 992S, 995H and 996H

Run Number	Fuel	Cladding	Atmosphere	Aging (hr)	Press. (atm-abs)*	Temp. (°C)*
CMF 990S	Simulant	Stainless	Steam-air	5.5	2.8	125
CMF 991S	Simulant	Zircaloy	Steam-air	6.4	2.8	125
CMF 992S	Simulant	Zircaloy	Steam-air	5.25	2.8	116
CMF 995H	1000 MWD UO ₂	Stainless	Steam-air	4.0	3.0	120
CMF 996H	7100 MWD UO ₂	Zircaloy	Steam-air	4.5	3.0	125

*Pressures and temperatures are those existing in the containment vessel at the start of the experiment.

2.3.2 Runs 990S, 991S, and 992S

Three nearly identical pellet type simulant runs were performed in the CMF in one series, 990S, 991S and 992S. Number 990S was a stainless clad capsule while the last two were Zircaloy clad specimens. In these two Zircloy clad runs, typical contrasting conditions existed during the melting, in that severe air-steam oxidation occurred with No. 991S while a relatively nonoxidizing steam-helium atmosphere protected the melt of Run 992S. Typical Zr-UO₂ behavior on melting appears to involve the molten Zr wetting the UO₂ spreading over the surface and penetrating into the interior or melting with the UO₂. Cracking of the melt occurs on cooling and sparking and burning will occur in air.

In Run 990S, simulated stainless steel clad UO₂ fuel was melted with air in the furnace tube and with a steam-air atmosphere at 27 psig in the containment tank. Aging time in the tank was approximately 5.5 hours.

In Run 991S, Zircaloy clad simulated UO₂ fuel was treated to or near the melting point of UO₂ with air in the furnace tube and with a steam air mixture at 27 psig in the containment tank; complete oxidation of the fuel to a ZrO₂-U₃O₈ mixture occurred as the fuel cooled below 1000°C.

In Run 992S, Zircaloy clad simulated UO₂ fuel was melted with a steam helium atmosphere in the furnace and with a steam-air mixture at 27 psig in the containment tank.

2.3.3 Distribution of Fission Products Released in CMF

It is interesting to compare the distribution of fission products released from high-burnup fuel (Runs 995H and 996H), with the distribution of simulated fission products released in earlier experiments (Runs 990S, 991S, and 992S). The following Table 2.3.2 shows a comparison of iodine distribution data:

Table 2.3.2 Distribution of Iodine Released from UO₂ with Simulated Fission Products and From High Burnup UO₂

	High-Burnup UO ₂		Simulant Experiments		
	Run 995H (1000 MWD)	Run 996H (7100 MWD)	Run 990S	Run 991S	Run 992S
Iodine Released	~100.0	90.2	~100.0	100.0	92.3
Iodine held in containment tank					
On tank walls	19.8	21.5	33.7	14.6	8.1
On deposition samples	7.2	25.1	0.1	20.8	1.4
In condensates	57.6	20.4	56.0	55.4	71.6
Total retained	84.6	67.0	89.9	90.8	81.1
Iodine removed from tank after aging by					
Pressure release	2.9	8.0	1.7	2.2	1.1
Argon displacement	4.8	12.3	4.4	3.0	5.0
Air sweep	1.2	2.9	1.8	0.9	2.6
Total iodine transported from tank	8.9	23.2	7.9	6.1	9.7
Retention of airborne iodine from tank					
On filters	0.35	0.71	0.05	0.1	0.15
On silver or copper screens	5.6	6.4	4.6	1.6	6.0
On charcoal papers			2.4	0.7	0.16
On charcoal cartridges	2.2	16.0	0.9	3.0	0.8
Iodine in penetrating form	0.6	0.02(?)	1.3	0.7	0.8

In all of the experiments, with the exception of 996H, the condensates removed over half of the activity from the containment tank. In the pressure release, argon displacement, and air sparging steps the fraction of the total iodine activity removed is very similar, with exception of this same Run 996H. It is especially interesting to find that only about 1% of the total iodine was converted to a penetrating, presumably organic, form in each of these experiments.

Table 2.3.3 gives a comparison of the distribution of cesium, tellurium, ruthenium, and strontium in the five runs. The effect of a longer flow path in the high burnup runs is shown by the greater deposition in the furnace tube and the duct connecting the furnace tube to the tank. There were few differences in the distribution of fission products reaching the tank. It is not clear at present whether the comparatively large amount of ruthenium in the condensate in the first simulant run is significant. Results of the other simulant experiments suggest that when the total amount of ruthenium reaching the tank is small, most of the material adheres to the tank wall, but when the amount is higher by a factor of 5 or 10, a significant fraction may be found in the condensate.

In the graphs of the airborne activity in the containment vessel with time, Figs. 2.3.2, 2.3.3, and 2.3.4, we find that the straight line portions of the cesium and strontium curves for the pellet simulant run (Fig. 2.3.2) and the irradiated UO_2 runs (Fig. 2.3.3 and 2.3.4) have similar slopes or half times. As most of the data, from which the ruthenium curves were derived, was of the "equal to or less than" variety, it is quite possible that all of these particulates (Cs, Sr, Ru) for any one run have the same slopes for their straight line portions. These similarities in the slopes of the pellet simulant and "hot" runs would indicate the presence of similar sized particles.

Table 2.3.3 Distribution of Fission Products Released
From Simulated Fuel and From High Burnup UO₂

	Amount of Fission Product Found (% of total inventory)				
	Furnace Tube and Duct to Tank	Aerosol Tank Walls	Condensate	Filters	Total Release From Fuel
<u>Cesium</u>					
Simulant (990S)	3.0	15.1	43.6	0.8	62.5
Simulant (991S)	-	4.5	3.5	0.19	8.2
Simulant (992S)	28.6	19.8	47.2	0.16	96.0
High Burnup (995H)	25.0	8.5	12.6	2.1	48.2
High Burnup (996H)	8.7	13.9	6.2	1.5	30.2
<u>Tellurium</u>					
Simulant (990S)	0.3	6.9	0.8	0.45	8.4
Simulant (991S)	-	36.2	0.36	9.2	45.7
Simulant (992S)	0.43	0.0043	0.00015	0.00006	0.43
High Burnup (995H)	18.1	12.4	0.7	0.5	31.7
High Burnup (996H)	0.7	1.5	0.04	0.12	2.4
<u>Ruthenium</u>					
Simulant (990S)	0.07	0.35	0.12	0.0006	0.48
Simulant (991S)	-	0.76	0.011	0.11	0.89
Simulant (992S)	0.002	0.07	0.018	0.028	0.12
High Burnup (995H)	0.26	0.054	0.001	0.002	0.32
High Burnup (996H)	0.17	0.052	0.002	0.005	0.23
<u>Strontium</u>					
Simulant (990S)	0.01	0.04	0.0003	0.0004	0.05
Simulant (991S)	-	0.026	0.009	0.0021	0.04
Simulant (992S)	*-	-	-	-	-
High Burnup (995H)	0.047	0.015	0.005	0.0001	0.01
High Burnup (996H)	0.05	0.011	0.014	0.002	0.77

*Incomplete analysis.

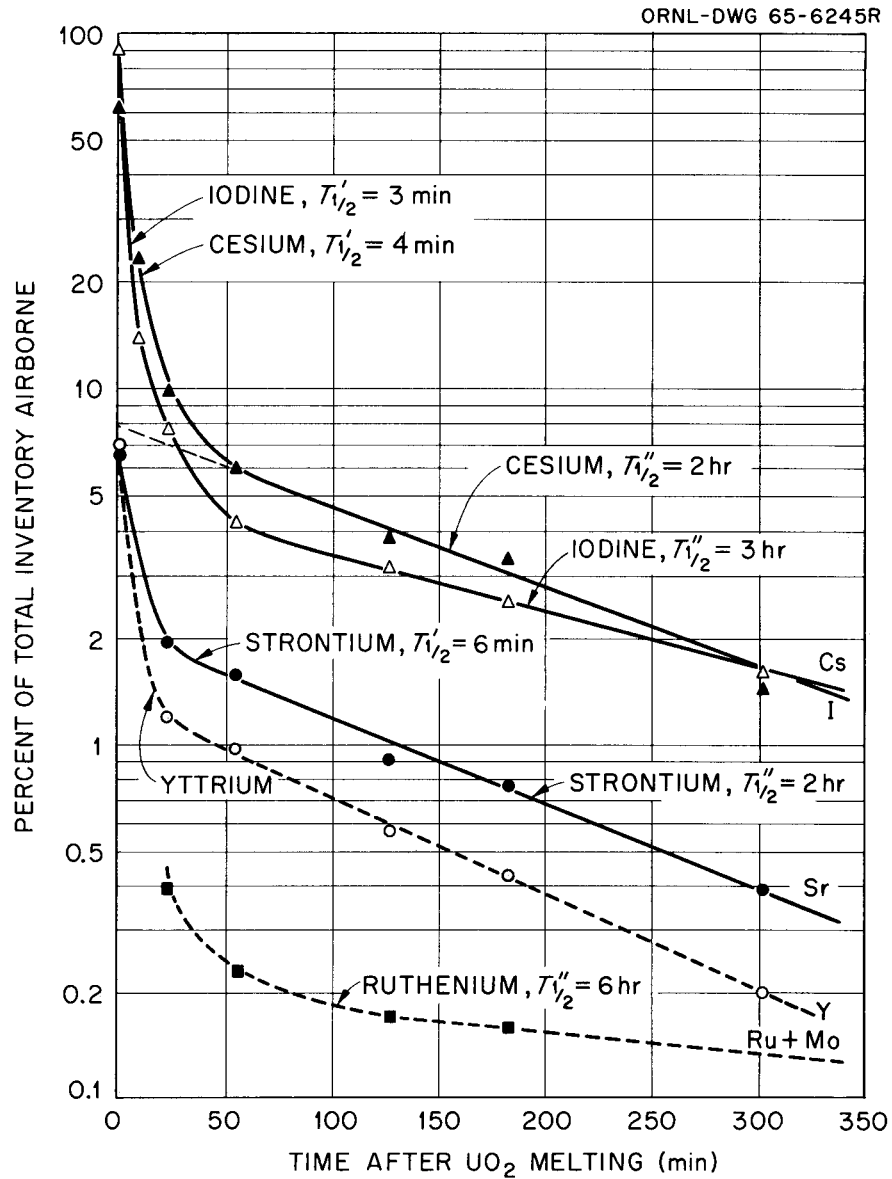


Fig. 2.3.2 Changes of Airborne Fission-Product Aerosol Concentration with Time in Run 992S.

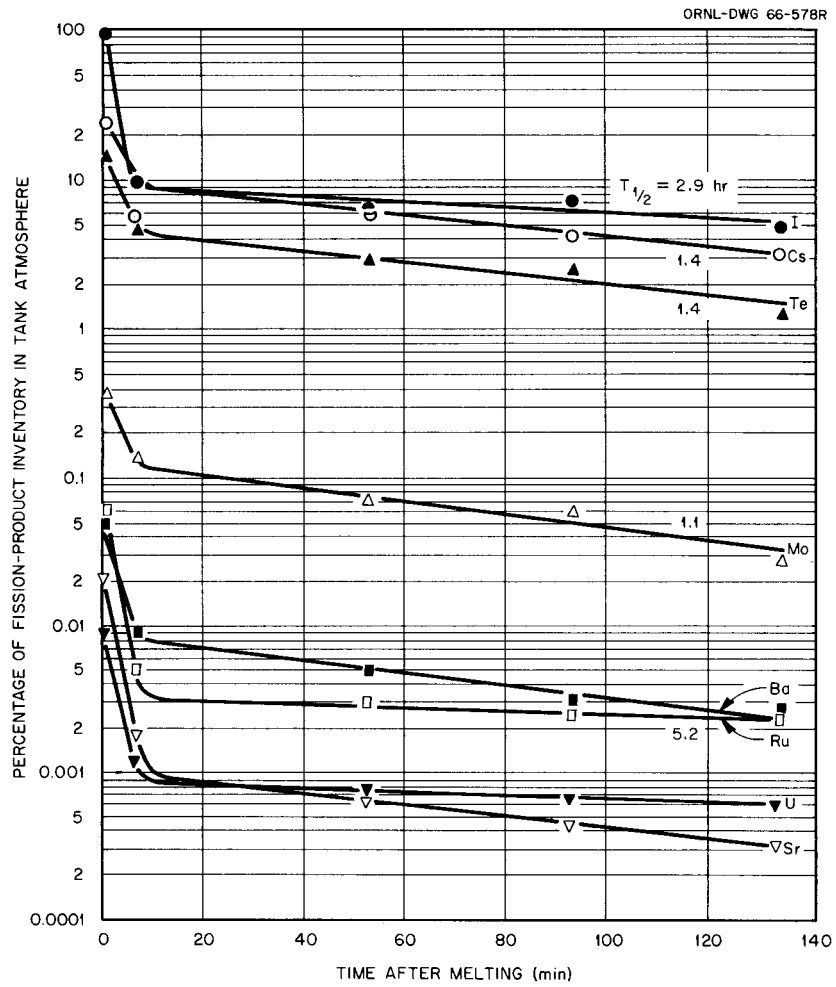


Fig. 2.3.3 Composition of CMF Tank Atmosphere as Determined by Gas Samples in Run 995H.

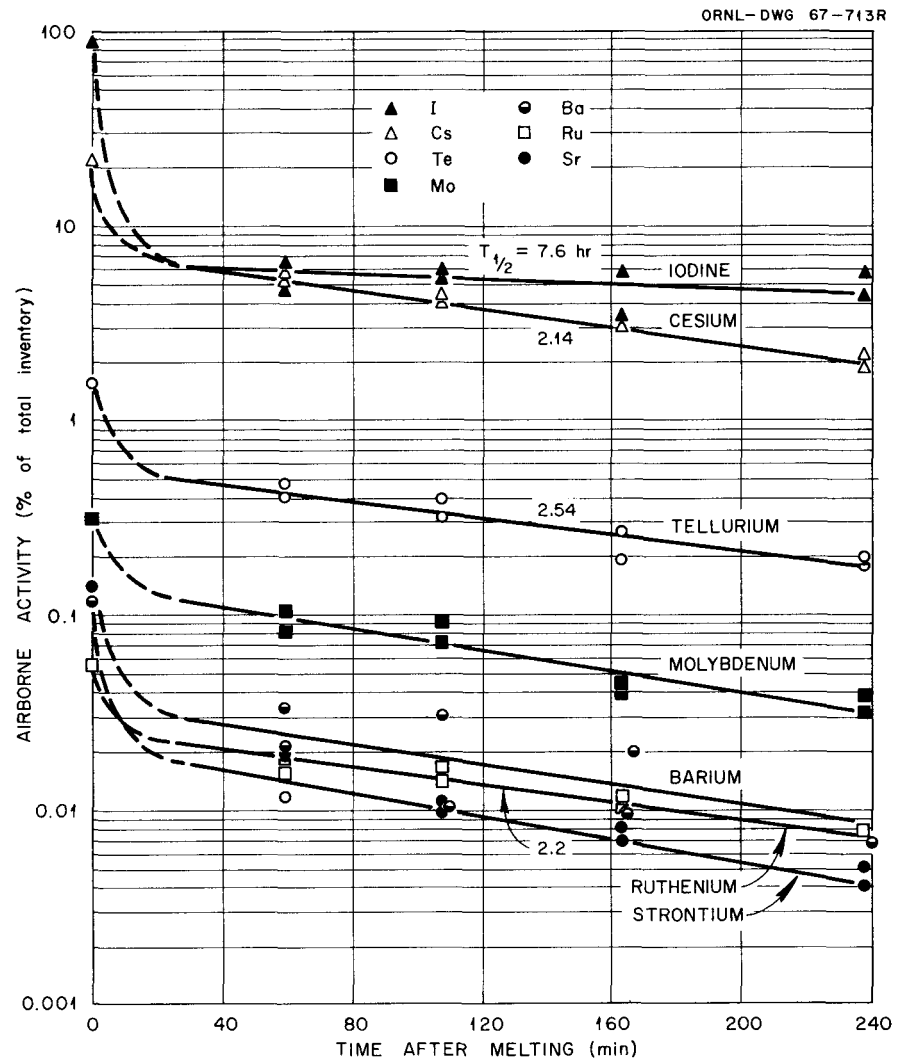


Fig. 2.3.4 Composition of CMF Tank Atmosphere as Determined by Gas Samples in Run 996H.

It is an accepted fact that the rate of condensation of steam in a containment vessel greatly influences the depletion rate of the airborne activities. The similarity in the depletion rate for the particulate activities in the pellet simulant and the hot runs, as shown above, is reflected in the similarities in the half-times for condensation rates as shown in Figs. 2.3.5 and 2.3.6.

2.3.4 Behavior of Iodine in UO₂ Fuel Melted in Air

As an additional comparison, some previous experiments in a series conducted in air — instead of steam and air — are summarized in Table 2.3.4. These include two at essentially trace level 979-T and 980-T (representing very low iodine concentration) and two at a higher iodine concentration 981-H (7000 MWD) and 982-S, a mixed pellet-and-iodine-tracer run.

As shown in **Table 2.3.4** the iodine released was slightly higher for the Runs 981H and 982S where higher iodine concentrations were present in the fuels. These two runs agree quite well throughout the table, with the exception of the iodine species found in the filters through which part of the tank atmosphere was vented during the pressure release steps at the end of the runs. The 49.4 value for Run 981H for molecular iodine (retained on silver or copper screens) is surprising, as this type of iodine would be expected to be greatly depleted by deposition on the tank walls during the aging period, and while some desorption from the walls does occur, it is difficult to imagine that desorption could account for such an amount.

The differences in iodine distribution is listed in Table 2.3.4 for the two trace irradiated UO₂ runs (979-T and 980-T), are not surprising and could be expected when very small concentrations of iodine are involved.

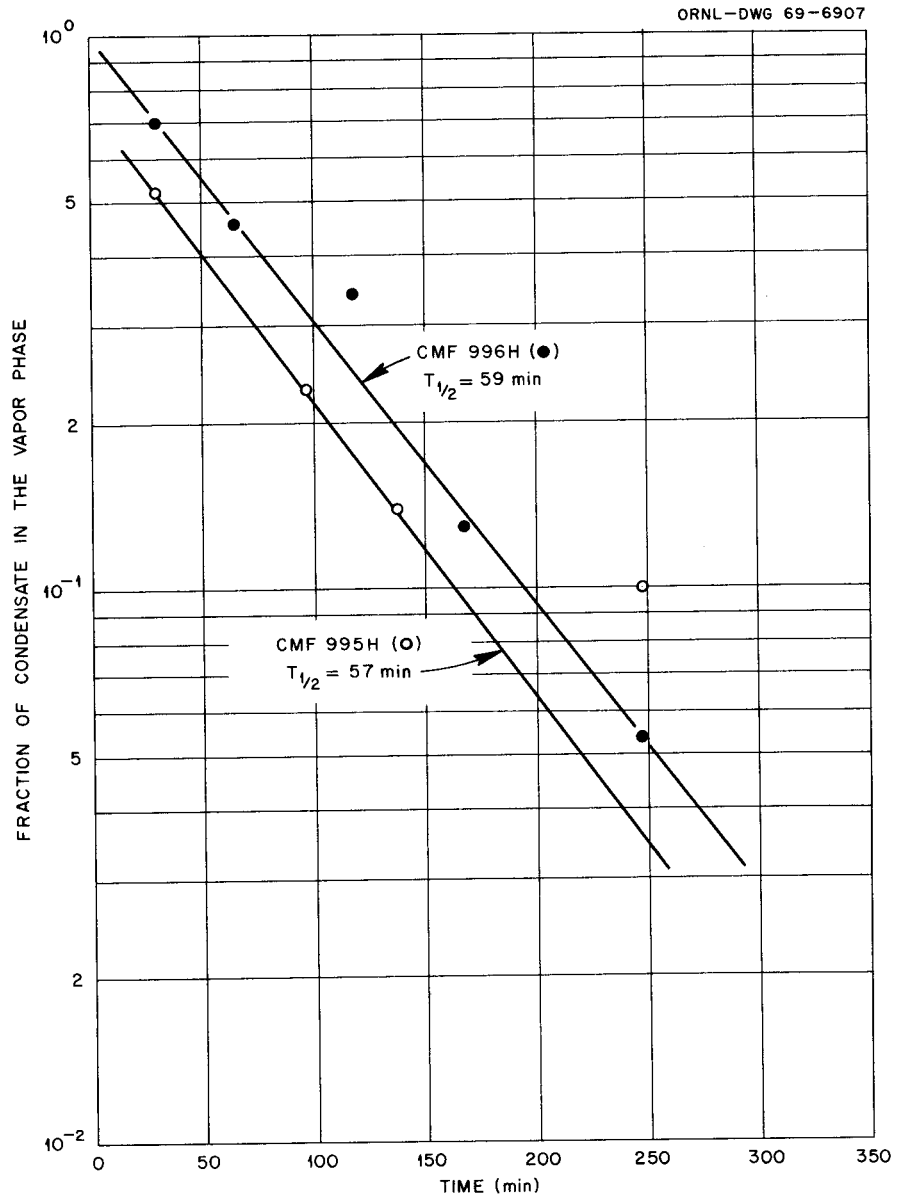


Fig. 2.3.5 Condensation Rates for CMF Runs 995H and 996H.

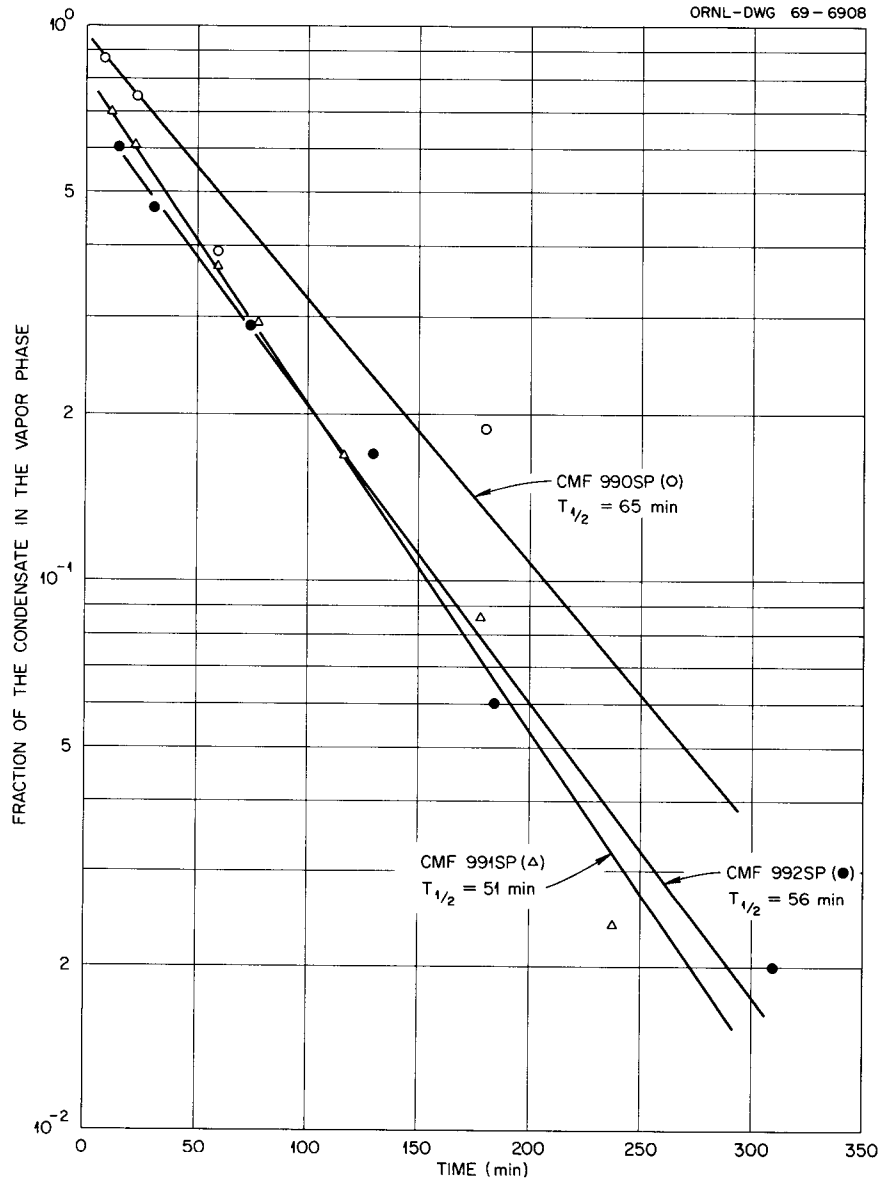


Fig. 2.3.6 Condensation Rates for Pellet Simulant Runs in the CMF.

Table 2.3.4 Distribution of Iodine Released in UO₂ Fuel Meltdown Tests in Air

	Irradiated UO ₂			
	Run 979T (trace)	Run 980T (trace)	Run 981H (7000 MWD)	*Run 982S
Iodine released	83.8	63.8	90.0	92.1
Iodine on tank walls	47.5	23.8	25.2	34.2
Iodine removed from tank after aging	29.5	26.7	61.9	57.2
Retention of airborne iodine from tank				
On filters	16.0	15.4	3.9	1.1
On silver of copper screens	4.8	8.1	49.4	2.0
On charcoal papers	-	-	4.1	14.7
On charcoal cartridges	8.7	3.2	4.5	39.4

*Run 982S was a ¹³¹I tracer simulant released by melting unirradiated UO₂.

If we examine the amount of iodine which was retained on charcoal (organic iodine) in the venting filters, we find that it is surprisingly high. We are, however, fully cognizant of the relatively large uncertainties in some of the values for "organic iodine." The crude techniques in use at the time these experiments were conducted must be taken into account.

2.4 Evaluation of the Pellet-Type Simulant in the CMF

The distribution of fission products released from high-burnup UO_2 and aged in a steam-air atmosphere in the CMF compared favorably with that of simulated fission products. Thus, the use of pellet simulated high-burnup fuel in fission-product release and transport experiments appears to be justified by these few experiments.

2.5 Fuel Preparation for the Nuclear Safety Pilot Plant

The fuel simulants were prepared as mixtures of UO_2 powder and suitable compounds of the fission products to be simulated. The simulant mixture was keyed to its iodine content according to proportions tabulated elsewhere,¹² as a guide to indicate appropriate molar ratios of the various isotopes. The fission-product elements and tracer isotopes used were the following:

<u>Element</u>	<u>Compound</u>	<u>Isotope</u>
Strontium	$\text{SrCO}_3 + \text{SrI}$	^{85}Sr
Ruthenium	Ru (elemental)	^{106}Ru
Iodine	$\text{SrI} + \text{NaI}$	^{131}I
Cesium	CsCO_3	^{134}Cs
Cerium	$\text{Ce}(\text{OH})_3$	^{144}Ce

In all cases, the tracer isotope was added while the element was in solution. Insoluble compounds were washed by decantation after precipitation and reslurried in water. Then about 10 g of UO_2 was added and the batch evaporated to dryness. The four simulant batches (Sr + I, Ru, Cs, and Ce) were then added to the remainder of the UO_2 required, blended in a cone-type blender, and cold-pressed into pellets. The pellet density turned out to be about 70% of theoretical. The pellets were then placed in a stainless steel can.

Significant differences between this form of doped UO_2 pellets and reactor grade UO_2 especially in the density and the oxygen to uranium ratio and in the chemical form as well as the uniformity of dispersion of fission products in the fuel were accepted as unavoidable. Other unknown effects include those of radiation and the fissioning process and the presence of other fission products. Depending primarily upon the expectation that the ultra high temperature to which the specimens are subjected during melting could override all the uncertain effects mentioned above, meltdown release experiments were conducted. It was gratifying to observe a reasonable correlation of the release data with that obtained in a high-burnup experiment.

For simulation experiments in the Nuclear Safety Pilot Plant, synthetic high burnup stainless clad UO_2 fuel elements were prepared. Stable Cs, I, Ce, and Ru were added in all three simulant experiments; Sr was used in two and Ba and Te in a third. The masses of these stable isotopes were maintained in the ratio calculated to exist in irradiated fuel. A gamma emitting isotope of each element was added so that we could use gamma ray spectrometry to analyze the samples. The radioisotopes were carefully homogenized with the stable isotopes, and the resulting mixture was blended with the UO_2 powder which was then cold-pressed into pellets. The pellets were then placed in stainless steel cans.

The synthetic fuel elements prepared as described above were then melted in a controlled atmosphere using a plasma torch. The plasma gas and shield gas served to sweep the resulting aerosol from the furnace into the model containment vessel of the pilot plant. Release of the fission products from the simulated fuel occurred in a chemical environment simulating that which would exist in a reactor core meltdown.

2.6 Simulant Evaluation Experiments in the NSPP

Seven of the first fifteen experiments in the Nuclear Safety Pilot Plant were concerned with evaluating simulants. Runs 8 and 9 were made with trace-irradiated stainless clad UO_2 fuel specimens, Runs 10-12 using stainless clad unirradiated UO_2 containing simulated fission products, and Runs 14 and 15 using Zircaloy clad UO_2 which had been irradiated to approximately 20,000 Mwd/tonne, stored for approximately 5 years and re-irradiated immediately prior to use to replenish the radioiodine. All of the experiments were done with the model containment vessel containing a mixture of air and steam simulating loss-of-coolant accident conditions.

While we saw difference in the behavior of fission products in these experiments, we are convinced that these were not due to whether real or simulated fission products were present. Rather, such factors as the chemical environment in which melting occurred and the degree of melting achieved appear to have had great influence.

We concluded that the chemical environment in the melt zone determines the chemical state of the fission products in the fuel and to a large extent, the percentage of each element which is released. This environment is principally influenced by the composition of the gases present and by the nature of the cladding metal.

In Runs 8 and 9 we observed that the cladding residue had a frothy appearance which we suspected indicated that a metal-water reaction had occurred. Subsequently, we found that other workers had observed the frothy residue when stainless-steel water reaction had occurred.¹³

In these two runs, we had placed 100 ml of water in the boat containing the fuel specimen to be evaporated as the boat and fuel were passed under the plasma torch. We adopted this procedure because we found that injecting steam into the furnace disturbed the plasma so much that we could not achieve satisfactory torch operation. We believe that all of this water was evaporated as the first pass of the fuel specimen under the torch was made. As a consequence of the metal-water reaction, free hydrogen undoubtedly existed in the melt area as long as the water was present and the atmosphere was reducing. Later, we believe only inert gas was present.

After these runs, we concluded that it would be better to maintain the same sort of atmosphere during the entire melting period of a run.

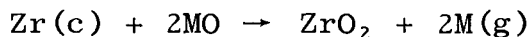
Accordingly, we defined two operating conditions: "Reducing" meant water was supplied to enable the cladding-water reaction to occur and that a mixture of argon and hydrogen was used as the sheath gas for the plasma. Thus the gas in contact with the melt always contained hydrogen. "Oxidizing" meant that water was not added to the boat, the furnace was purged continuously as the model containment vessel was heated (by open steam) and the plasma sheath gas was air. Thus metal-water reaction could not occur and the gas in contact with the melt contained oxygen. We maintained the "reducing" condition in Runs 10, 12, and 14 and the "oxidizing" condition in Runs 11 and 15.

The change from stainless cladding in Runs 8-12 to Zircaloy in Runs 14 and 15 appears to have considerable influence. The zirconium appears to have gettered all of

oxygen from the sheath gas and probably to have reduced some fission product oxides.

Table 2.6.1 shows the percentages of several fission products transported to the MCV in Runs 8-15. In Runs 8 and 14, there was very limited melting, and we believe the lack of melting accounted for the generally low transfer in these two experiments. Strontium transfer was low in all runs except No. 15, and barium transfer was low except in Runs 14 and 15.

Run 14 was intended to be reducing. Run 15 was run under intended oxidizing conditions, but the zirconium in the cladding apparently consumed all of the oxygen. We believe the alkaline earth oxides were reduced in these two runs. The free energy change for the reaction:



(M stands for Sr or Ba) is given in Table 2.6.2.

This indicates that we should expect barium to be reduced above 2000^oK and strontium above approximately 2200^o. Thus the observed high barium release in both runs and high strontium release in the second only is consistent with the apparent temperature history.

Table 2.6.2 Free Energy Change for Reaction Between Zirconium Metal and Alkaline Earth Oxides

	ΔG , cal/mol at Temperature	
	2000 ^o K	2500 ^o K
Barium	-373	-35,207
Strontium	+4427	-10,007

The iodine data show that a maximum of 35% of the fuel iodine inventory was transferred into the model containment vessel when reducing conditions existed. Except in Runs 11 and 12, 80-90% of the iodine which was not transferred was

Table 2.6.1 Percentages of Fuel Inventory of Several Fission Product Elements Transferred to the Model Containment Vessel

Run:	8	9	10 ⁽²⁾	11 ⁽¹⁾	12 ⁽²⁾	14* ⁽²⁾	15* ⁽¹⁾
Strontium	0.02	0.08	0.025	0.021		0.19	15.17
Barium	0.18	0.06	-	-	0.024	2.19	14.2
Iodine	2.3	35.1	24.0	84.0	8.0	2.4	27.3
Tellurium	0.3	8.5	-	-	2.6	-	-
Cesium	0.12	10.5	19.0	26.0	4.2	0.8	43.0
Cerium	0.02	0.2	0.22	0.008	0.05	0.17	1.28
Ruthenium	0.02	1.9	1.2	11.7	0.086	0.12	0.58

*High burn-up specimens.

(1)Oxidizing conditions.

(2)Reducing conditions.

found with the fuel residue. In these two runs a major part of the iodine which failed to transfer was found in the furnace.

In Run 11, under oxidizing conditions, 96% of the iodine was released from the fuel and 84% was transferred into the model containment vessel. Under the reducing conditions in Run 12, 74% of the iodine was released from the fuel but only 9% reached the containment vessel, the other 65% deposited in the furnace.

Cesium release was markedly affected by the degree of melting and very little by varying the furnace atmosphere. As was the case for iodine, in Run 12 there was significant deposition of the cesium in the furnace. Eighty-five percent of the cesium inventory was released from the fuel, but 81% deposited in the furnace and only 4% was transferred into the model containment vessel. The unique feature of Run 12 was that it took 3-1/2 hr to heat up to starting conditions, compared with 3/4 hr in the other runs. We suggest that considerably more condensate was accumulated on the furnace surfaces (the furnace body and lid are water-jacketed, although these were maintained at 90°C to minimize condensation) than when the vessel was heated rapidly. An accumulation of condensate would explain the abnormally high deposition.

Cerium release was very low except in Run 15. In that run, 35% was released from the fuel; all but 1.3% remained in the furnace. As with the alkaline earths, reduction of cerium oxide by the zirconium metal in the melt appears to be a possible explanation the behavior observed.

Ruthenium behaved about as expected. We observed large transfer into the model containment vessel only for the oxidizing conditions of Run 11.

It is unfortunate that we have no simulant run using Zircaloy-clad specimens. Run 13 had been scheduled to be such. However, it had to be abandoned in order to meet a schedule commitment for Run 14, and we were unable to

obtain support for a run using Zircaloy-clad simulated fuel at a later date. Such a run would have confirmed or refuted our opinion that the differences we have seen between Runs 14 and 15 and the others are due to the chemical effect of the cladding rather than the irradiation history.

Table 2.6.3 indicates the maximum percentage of the inventory in the model containment vessel represented by any of the gas samples. The data show erratic behavior. In every case where we have data, the iodine concentration is a fraction of what it would be if all of the iodine reaching the containment vessel were dispersed uniformly. In Run 14, the iodine data from the May packs showed a pattern of erratic behavior which we recognized from previous experience with shorter-lived isotopes as indicating too much decay correction had had to be applied. Therefore, we discarded the iodine data from this run.

It is shown in Table 2.6.3 that the maximum concentration is substantially higher than the average inventory value for certain of the aerosols in part of the runs. We believe this can be explained as follows: when a fluid circulates in a closed tank it is quite common for stagnant eddies to develop. We feel that such a thing must have happened here and that the eddy was located so that the aerosol entering from the furnace got trapped in the eddy instead of being dispersed and diluted as it entered the containment vessel.

Possibly it is significant that the maxima tend to be higher for Runs 8 and 14 where practically no melting occurred than for other runs. The low concentrations in the containment vessel atmosphere could very well have led to smaller particle size and thus to less effective removal. In Run 14 we observed that a maximum in concentration of several of the fission products occurred at progressively later times as the elevation in the vessel decreased. It looked like a cloud of particles was settling, and the velocity was that of approximately 3- μ diameter water drops.

Table 2.6.3 Maximum Percentage of the Model Containment
Vessel Inventory of the Given Fission Product
Found in Gas Samples

	Run	8	9	10	11	12	14	15
Strontium		--	--	---	--	--	130	--
Barium		36	10	---	--	--	15	12
Iodine		21	11	0.7	12	12	--	10
Cesium		1130	20	0.6	58	17	400	6
Cerium		89	20	---	--	--	300	68
Ruthenium		160	10	---	17	--	77	24
Tellurium		43	9	---	--	--	--	--

We suggested that particles of 0.1 to 0.5- μ diameter acted as condensation nuclei and that the drops grew to approximately 3- μ diameter. We saw no behavior of this type in the rest of the runs.

As we have described, we observed many differences in behavior of the several isotopes during these runs. However, we are convinced that these can be accounted for by the time-temperature history to which the sample was subjected and the chemical environment in which release of the fission products (real or simulated) occurred. We observed no effects which could not be accounted for by time-temperature history and melt environment, and we have no reason to believe simulants behave in a different way than real fission products in the NSPP.

3.0 CSE SIMULANT TESTS OUT-OF-PILE

3.1 Introduction

Fission-product aerosols simulated in experiments performed in the Containment System Experiment (CSE) are generated by separate vaporization of the simulants. Rogers⁹ pointed out that in the 30,000-ft³ CSE containment tank, use of irradiated fuel to furnish realistic fission-product levels was impractical. Neither was it feasible to use simulated high-burnup fuel pellets of the type used in the CMF and in the NSPP. The simulation technique devised for the CSE experiments, described by Hilliard and McCormack,¹ involves vaporization of suitable quantities of fission-product elements containing radioactive tracers and passing the vapor over molten, unirradiated UO₂ before it enters the containment vessel. In order to determine how well the aerosols produced by this technique imitate those produced by overheated high-burnup fuel, it was necessary to make direct comparisons of simulants with high-burnup fuel under similar conditions in the CMF and CRI.

In order to perform CSE-type simulation experiments in the CMF, it was necessary to modify the experimental arrangement described by Hilliard and McCormack rather extensively to adapt it to the CMF fuel meltdown arrangement, but the differences related mainly to methods of getting the vaporized materials into the pressurized meltdown furnace. In addition, we chose to provide a steam-air environment in the vicinity of the molten UO₂ and in the containment tank, at 30 lb total pressure, rather than air, because our recent experiments with high-burnup fuel were all carried out with a steam-air atmosphere in accord with the LOFT model.

3.2 Description of Simulant Vaporizer Unit

As shown in Fig. 3.2.1, two ribbon heating units were inserted through a glass envelope which was fitted to the end of the quartz meltdown tube by means of a tapered joint. A platinum ribbon filament that operated at a temperature between 1400 and 1600°C in the furnace-tube atmosphere was used to vaporize tellurium (in the form of TeO_2), cesium (introduced as Cs_2CO_3), and ruthenium metal. Cesium, which is probably vaporized as the metal, will quickly be re-oxidized in the furnace atmosphere. Ruthenium metal undoubtedly is converted to a volatile oxide, RuO_3 or RuO_4 . The other heater filament, which was a V-shaped tantalum ribbon (1/8-in. wide and 1/2-in. long), was heated in a helium atmosphere in a small glass envelope with only a 1/16-in.-diam hole through which helium carrying the vaporized material flows into the furnace tube. A mixture of BaCO_3 or SrCO_3 and finely divided zirconium metal was placed on the tantalum ribbon to increase the volatility of barium as the metal.

Iodine in the form of I_2 was introduced through a side arm attached to the outside pressurized-tube extension, as shown in Fig. 3.2.2. A glass capsule containing crystalline I_2 was inserted in the Teflon-lined side arm, and it was crushed while a stream of hot air was introduced to carry the iodine into the inner (furnace) tube.

Steam was added through the ball joint at the end of the glass envelope. Water that is supplied under pressure at a carefully controlled rate was converted to steam by a miniature water vaporizer located in the outer pressurized shell quite close to the ball joint entrance to the furnace tube.

Preliminary testing centered on achieving satisfactory volatilization of barium, the least volatile species expected to be used in these experiments. We found that a

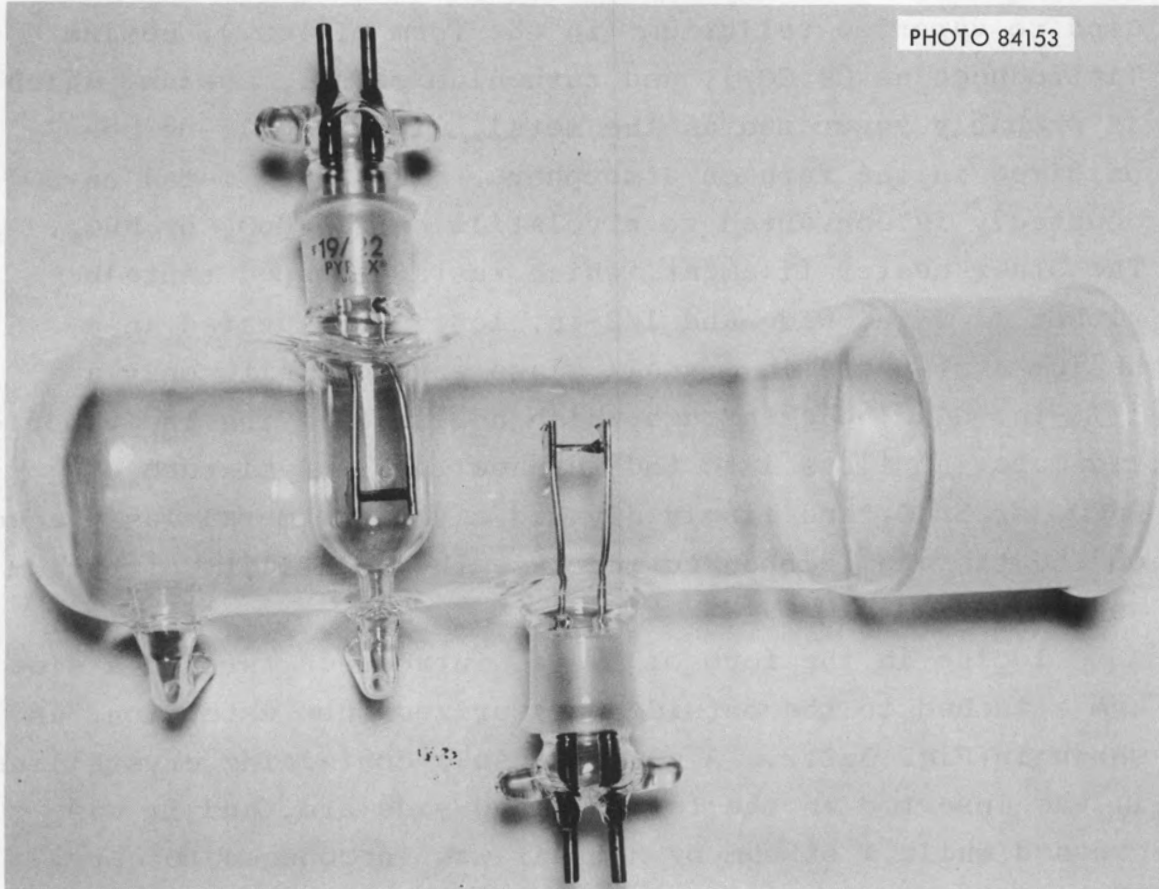


Fig. 3.2.1 Electrically Heated CSE Simulant Vaporizer.

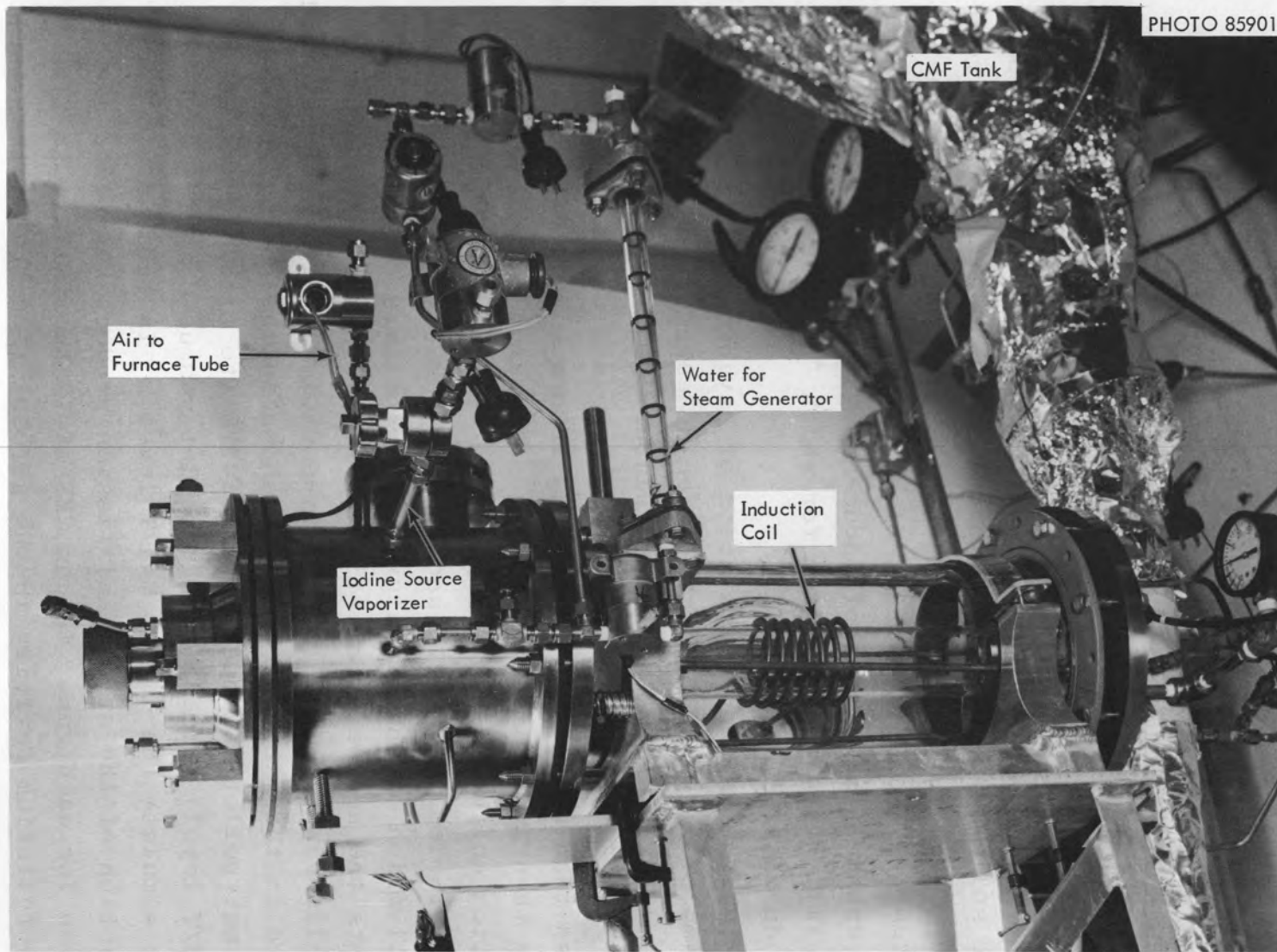


Fig. 3.2.2 CSE Type UO_2 Furnace and Simulant Vaporizer.

temperature of 1800°C was needed to volatilize half of the barium activity from a BaCO₃-Zr metal mixture in a flowing helium atmosphere under ideal conditions and applicable time periods.

3.3 Fuel Preparation

Due to the necessity of handling an unusually small sample of fission product elements with tracers added or induced, it became obvious that some method of compacting the solid tracer to permit handling as a unit was required.

There were also some advantages to be gained in the selection in certain cases of separated isotopes in order to enhance the amount of induced activity. This was especially true of tellurium for which ¹²⁴Te was chosen to produce the 58 d ¹²⁵Te.

With the added limitation of having only a few milligrams of a total solids to place on each filament, it was deemed practical to devise miniature pellet dies as shown in Fig. 3.3.1. The smaller of these was capable of pressing less than a milligram of solids into a single cylinder which was then irradiated in-pile and recovered intact for evaporation on the filament.

Tables 3.3.1, .2, and .3 show some typical results of activation of the miniature tracer pellets. Table 3.3.1 lists the nuclear properties of some of the most useful nuclides while Table 3.3.2 gives typical weights of materials used in the miniature pellets shown in the photograph. A 10 mg. pellet was used in CMF 1007S (to simulate the 2000 Mwd/T level) while a 50 mg. pellet was used in CMF 1008S (to simulate the 10,000 Mwd/T level). In Table 3.3.3 the fraction of the artificial fission product vaporized is given for each run. In Run CMF 1007S the failure to find the tellurium activity in the aerosol is probably the result of using an unenriched tellurium source.

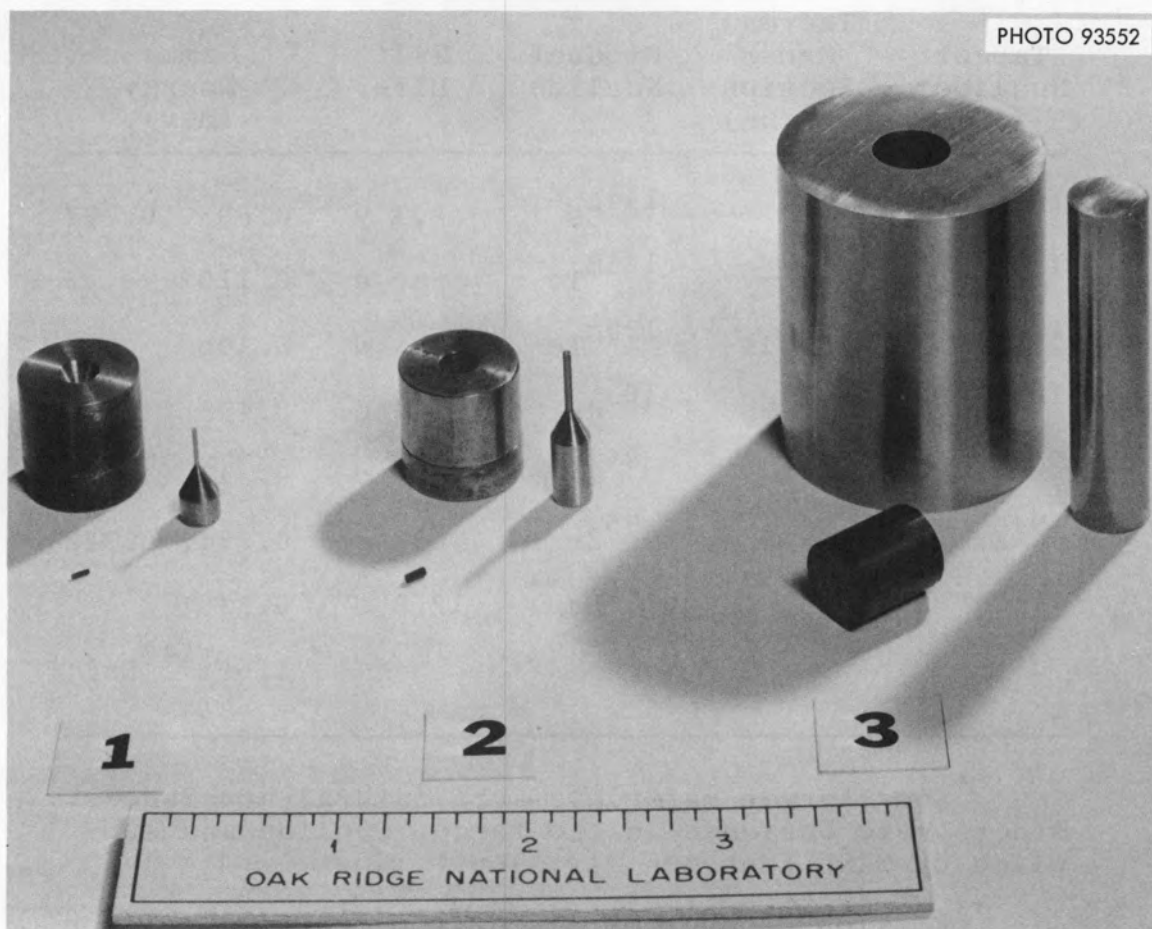


Fig. 3.3.1 Punch and Die Combinations for the Production of Pellets to be Used in the CSE Vaporizer Unit.

Table 3.3.1 Nuclear Properties of Nuclides
Used as Fission Product Simulants

Target Nuclide*	Thermal Cross Section (barns)	Product Nuclide	Half Life	Gamma Energy (mev)
^{133}Cs	26	^{134}Cs	2.3 y	0.605, 0.797
^{124}Te	6	$^{125\text{m}}\text{Te}$	58 d	0.110
^{128}Te	0.015	$^{129\text{m}}\text{Te}$	33 d	0.106
^{102}Ru	1.2	^{103}Ru	41 d	0.498
^{84}Sr	1.0	^{85}Sr	65 d	0.513 (^{85}Rb)
^{94}Zr	0.08	^{95}Zr	63 d	0.754, 0.722
		$^{140}\text{Ba}^{**}$	12.8 d	0.53
				1.6 (^{140}La)

*Some target materials were natural abundances, others were enriched in the target nuclide and supplied by ORNL Isotopes Division.

**Fission product obtained from Isotope Division.

Table 3.3.2 Composition of Simulated Fission Product Pellets
 (To simulate 20g UO₂ irradiated to 2,000 or 10,000 Mwd/T)

Pellet Type	Method of Heating	Element	Compound	Weight % in Mix		Pellet Weights		
				Element	Compound	CMF 1007S	CMF 1008S	CRI 107S
A	Pt Filament (1500°C)	Cs	Cs ₂ CO ₃	27.4	33.6			
		Te	TeO ₂	14.1	17.6	5.5 mg	25 mg	24.1 mg
		Ru	Metal	48.8	48.8			
B*	Ta Filament (>2000°C)	Sr	SrCO ₃	36.1	61.6		20 mg	
		Sr	Metal	38.4	38.4			
C*	Ta Filament (>2000°C)	Ba	BaCO ₃	48.6	68.4	5.5 mg		17.5 mg
		Sr	Metal	31.6	31.6			

* Barium and strontium were used alternatively.

Table 3.3.3 Simulant Sources and Release Fractions
in Aerosol CSE Simulation Experiments

Run No.	Simulant Nuclides				
	^{131}I	^{134}Cs	^{125}Te	^{103}Ru	^{85}Sr
<u>CMF-1007S</u>					
Source Activity, mc	45	0.85	0.016	0.26	--
% Released	100	100	not detected	23	
<u>CMF-1008S</u>					
Source Activity, mc	5.4	2.7	0.052	0.81	0.26
% Released	100	100	98	9.1	53
<u>CRI-107S</u>					
Source Activity, mc	48	10.3	0.102	1.46	0.87
% Released	100	97	84	6.6	1.0*

*Sr-Zr pellet in CRI-107S not heated to required temperature due to low electrical power.

3.4 Behavior of Simulants in the CMF

We completed two runs that simulated fuel with burnup levels of 1000 and 7000 Mwd/T. These are listed in Table 3.4.1 as CMF Runs 1007S and 1008S. Technical difficulties have limited our success in generating suitable fractions of elements other than iodine, cesium, and ruthenium; however, a fair amount of data has been accumulated with these three elements. We have compared the results of the two runs in Figs. 3.4.1 and 3.4.2 and in Table 3.4.2. The major differences in amount of reactivity remaining airborne are attributed to the effect of having a delay in Run 1008S that allowed most of the steam to condense before the aerosol was generated.

From the condensate collection rate (summary in Table 3.4.3), it was possible to evaluate the effect of the lower condensation rate in Run 1008S. The rate of steam condensation which is inferred is approximately equal to a 1-hr delay or about 1 ml/min initial condensation rate in 1008S compared to about 5 ml/min in 1007S. This suggests that the slopes of the two iodine deposition curves in Fig. 3.4.1 and 3.4.2 should be similar if the first hour in Run 1007S is ignored. This is indeed the case and clearly illustrates the strong influence of the steam condensation process for iodine removal.

In Fig. 3.4.1, showing the airborne concentration of activities with time in the containment vessel during Run CMF 1007S, the half-times for cesium and ruthenium are fairly close to that for the straight line portion of the iodine curve. In Fig. 3.4.2 which is a similar plot for CMF 1008S, the half times for the cesium and iodine are very similar while that for ruthenium was impossible to evaluate because of the extreme variation in values.

The half-times for the concentration of airborne cesium with time for the simulant Runs 1007S and 1008S (Figs. 3.4.1

Table 3.4.1 Experimental Conditions for Runs 995H, 996H, 1007S and 1008S

Run Number	Fuel	Cladding	Atmosphere	Aging (hr)	Pressure (atm abs)*	Temp. (°C)*
CMF 995H	1000 Mwd UO ₂	Stainless	Steam-air	4.0	3.	120
CMF 996H	7100 Mwd UO ₂	Zircaloy	Steam-air	4.5	3.	125
CMF 1007S	CSE Simulant (1000 Mwd)	Zircaloy	Steam-air	4.7	3.	97
CMF 1008S	CSE Simulant (7100 Mwd)	Zircaloy	Steam-air	4.7	3.	101

*Pressures and temperatures are those existing in the containment vessel at the start of the experiment.

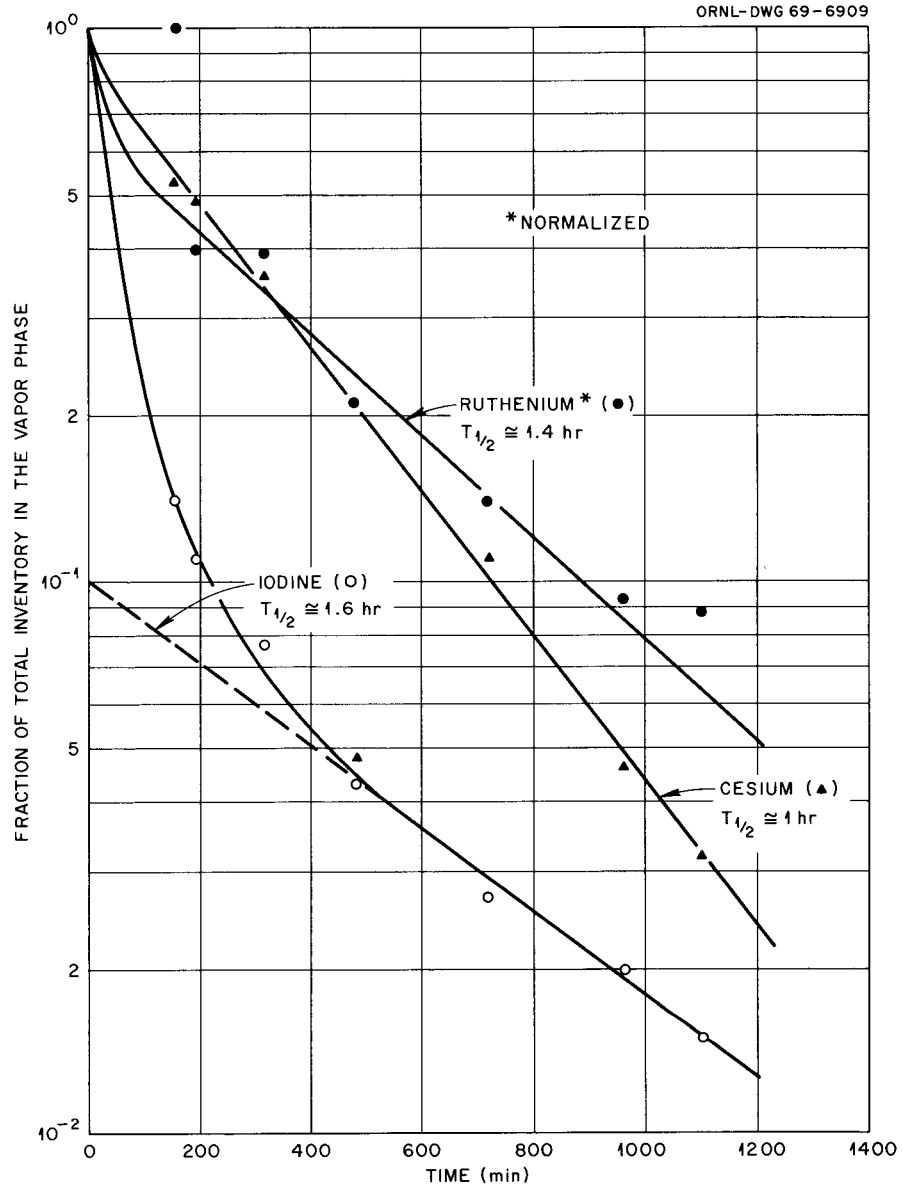


Fig. 3.4.1 Variation of Airborne Activity with Time in the CMF Containment Tank During Experiment 1007S.

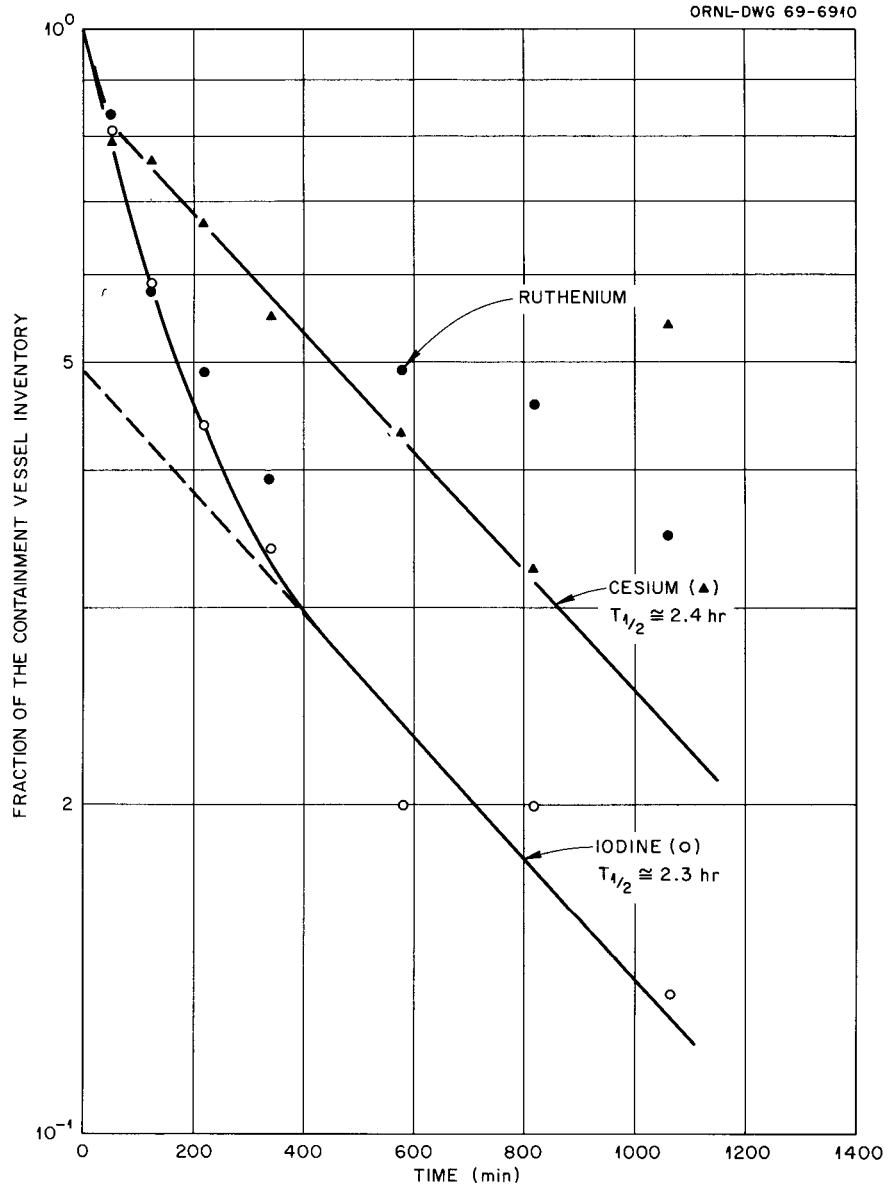


Fig. 3.4.2 Variation of Airborne Activity with Time in the Containment Tank During Experiment 1008S.

Table 3.4.2 Comparisons of Radioactivity Distribution Obtained in CMF Runs

	Iodine				Cesium				Ruthenium			
	Run 995H	Run 1007S	Run 996H	Run 1008S	Run 995H	Run 1007S	Run 996H	Run 1008S	Run 995H	Run 1007S	Run 996H	Run 1008S
Activity, %*												
Tank washes and deposition coupons	22.0	26.0	51.6	38.9	6.4	64.3	63.8	67.9	64.2	88.5	88.0	78.5
Condensates	67.4	66.9	22.6	45.1	80.0	31.0	28.7	15.0	10.6	5.6	3.5	8.9
Total	89.4	92.9	74.2	84.0	86.4	95.3	92.5	82.9	74.8	94.1	91.5	87.4
Airborne activity at end of aging period, % *												
Gas samples	0.17	1.8	0.1	2.1	0.86	3.8	0.4	3.1	0.8	5.0	0.5	3.0
Released by venting	3.2	0.57	9.0	6.0	2.9	0.03	1.1	8.4	4.5	0.04	1.2	5.2
Recovered by argon sweep	5.7	4.25	13.1	7.9	9.8	0.61	5.9	5.5	19.8	0.65	6.7	4.5
Total	10.6	6.52	25.8	16.0	13.56	4.4	7.5	17.0	25.29	5.69	8.4	12.7

*Percent of total activity in the containment tank.

Table 3.4.3 Condensation Data for CSE simulant Runs in the CMF and Their Counter-Parts

Run No.	CMF 1007S		CMF 995H		CMF 1008S		CMF 996H	
Date of Run	3-22-67		10-29-65		4-20-67		4-11-66	
Fuel	CSE, 1000 Mwd Simulant		1000 Mwd UO ₂		CSE, 7000 Mwd Simulant		7100 Mwd UO ₂	
Elapsed Time (min)	Total Condensate (ml)	$\Delta v/\Delta t$ (cc/min)	Total Condensate (ml)	$\Delta v/\Delta t$ (cc/min)	Total Condensate (ml)	$\Delta v/\Delta t$ (cc/min)	Total Condensate (ml)	$\Delta v/\Delta t$ (cc/min)
9	48	5.3						
30			129	4.3			69	2.3
33	140	3.8						
49	168	1.8						
50					48	0.96		
65							123	1.5
79	180	0.4						
95					72	0.53		
97			206	1.1				
118							150	0.51
137			230	0.6				
155					92			
168							197	0.94
180	204	0.24						
215					108	0.27		
247			241	0.1			214	0.22
275	216	0.13			112	0.067		
300					115	0.006		
$T_{1/2}^*$ (min)	26		57		71		59	

*Obtained by plotting fraction of total condensate in tank atmosphere, versus time.

and 3.4.2), and those for the comparable "hot" UO₂ runs 995H and 996H (Figs. 3.4.3 and 3.4.4), are 1.0, 2.4, 1.4, and 2.1 hours, respectively, and the corresponding condensation half-times for these runs, as listed in Table 3.4.3, are 26, 71, 57, and 59 minutes, respectively. The correlation between depletion and condensation rates, as shown by these values, again points out the importance of steam condensation on airborne activity depletion, as well as the validity of the CSE simulants as they fit with the irradiated UO₂ runs in the series very well.

3.5 Behavior of Simulants in the CRI

The experimental procedure in the CRI was, with the exception of the use of the vaporizer unit in 107S, the same for the irradiated UO₂ in Run 114H. The activity was liberated from its source and blown into the containment vessel, and once there, was isolated for a period of approximately twenty hours. During this "aging period," May pack type gas samples were taken of the tank contents as well as gas samples for particle size determinations with a low pressure cascade impactor. During the run, accumulated condensate was drawn from the containment vessel at various times. At the end of the aging period, the excess pressure on the containment vessel was vented through filters, and then the containment vessels atmosphere was decontaminated by recycling through filters.

A flow diagram of the CRI system is shown in Fig. 3.5.1. The cylindrical section of the containment vessel is 1.66 meters in diameter and 1.41 meters tall. The average height for the containment vessel, including the dished head and conic section, is about 2 meters with an overall height of 2.58 meters. The containment vessel volume is 4.62×10^6 cm³, and the surface area is 1.34×10^5 cm². A more detailed discussion of the construction and operation of the CRI can be found in a previous report.¹⁴

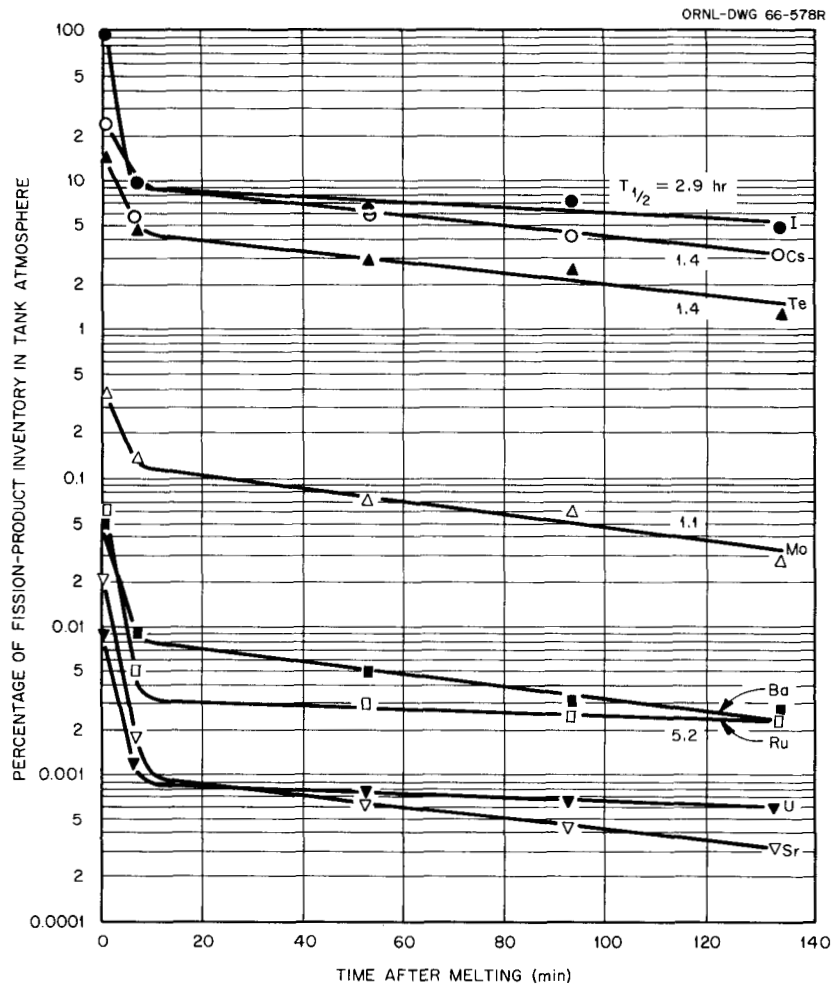


Fig. 3.4.3 Composition of CMF Tank Atmosphere as Determined by Gas Samples in Run 995H.

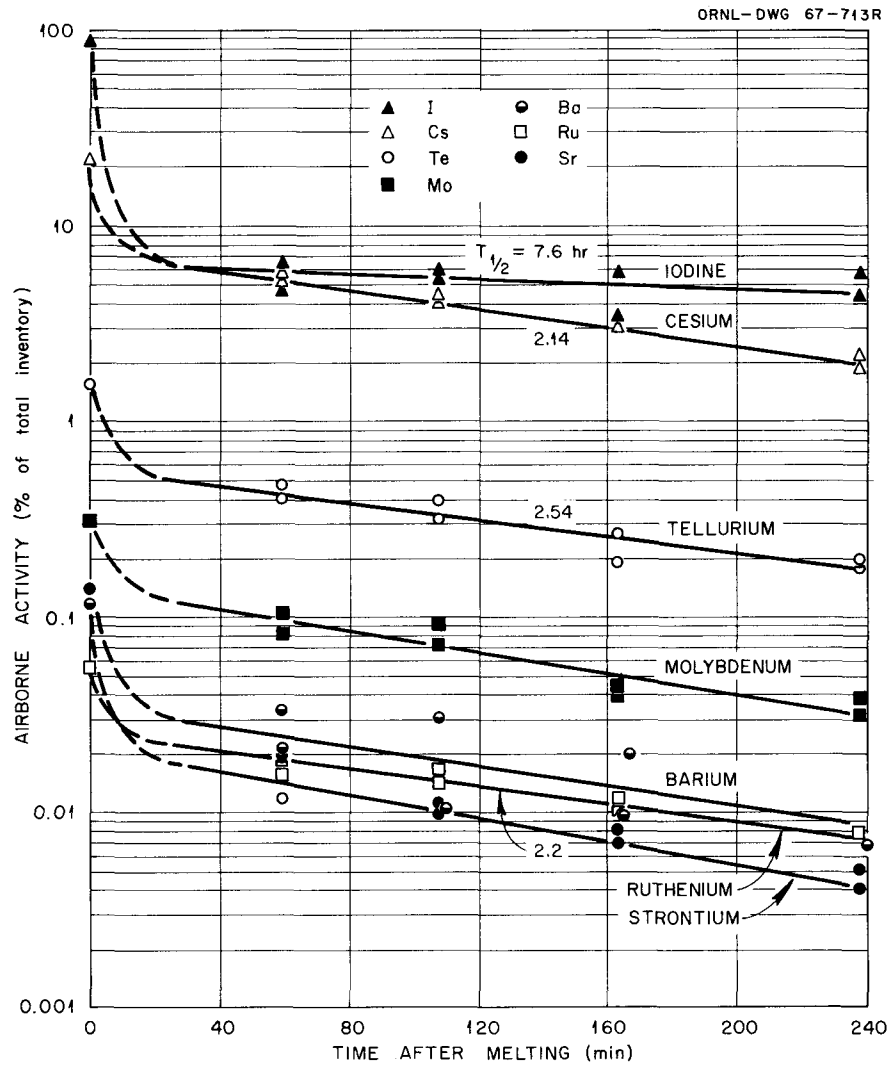


Fig. 3.4.4 Composition of CMF Tank Atmosphere as Determined by Gas Samples in Run 996H.

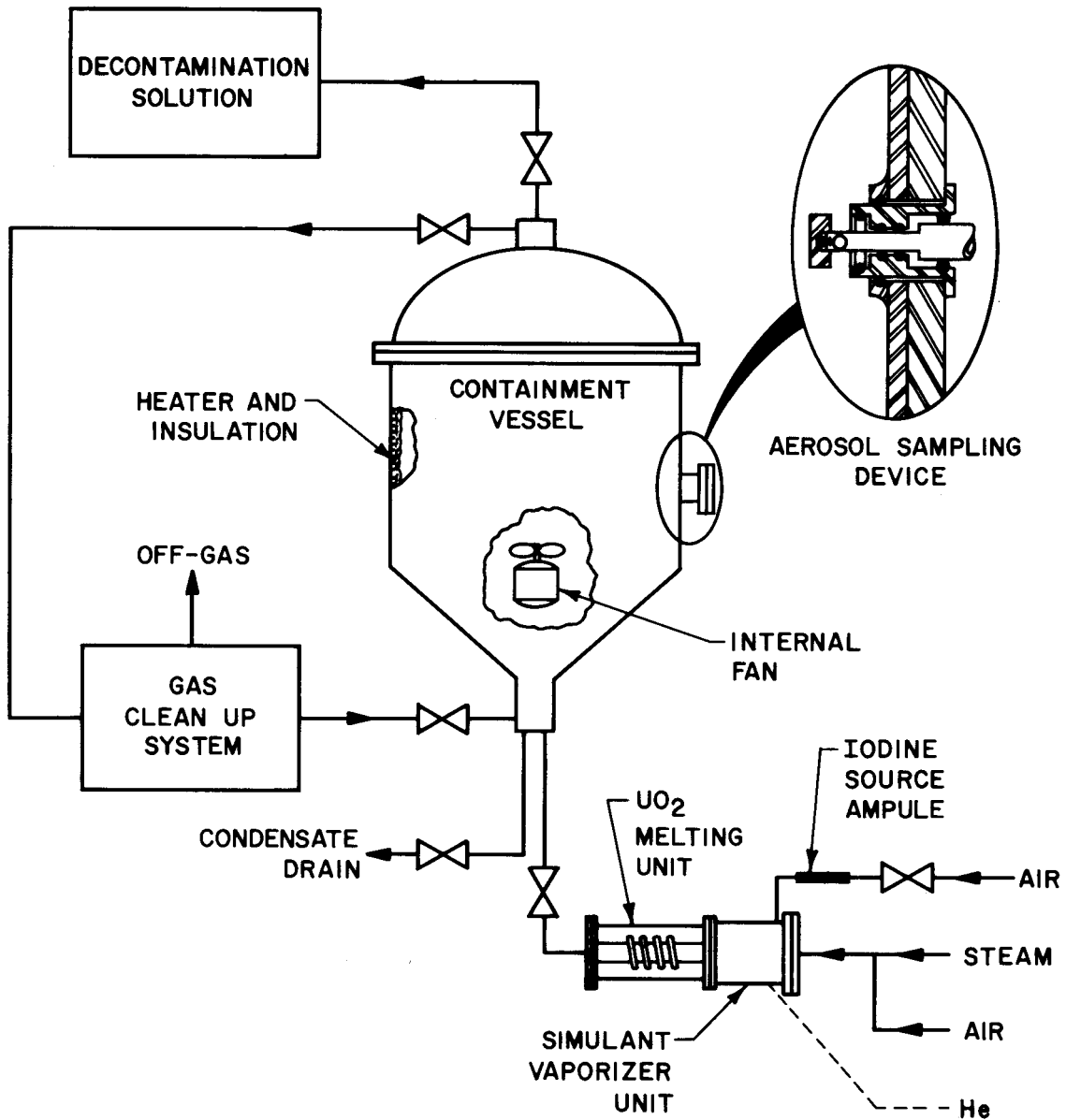


Fig. 3.5.1 The CRI Facility as Modified for Fission Product Simulation Studies.

3.5.1 Run 107S

Run 107S was conducted as a CSE fission-product simulant validation test. The objective was to provide the separately vaporized fission-product tracer elements in the mixed aerosol in the manner used at Battelle's Pacific Northwest Laboratory,² and to use the deposition behavior data later in comparison with one that has real fission-product aerosols from highly irradiated UO₂ (114H). In the simulant run, molten Zircaloy-clad UO₂ was used as the aerosol-generating source, and the gaseous iodine, cesium, and tellurium were vaporized and passed over the molten mass before they reached the containment vessel.

3.5.2 Run 114H

In Run 114H, 40 grams of irradiated (6000 Mwd/T) UO₂ were clad in Zircaloy and melted in a steam-air atmosphere with induction heating. This run was performed for comparison with the simulant Run 107S, however the iodine present in 114H fuel was calculated to be just over 2.2 mg while there was 9 mg present in 107S. In general, with the exception of the weight of iodine, the conditions for the two runs were very similar.

On examining Table 3.5.1 and Fig. 3.5.2, it is evident that the conditions of temperature, pressure, and humidity are practically identical for the simulant Run 107S and the irradiated UO₂ Run 114H. In Fig. 3.5.3, the condensation rates for the two runs, as calculated from condensate volumes, are shown and the half-times for condensation are practically identical.

In Table 3.5.2, the distribution of fission activities is listed for the simulant 107S and the "hot" 114H runs. It is interesting to note that the total release of the listed activities is greater in the simulant run than in the "hot" run. In Table 3.5.3, the distribution of the iodine

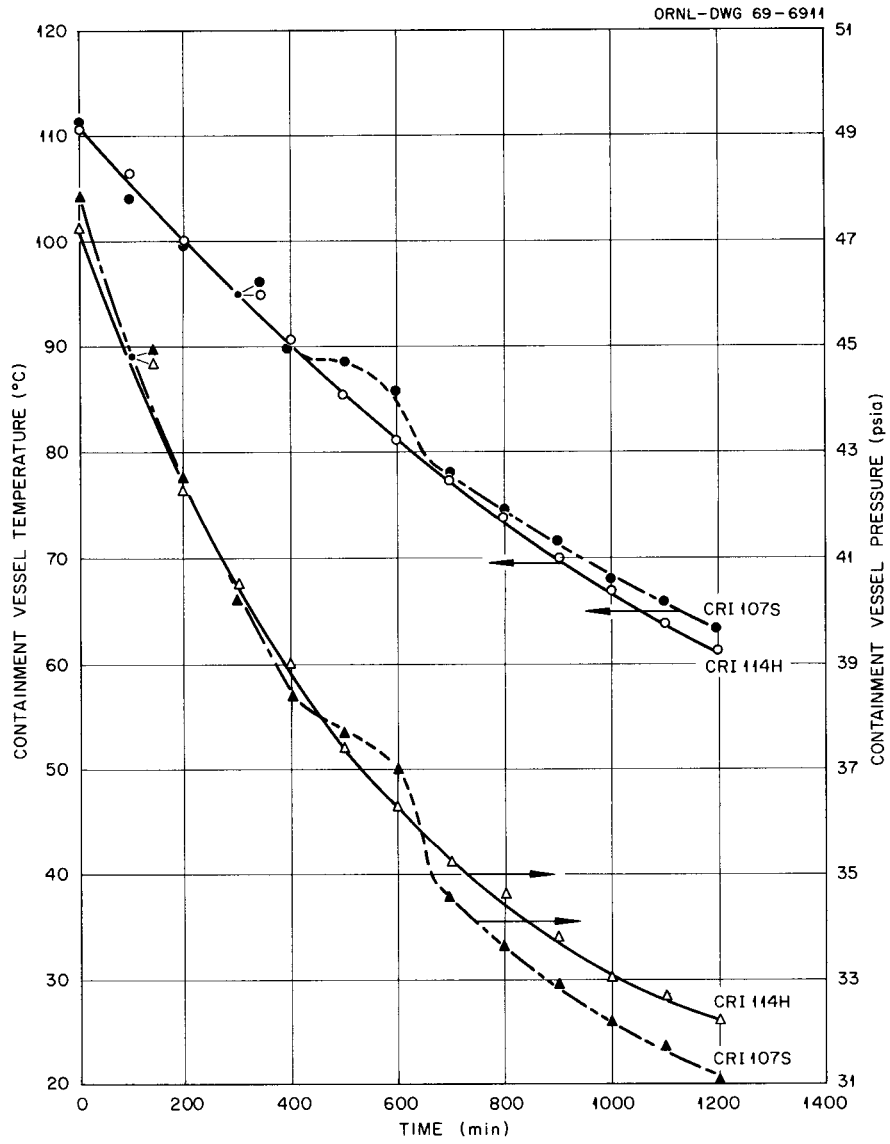


Fig. 3.5.2 Temperature and Pressure Conditions Existing in the CRI Containment Vessel.

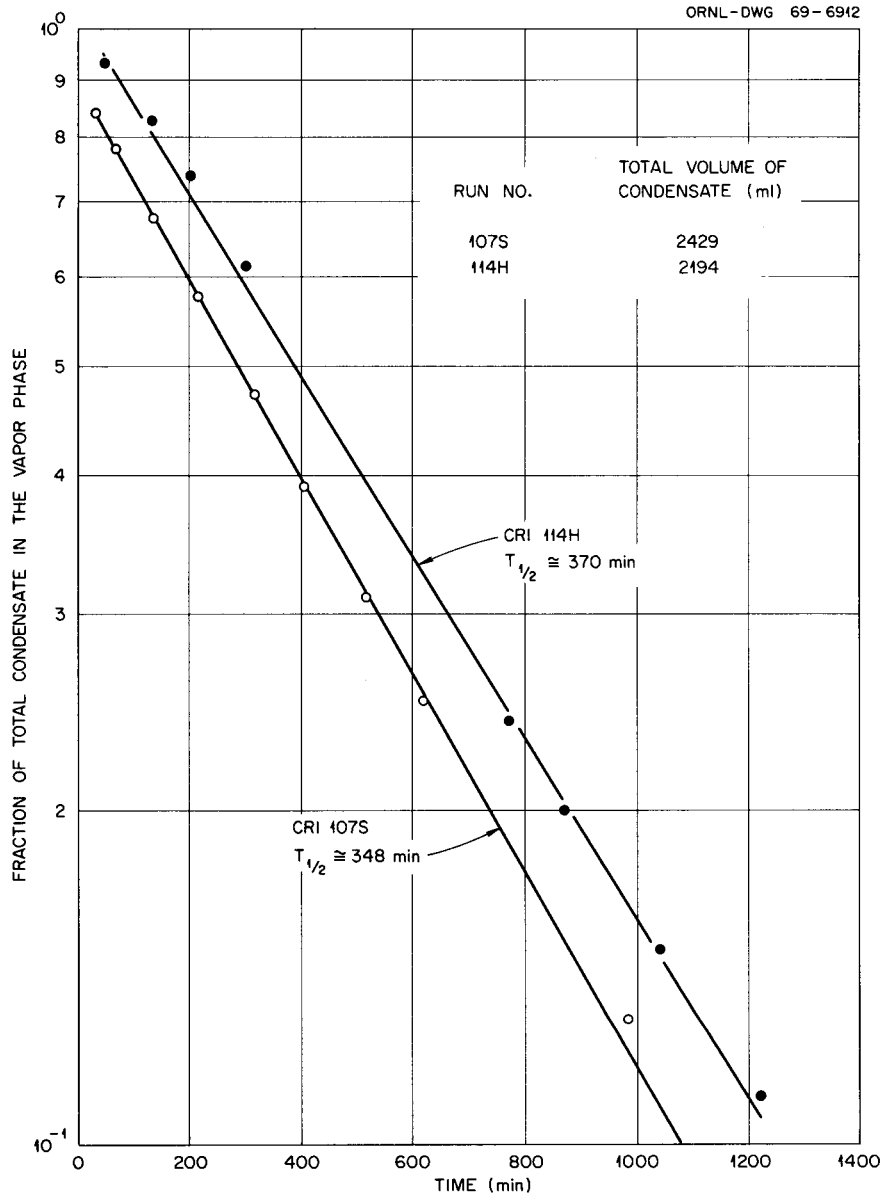


Fig. 3.5.3 Condensation Versus Time for CRI Runs 107S and 114H.

Table 3.5.1 Conditions for CSE Fission-Product
Simulant Validation Test 107S and Experiment
with Irradiated UO₂, 114H

	Run 107S CSE Simulant	Run 114H 6000 Mwd/T UO ₂
Atmosphere	air-steam	air-steam
Aging time, hr	20.6	20.2
Conditions in containment vessel at zero time		
Pressure, atm. abs.	3.3	3.6
Temperature, °C	110.5	111.0
Relative humidity, %	64	72
Conditions in containment vessel just prior to venting		
Pressure, atm. abs.	2.2	2.1
Temperature, °C	61.5	62.2
Relative humidity, %	100	100
Cladding on UO ₂ pellets	Zircaloy 2	Zircaloy 2

Table 3.5.2 Observed Release of Fission Products in CRI 107S and CRI 114H

	Percent of Total Inventory					
	In CRI Tank		Deposited in Transport Line		Total Release	
	CRI 107S	CRI 114H	CRI 107S	CRI 114H	CRI 107S	CRI 114H
Iodine	62.0	59.0	34.3	14.5	96.3	73.5
Tellurium	66.4	14.1	7.1	0.2	73.5	14.3
Cesium	47.3	20.1	9.9	0.8	57.2	20.9
Ruthenium	18.5	2.4	7.9	0.2	26.4	2.6

Table 3.5.3 Distribution of Activities in CSE Simulant and Irradiated UO₂
Run in the Containment Research Installation

	Iodine		Cesium		Ruthenium	
	CRI 107S	CRI 114H	CRI 107S	CRI 114H	CRI 107S	CRI 114H
Time in containment vessel, hr	20.6	20.2	20.6	20.2	20.6	20.2
<u>Activity, %</u>						
Tank washes and deposition coupons	84.0	84.3	62.0	72.0	91.3	86.1
Condensates	14.9	13.5	26.7	21.3	0.3	12.9
Total	98.9	97.8	88.7	93.3	91.6	99.0
<u>Airborne activity at end of aging period, %</u>						
Gas samples	0.05	0.11	0.86	1.0	1.7	0.63
Released by venting	0.55	0.77	4.4	2.4	6.3	0.002
Recovered by cyclic filtering	0.50	1.34	6.0	3.3	0.4	0.36
Total	1.1	2.2	11.3	6.7	8.4	1.0

activity in the containment vessel is listed, and the values are very close for the two runs. Figures 3.5.4 and 3.5.5 show the distribution of iodine activity with time in the containment vessel during the two runs and, as would be expected from the data in Table 3.5.3, the shape of the curves is similar for the two runs.

In Figs. 3.5.6 and 3.5.7, the distribution of airborne activities in the containment vessel during the runs is shown, and the iodine curves for the first 600 minutes are very much alike, however 107S shows a rise in airborne iodine activity shortly after about 600 minutes of the run, this rise is probably due to desorption of iodine activity from the containment vessel walls. On examining the temperature curve for 107S, as shown in Fig. 3.5.2, we find that the temperature of the containment vessel showed an unusual rise from the smooth decay at about this time, and this increase in the temperature of the walls could certainly cause a portion of the deposited iodine to desorb. Also in Figs. 3.5.6 and 3.5.7, we find a discrepancy in the half-lives for the straight line portions of the particulate activities (Ru, Te, and Cs). In the simulant Run 107S the average value for these activities is approximately 8 hours, while the average value for those listed for Cs and Te in Run 114H is approximately 5 hours. The difference in the half-lives for these activities in the two runs cannot be due to differences in condensation rates, since these rates were shown to be practically identical (Fig. 3.5.3).

Figures 3.5.8 and 3.5.9 show the concentration of iodine species in the containment vessel atmosphere with time for 107S and 114H, respectively. It should be noted that the shape of the curves for particulate, molecular, and organic iodine are very similar for about the first 600 minutes of the two runs. In Run 107S, the particulate iodine is the major portion of the iodine activity while the molecular iodine is the greater portion in Run 114H. The data for the

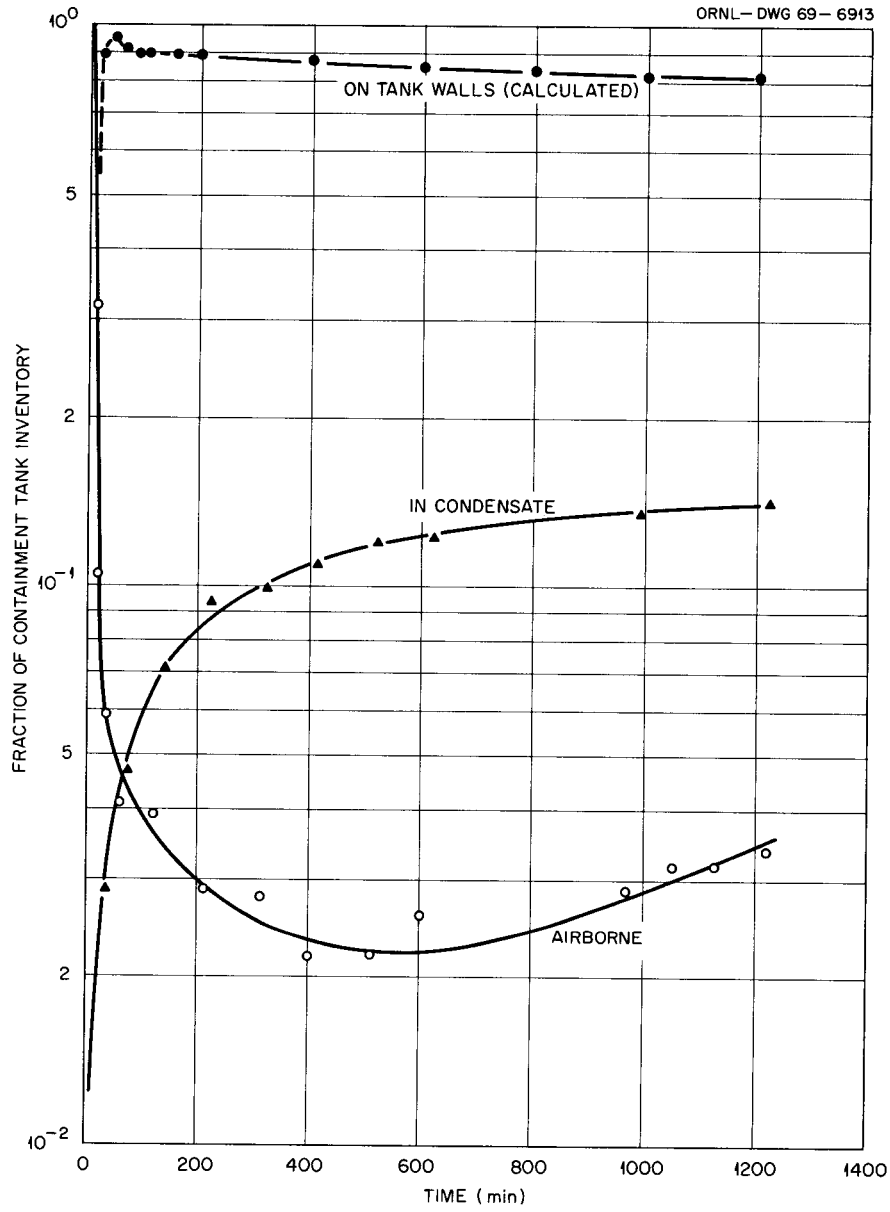


Fig. 3.5.4 Distribution of Iodine Activity in the Containment Vessel During Run CRI 107S.

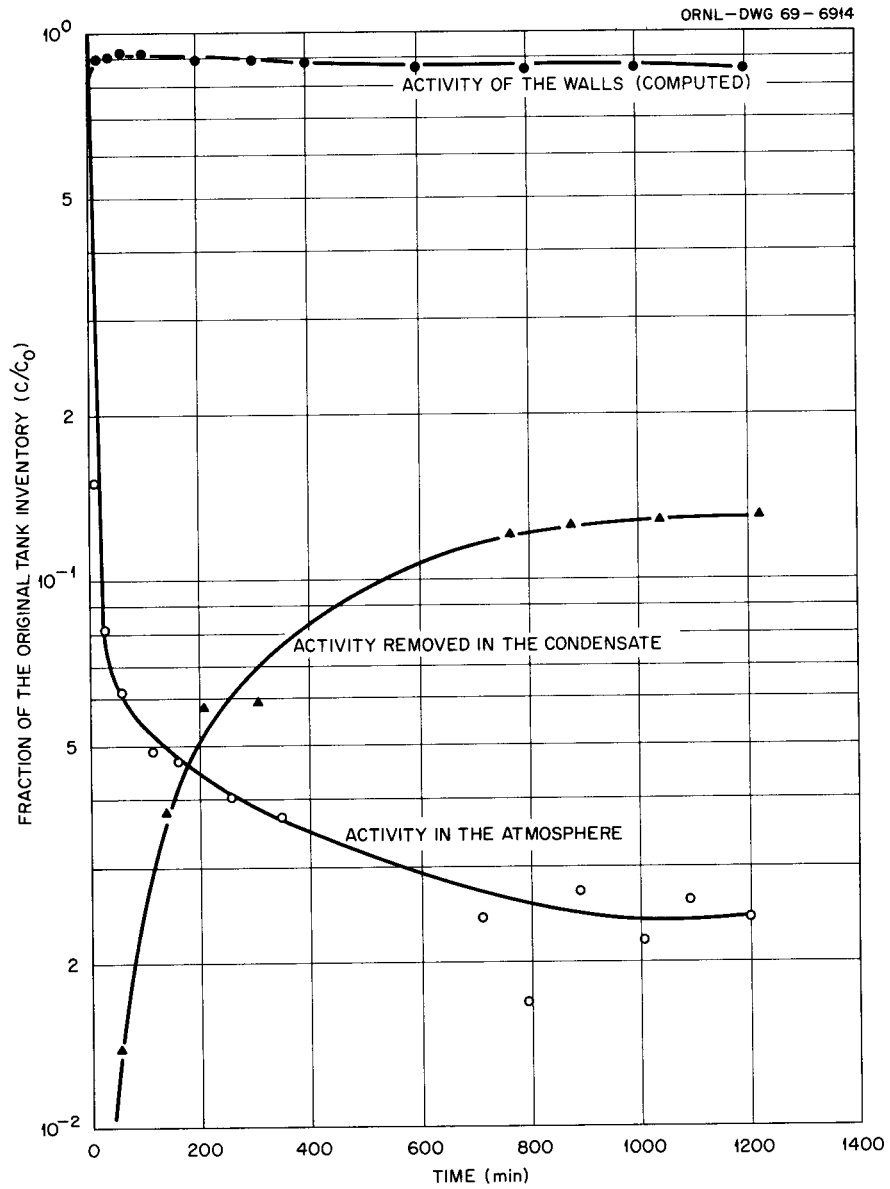


Fig. 3.5.5 Distribution of Iodine Activity in the Containment Vessel Run CRI 114H.

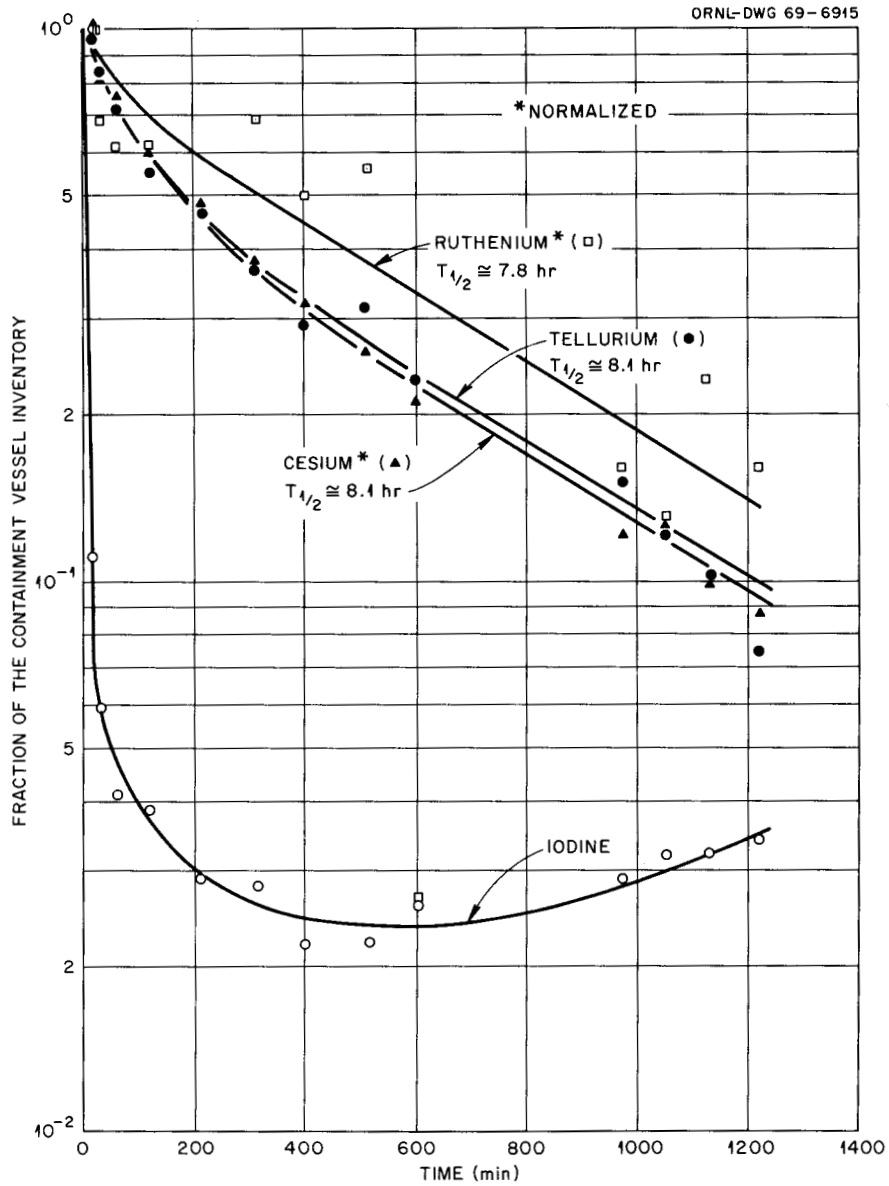


Fig. 3.5.6 Variation in Airborne Activity in the CRI Containment Vessel with Time During Run 107S.

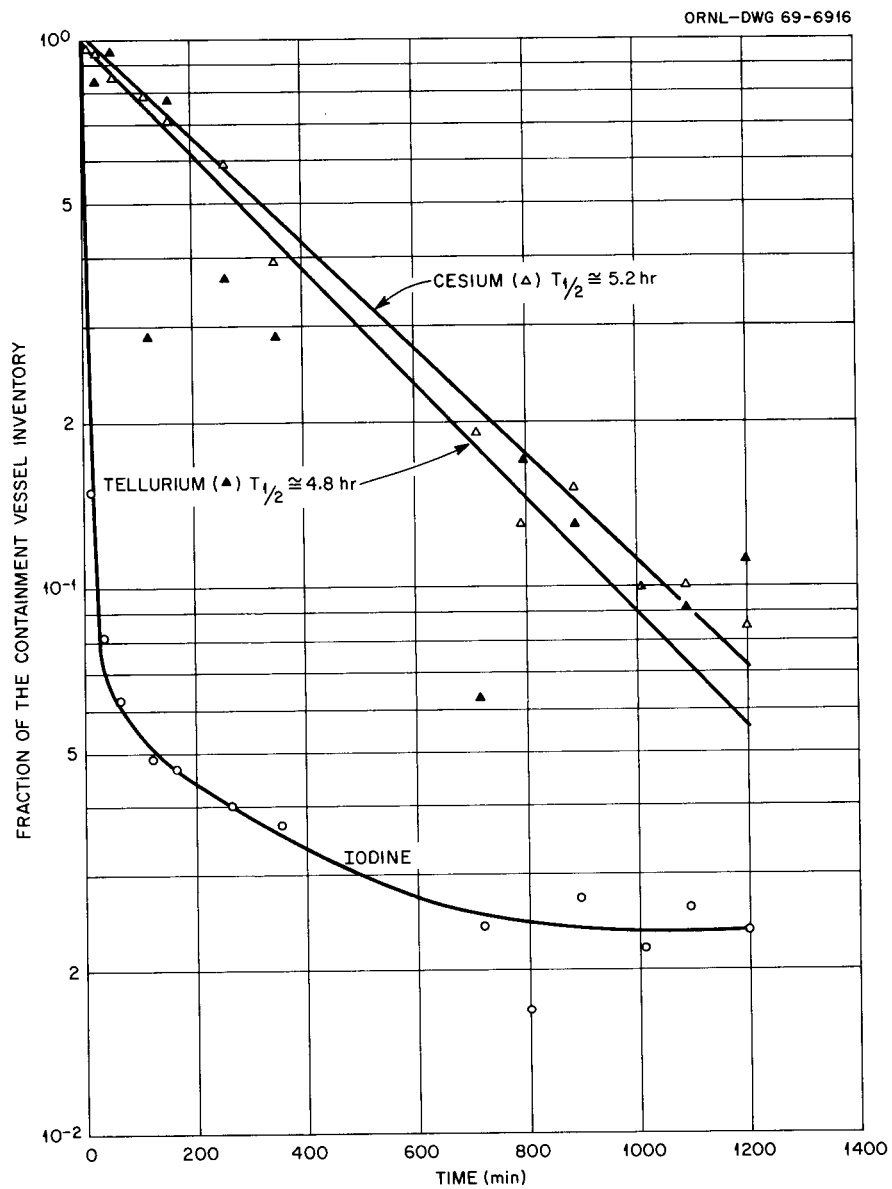


Fig. 3.5.7 Distribution of Activity in the Containment Tank With Time During Run 114H.

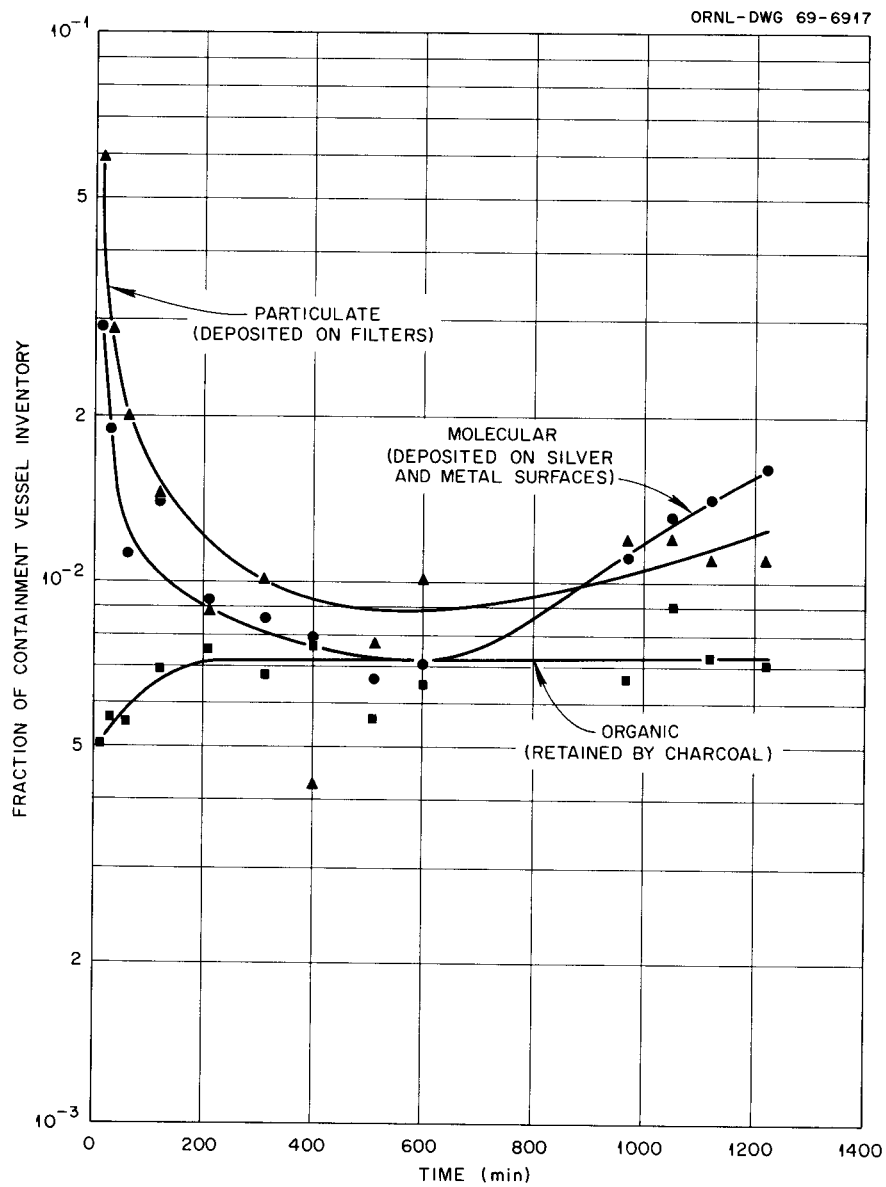


Fig. 3.5.8 Distribution of Iodine Species During CRI Experiment 107S.

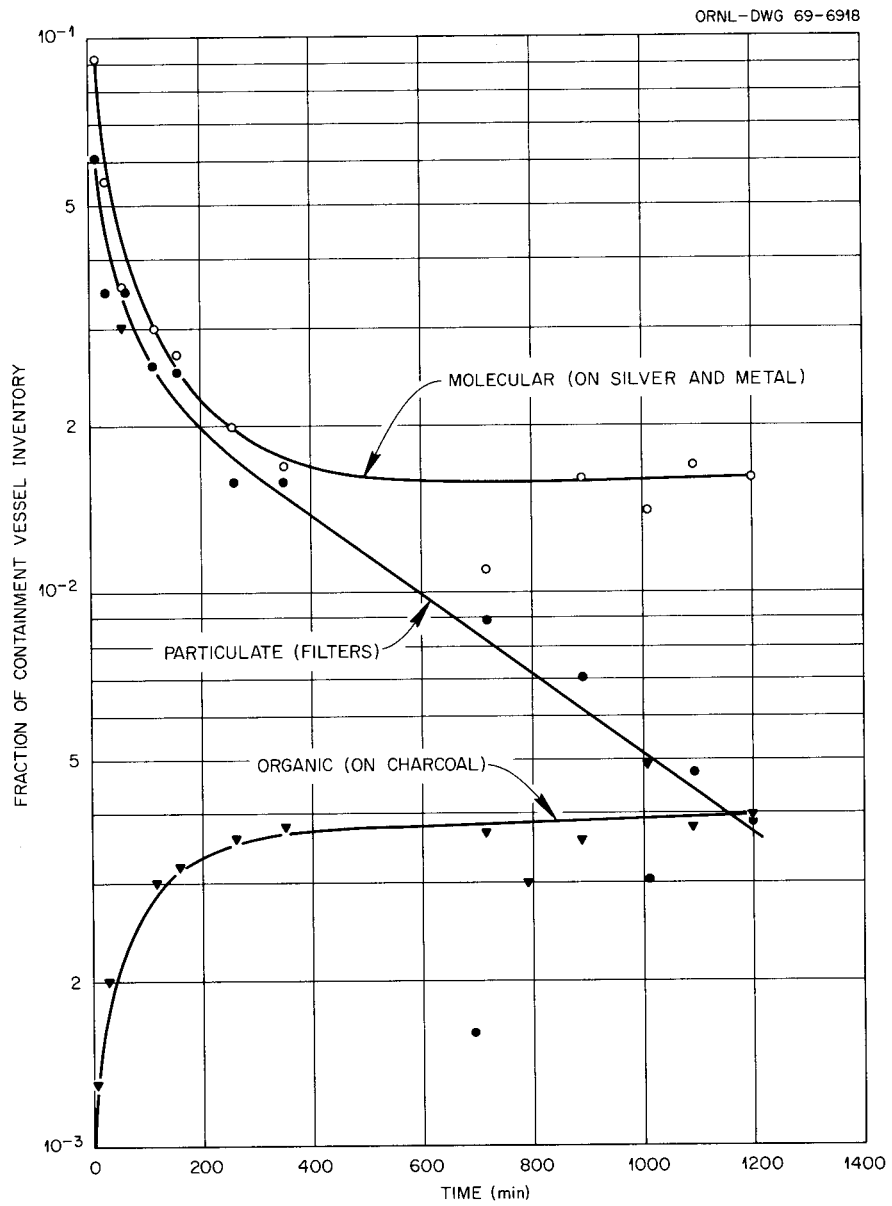


Fig. 3.5.9 Concentration of Iodine Species with Time in CRI Run 114H.

two graphs was derived from gas sample data using the common assumptions that iodine activity on filter components is particulate, on silver components and exposed metal surfaces is molecular, and that retained by charcoal is organic. In Run 107S the sampler components were arranged in the following sequence: filters, silver membranes, and then charcoal. In 114H gas samplers the arrangement was silver honeycomb or silver screens, filters, and charcoal. Since the filters in 107S samplers were not preceded by silver as were those in 114H, the higher values for particulate iodine in 107S could be due to the partial adsorption of molecular iodine by these filters.

The iodine activity retained on the charcoal portion of the gas samplers, as shown in Figs. 3.5.8 and 3.5.9, would indicate that organic forms of iodine account for 0.73% and 0.4% of the containment vessel inventory in Runs 107S and 114H, respectively. Using an elution technique that depends on the accepted fact that CH_3I can be eluted from charcoal with a flow of moisture saturated air, the CH_3I was found to be approximately 0.32% for 107S and 0.12% for 114H. These two values of 0.32% and 0.12%, while considerably lower in value than those found by charcoal retention (0.73% and 0.4%), indicate that the simulant run (107S) has about 3 times as much organic iodine as the "hot" run (114H).

3.6 Evaluation of CSE-Type Simulant

The simulant test results for the CSE vaporization process like those for the CMF pellet-additive method seem to give reasonably similar results to those obtained with irradiated fuel. There are perhaps more variations between our own individual simulant runs than between one of these and the most nearly identical hot run.

As a general conclusion, it should be stated that the effect which we thought might be observed, that of a non-homogeneous fuel composition and unrealistic release of the

aerosol to produce non-uniform settling rates for different aerosol solids was not observed.

It appears, from the experimental results, that regardless of source of aerosol (simulant or hot run) the characteristics of the resulting aerosol are such that the settling times during aging are not very different providing the environmental conditions are alike. For example, it seems that the results are more sensitive to variations in certain environmental parameters — such as rate of steam condensation — than to the origin of the aerosol, simulant or hot run. Accordingly, from the results obtained it appears that the use of simulant produces valid and realistic results.

4.0 CSE SIMULANT TESTS IN-PILE

4.1 Introduction

The in-pile testing of a proposed simulation technique is the only method of direct comparison between the behavior of real fission products and their simulated fission products analogs. Except for the method of generation (i.e. fissioning UO_2 vs vaporization) and radioactive decay, the simulated fission product aerosol and the true fission product aerosol experience, simultaneously, identical environmental conditions throughout the experimental system. In addition, the fission products and their analogs are collected simultaneously on each sampling device to eliminate discrepancies in sampling. Although basic aerosol parameters were not measured in this study, the relative behavior of the two types of aerosols is an important indication of their degree of similarity.

The method of simulation that we have investigated is that developed for the Containment Systems Experiment (CSE) at Hanford. Their method of aerosol generation is the volatilization of several selected elements (I, Cs, Ru, and Te) individually, then mixing these vapors with those produced from UO_2 in a R.F. induction furnace. The resulting aerosol is then passed through relatively long lines into their containment vessel. In this study we have tried to duplicate as closely as possible the CSE method of simulant vaporization within the restrictions imposed by an in-pile experiment. The main differences in our method of simulation and that of the CSE was in the length of line between the vaporization section and the UO_2 , the method of heating the UO_2 (i.e., fission heat vs R.F. induction heating) and the presence of real fission products accompanied by their radioactive environment.

Two experiments were designed to evaluate the degree of similarity between the CSE simulation technique and real fission products. The first experiment employed a fuel element that had been irradiated to a fairly high burnup and no simulants. The second experiment contained simulants and fresh fuel. The mass of material to be transported in both experiments was approximately equal. Trace irradiation of the fuel was performed before meltdown in both experiments. The detection of a simulated fission product in the presence of real fission products was accomplished by neutron activation of the stable simulant nuclides. It was felt, therefore, that we could evaluate the behavior of real and simulated fission products in these two experiments and detect any possible irregularities during the second experiment by comparing the results of the simulants and fission products from the trace irradiation directly.

4.2 Experimental Facilities

The simulant fission product generator was patterned after the one designed for the CSE experiments in that each isotope was individually vaporized. In addition, the iodine was generated in a separate chamber and mixed with the other simulants before being passed over the molten UO_2 . The simulant generator is shown in figure 4.2.1.

The main chamber consisted of platinum resistance wire in an alumina support. The simulants were placed in individual platinum mesh baskets which were tack welded to a platinum sheathed thermocouple. The simulants in this chamber were ruthenium as (99.7%) Ru metal, tellurium as (97% ^{127}Te) TeO_2 and cesium as (100% ^{133}Cs) CsHC_2O_4 . Cesium bioxalate was used as suggested by CSE personnel¹⁵ in that it is non-hygroscopic and decomposes at fairly low temperatures to cesium oxide. This chamber attained a temperature in excess of 1300°C for four minutes and then was pushed to

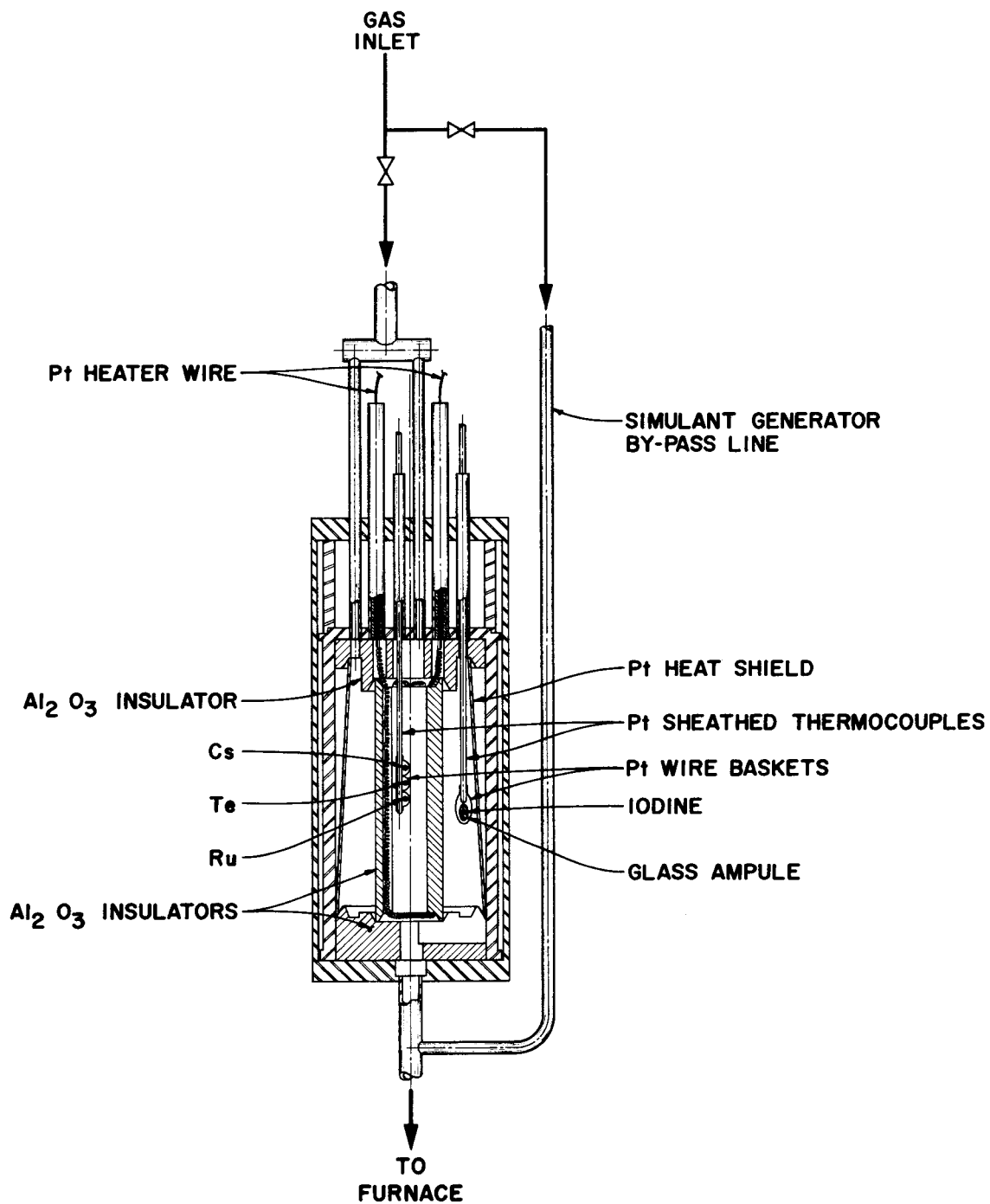


Fig. 4.2.1 In-Pile Simulant Generator.

over 1500°C before the heating element burned out.

The iodine chamber was located directly outside the alumina support and was heated by convection and radiation from the main chamber. The iodine simulant as (100% ^{127}I) elemental iodine was sealed in a glass ampoule was broken by internal pressure as the temperature of this chamber increased to approximately 600°C during steady operation and 800°C before the heaters burned out.

Prior to fuel meltdown and during heatup of the generator, the sweep gas completely bypassed the generator. During the meltdown however, the gas entering the generator was split approximately 60% to the main chamber and 40% to the iodine chamber. These gas streams were recombined at the exit of the simulant furnace and then passed down to the fuel section. The simulant generator was located sufficiently distant from the reactor core during pre-meltdown irradiation to prevent significant activation of the simulants during this period.

The fuel for these experiments consisted of pressed UO_2 pellets one inch long by 0.21 inches in diameter. The original enrichment for the high burnup experiment was 10.24% and it was 6.49% for the trace irradiated experiment. In both experiments the fuel pellets were encapsulated in Zircaloy 4 tubing. The in-pile UO_2 furnace is shown in Fig. 4.2.2 This furnace consisted of the encapsulated fuel surrounded by a high density thoria cylinder and sat in a thoria pedestal. The thoria in turn was surrounded by a zirconia insulator. The sweep gas was admitted to the furnace area below the fuel. It passed over the fuel and out the top of the furnace through a thoria end-cap.

The aging chamber, Fig. 4.2.3 is an instrumented 55-gal (208 l) stainless steel drum that can be heated and maintained at temperatures in excess of 100°C. This chamber has facilities for withdrawing aqueous samples and for sampling airborne constituents during the post-meltdown period.

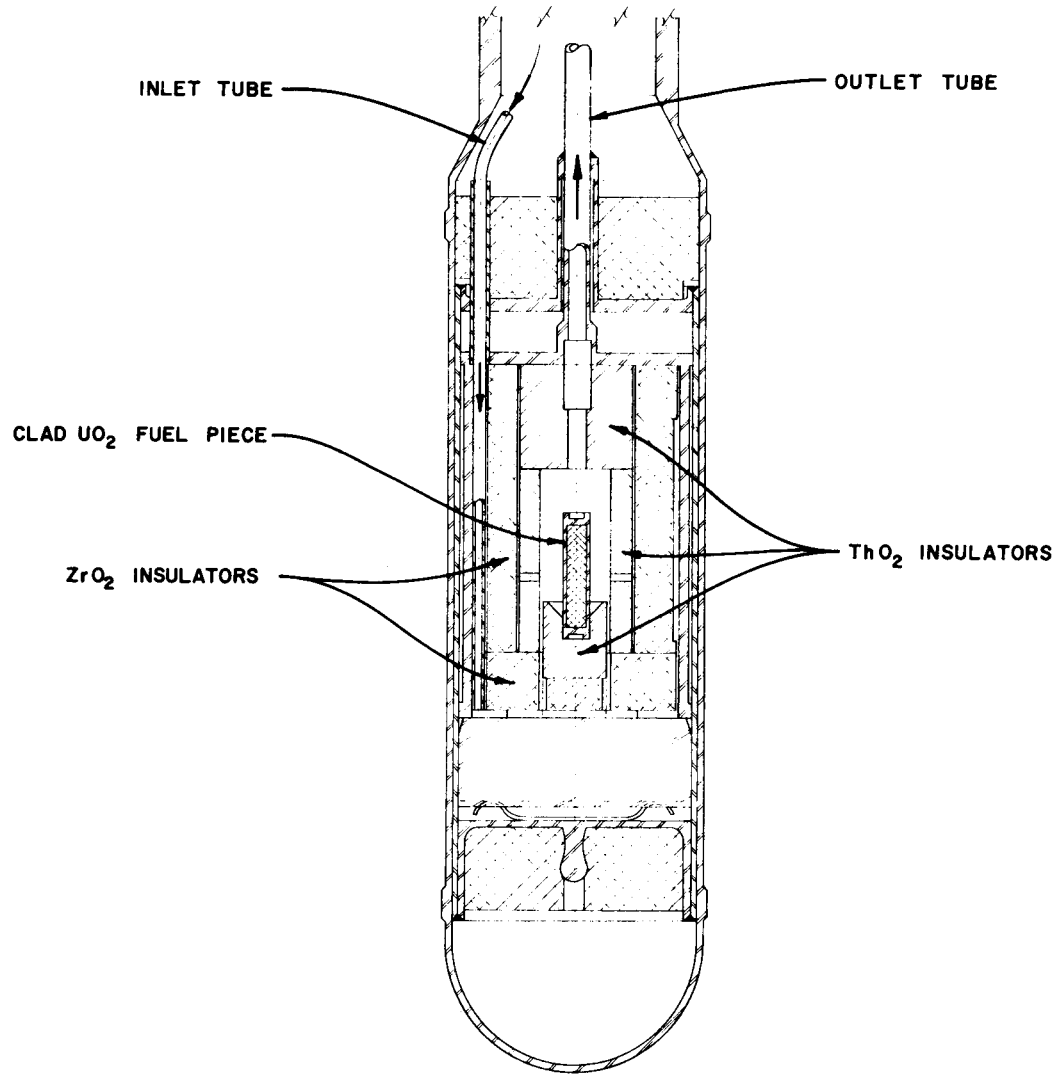


Fig. 4.2.2 Furnace for In-Pile Melting of UO₂.

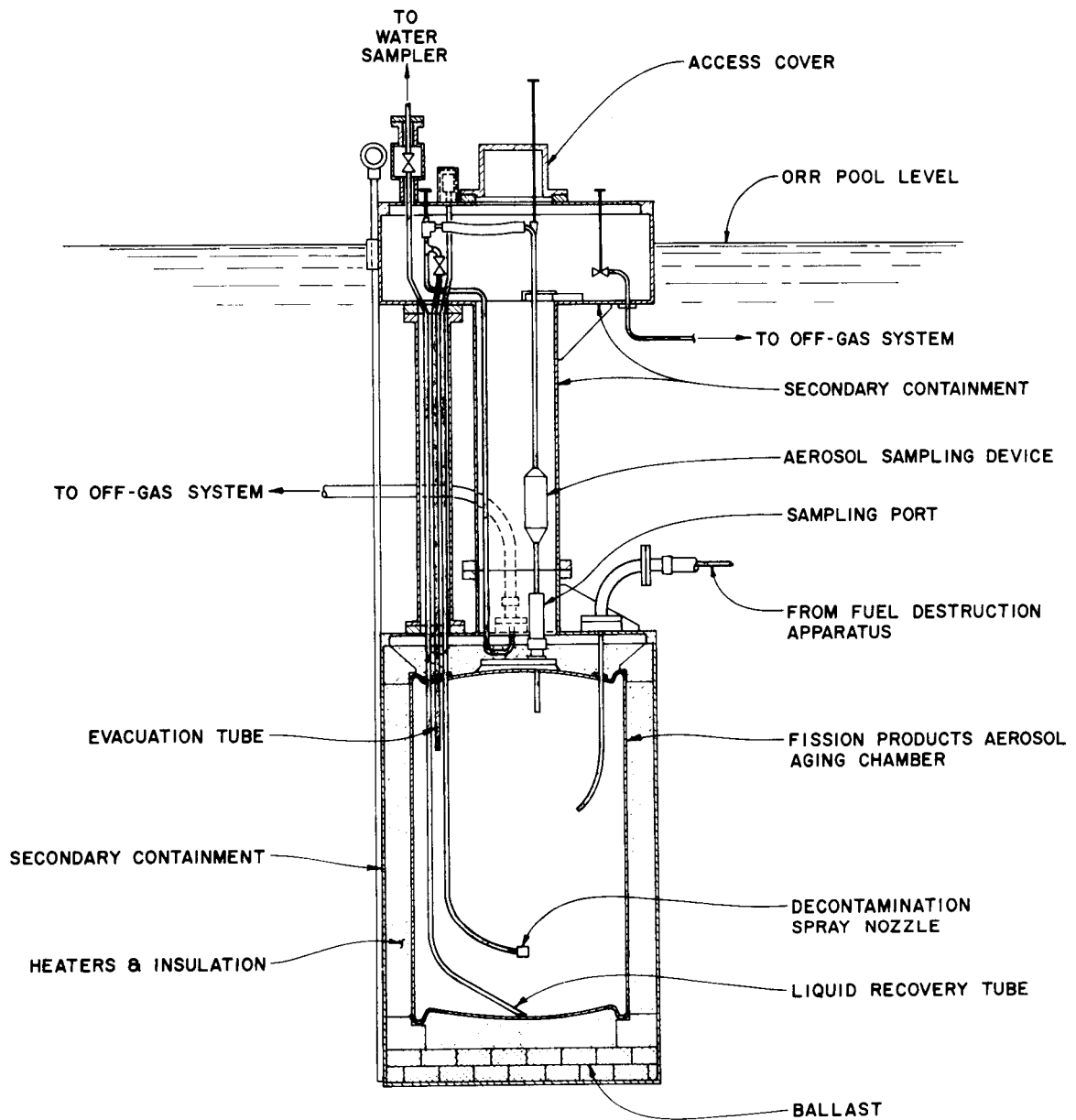


Fig. 4.2.3 Aging Vessel for Fission Product Aerosols.

4.3 Experimental Procedure

The experimental procedures for the two experiments were essentially the same, except for the absence of the simulant generator in the high burnup run. As discussed previously, the reason for these two experiments was to compare the transport and aging behavior of roughly similar amounts of material. Table 4.3.1 shows the amounts of fission product or simulant present before trace irradiation in these two experiments.

Table 4.3.1 Amounts of Fission Products or Simulants Present Prior to Fuel Meltdown^a

Element ^b	High Burnup Experiment	Simulant Experiment
Iodine	0.62 mg	8.1 mg
Cesium	9.87 mg	40.3 mg
Ruthenium	4.63 mg	25.0 mg
Tellurium	1.36 mg	17.8 mg

^aDoes not include fission products produced prior to or during fuel meltdown.

^bHigh Burnup Experiment: $^{127,129}\text{I}$, 133,135 , ^{137}Cs , $^{101,102,103,104,106}\text{Ru}$, and 125,126,127,128 , ^{130}Te .

Simulant Experiment: ^{127}I , ^{133}Cs , ^{104}Ru , and ^{126}Te .

The excess amounts of simulant elements were deemed necessary in order to provide for mass losses up to the fuel furnace and to increase the chances of their detectability by activation analysis in the presence of fission products. Trace irradiation prior to each meltdown was performed in order to provide sufficient identical fission products in

both experiments for radiochemical analysis. The amounts of fission products produced during trace irradiation and meltdown were identical in both cases.

Prior to fuel meltdown, the aging vessel was equilibrated at 80°C with a pool of water on the bottom of the vessel several degrees warmer in order to provide a condensing steam environment. These conditions were chosen to emulate the CSE conditions at Hanford.

Figure 4.3.1 is a schematic diagram of the operating system for these experiments. The air atmosphere passed through the simulant-generator, over the molten fuel, and then the stream was split, part to the hood sampler (10%) and the rest into the aging vessel. The hood aerosol sampler is indicative of the initial distribution of species entering the aging vessel. Seven aerosol samples and fourteen water samples were obtained during the twelve hour aging period after each meltdown.

The water samples were taken by sequential valving of evacuated bottles connected to a tube that dipped into the pool of water on the bottom of the vessel. Samples of the vessel atmosphere were obtained by inserting the entrance tube of the aerosol sampler through a ball valve directly into the aging vessel. The entrance tube was analyzed together with the rest of the sampler and eliminated problems associated with manifolded systems. The aerosol sampling devices were of the honeycomb design, Fig. 4.3.2. Bennett, Hinds, and Adams⁷ have shown that this sampler adequately distinguishes between molecular and particulate forms of iodine. These samplers were electrically heated to 100°C to prevent condensation of water vapor during the sampling period. The sampler itself consisted of the entrance tube and a silver plated aluminum honeycomb section for deposition of molecular species. Then an absolute filter section to trap out particulate associated species and, finally, two charcoal beds to trap out organic iodides.

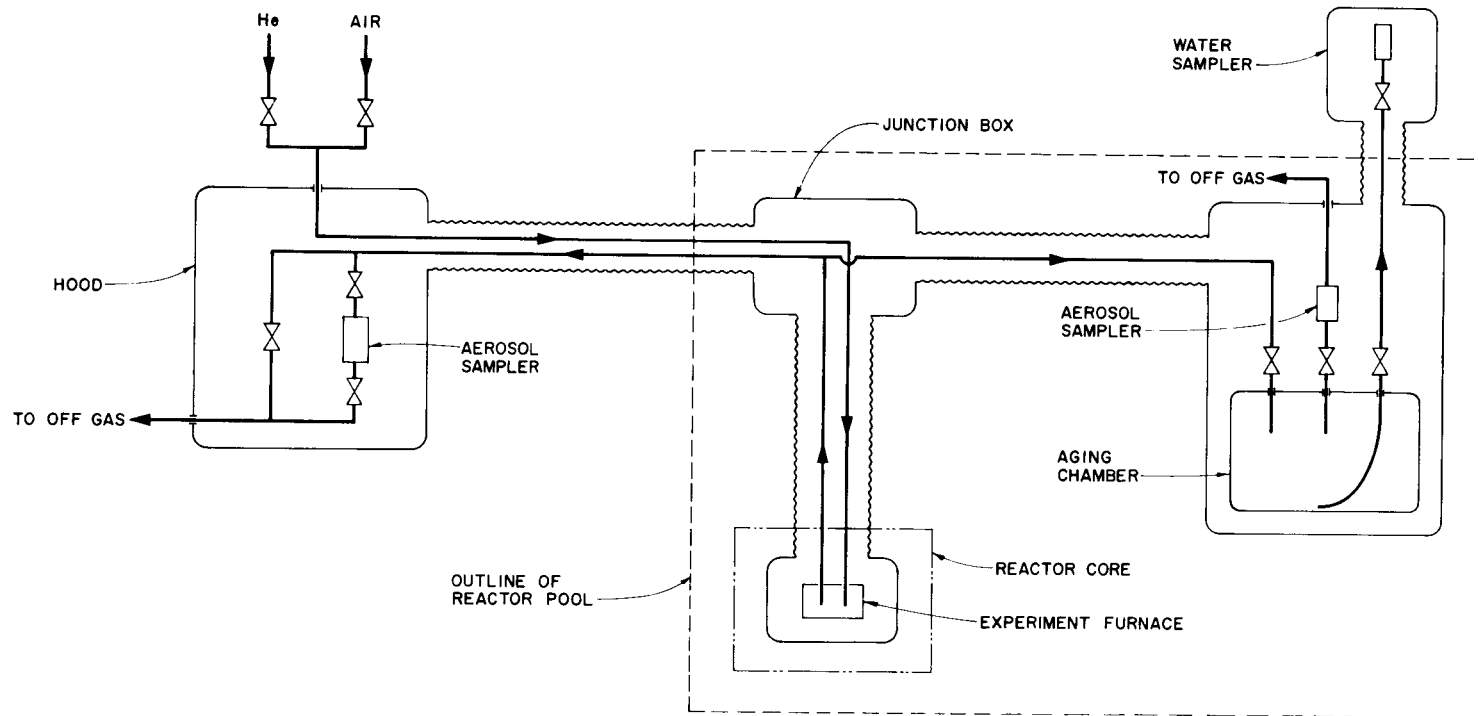


Fig. 4.3.1 Flow Diagram for In-Pile Fuel Melting Program.

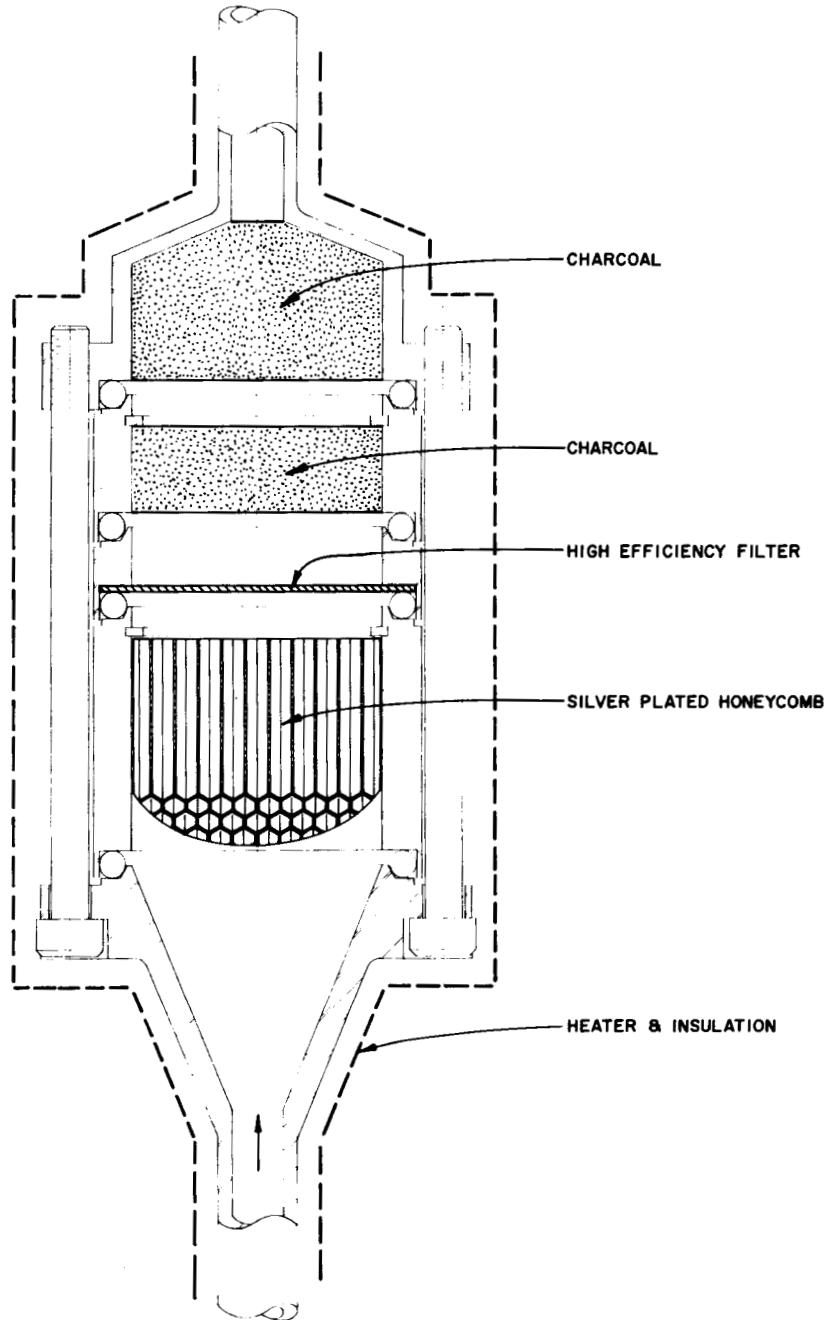


Fig. 4.3.2 Heated Honeycomb Sampler.

The complete rig was disassembled in the hot cells. All transfer lines and components were sent for fission product and simulant analysis. In both experiments the fission products were assayed by γ -stripping techniques. Analysis of the simulant experiment was more complex. Initially all samples were leached and then analyzed for fission products by γ -analysis. After suitable decay time, aliquots of the leach solutions were analyzed for the simulant concentrations by neutron activation.

4.4 Experimental Results

Due to problems in the analytical determination of the simulants Cs, Ru, and Te, we can only report on the relationship between the real and simulant iodine aerosols. Table 4.4.1 shows the distribution of all iodine species at various locations in the experimental rig. The values shown for the real fission products are the percent of theoretical, based on the flux-time history, while that shown for the simulant iodine is the percent of the initial iodine loading corrected for plateout prior to the UO₂ furnace.

Table 4.4.1 Fission Product and Simulant Iodine Distribution

Experimental Section	High Burnup Experiment	Comparison Experiment	
		Fission Product	Simulant
UO ₂ fuel furnace	34 ^a	9 ^a	5 ^b
Transfer lines	24	20	17
Aging Chamber	10	64	73
Hood Sampler	28	18	5
Total	96	111	100

^aPercent of theoretical.

^bPercent of initial loading corrected for plateout prior to UO₂ furnace.

It is apparent that there is a greater disparity between the real fission product iodine distributions in the high burnup and comparison experiments than between the simulants and real fission products in the same experiment. These results show the necessity for evaluating a simulation technique simultaneously with a real meltdown. Except for the percents remaining in the fuel furnace, the discrepancies between experiments can be ascribed to experimental variations. The small differences in plateout between the two experiments are probably due to the existence of two cold sections in the high burnup experiments transfer lines. The disparity between the relative amounts going to the hood samplers in the two experiments was due to a valving problem we had on the high burnup experiment. We cannot, however, reconcile the differences in the percents of real fission product iodine remaining in the fuel area between these two experiments in that they were operated in an identical manner.

On the other hand, differences between real and simulant fission product iodine can only be due to inherent differences in their aerosol characteristics. That only half the percentage of simulant iodine compared to real fission product iodine remained in the fuel furnace area is certainly attributable to the fact that the simulant iodine totally passed over the molten UO_2 while most of the fission product iodine had to diffuse from the molten mass. However, the reason that the ratio between the amounts that went to the aging chamber and the hood sampler is so different for the simulants (15:1) and the real fission product (4:1) iodine must be due to the overall makeup of their respective aerosols. The hood sampler was taken in order that we might assess the initial distribution of the iodine species entering the aging chamber. Table 4.4.2 shows the distribution of the hood sampler according to the hypothesized species. The values shown are percents of the total iodine loading in the sampler.

Table 4.4.2 Iodine Specie Distribution in Hood Sampler

Specie	High Burnup	Comparison Experiment	
		Fission Product	Simulant
Molecular	2	48	66
Particulate	96	49	32
Organic	2	3	2

Certainly part of the explanation for the overwhelming percent of particulate associated iodine in the high burnup experiment must be due to the presence of the two cold sections, one of which was at the entrance to the hood sampler. The data in Table 4.4.2 indicate that there is a difference in the forms of the iodine species between real and simulant fission product aerosols. The difference in the ratio of the molecular to particulate associated iodine forms for the real fission product iodine (1:1) and simulant iodine (2:1) again is probable attributable to the residence time of the iodine in intimate contact with the molten UO_2 . It is interesting to note that Hilliard, Coleman, and McCormack² found, on the average, the same relative distribution of molecular and particulate associated species between irradiated and simulant tests in the ADF.

The most critical evaluation of the forms of the simulant and real fission product aerosols would have been their behavior in the aging vessel. Unfortunately, even with fairly high sensitivity for iodine detection, the amounts of simulant iodine on the various components of the honeycomb samplers were below the limits of detection. We are currently trying another approach to improve these detection limits and get some useful data in this area. Since the in-pile testing was performed to evaluate the CSE method, we have analyzed the available fission product data to see how

it compares with the results obtained at Hanford. Figures 4.4.1 and 4.4.2 show the airborne fission product iodine distributions during the 12-hour aging period for the high burnup and comparison experiments. Figure 4.4.3 is a composite of certain non-volatile fission product aerosols from both experiments. System parameters for our set of experiments and the Hanford experiments² were the same except for total pressure, steam flux, surface to volume ratio of the containment chambers, and a high radiation environment. The first three are explicit parameters in all theoretical treatments of containment behavior and should provide a good test of the CSE developed theory.¹⁶ The main difference, therefore, between the in-pile tests and those at Hanford was the presence of a real fission product aerosol.

According to the CSE theory the gas phase molecular iodine concentration should be of the form:

$$\frac{C_g}{C_o} = \left[1 - \frac{K_c HV}{(K_c + K_s)L} \right] e^{-\frac{A}{V} (K_c + K_s)t} + \frac{K_c HV}{(K_c + K_s)L} e^{-\left(\frac{W_s}{\rho_L} + \frac{K_f A}{L}\right)t}$$

where C_g = the gas phase concentration at time t

C_o = the initial gas phase concentration

K_c = gas phase mass transfer coefficient due to concentration gradient, cm/sec

K_s = mass transfer coefficient due to condensing steam flux, cm/sec

H = gas liquid equilibrium coefficient

V = total volume of contained gas phase cm^3

L = liquid holdup in vessel cm^3

M_1 = final slope = $\frac{W_s}{\rho_L L} + \frac{K_f A}{L}$

M_2 = initial slope = $(K_c + K_s)(A/V)$

A = internal surface area of containment

(continued)

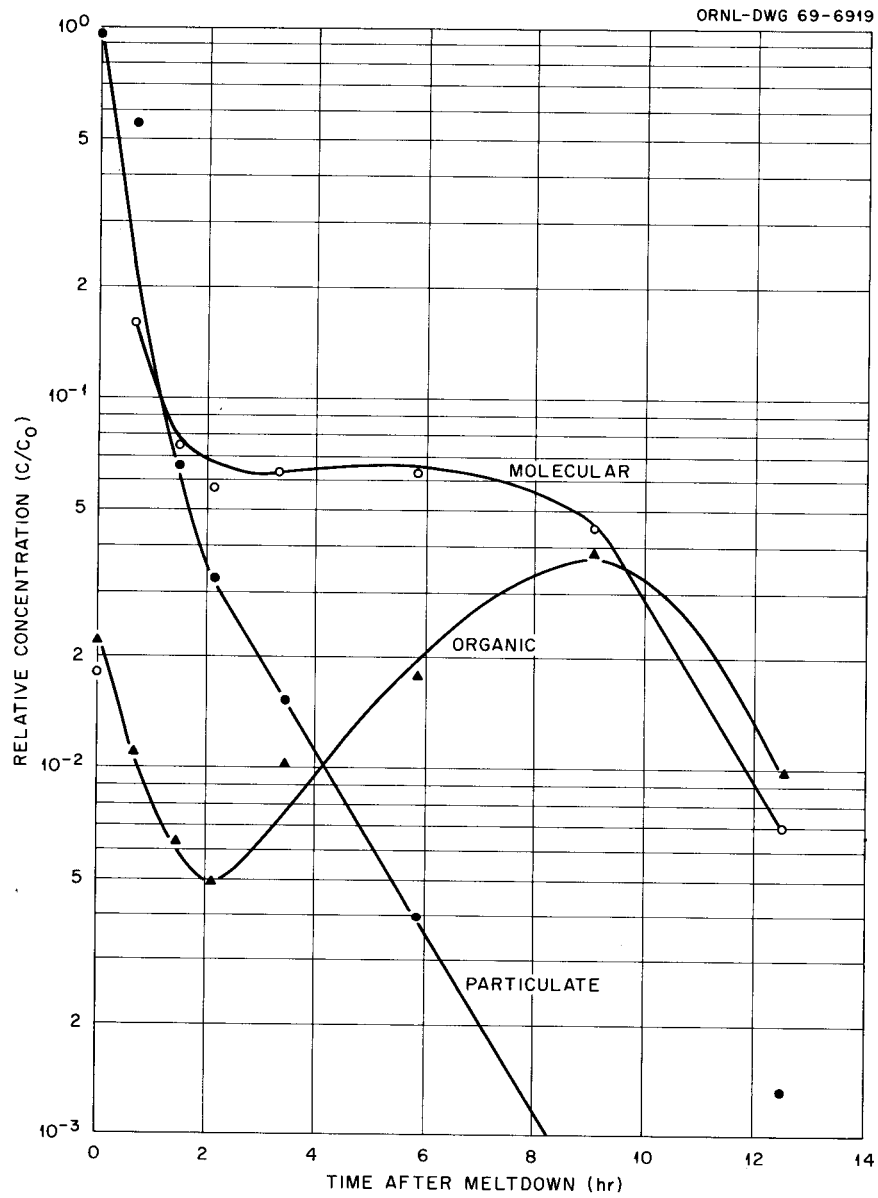


Fig. 4.4.1 Behavior of Airborne Fission Product Iodine (High Burnup Experiment).

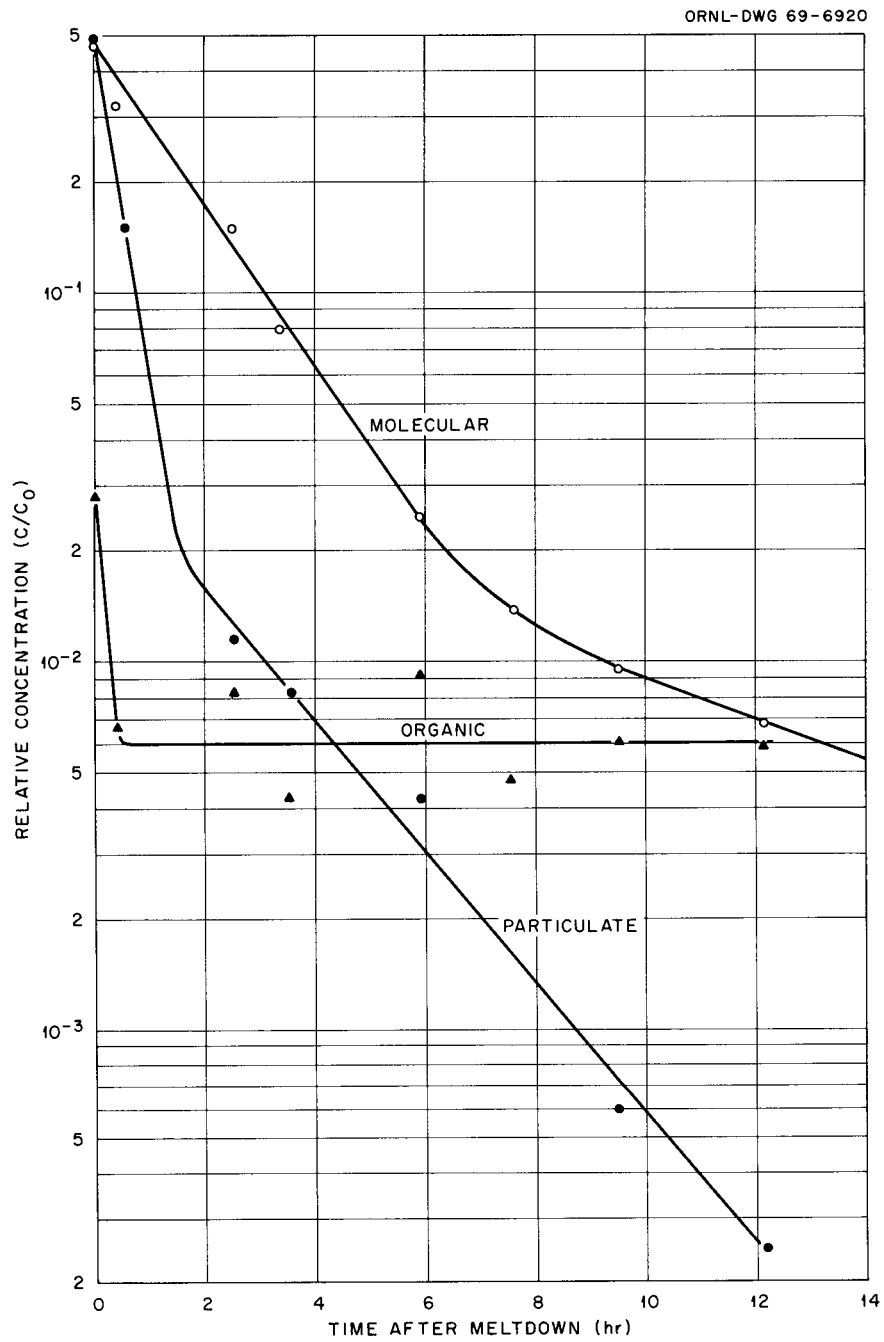


Fig. 4.4.2 Aging Behavior of Airborne Fission Product Iodine (Comparison Experiment).

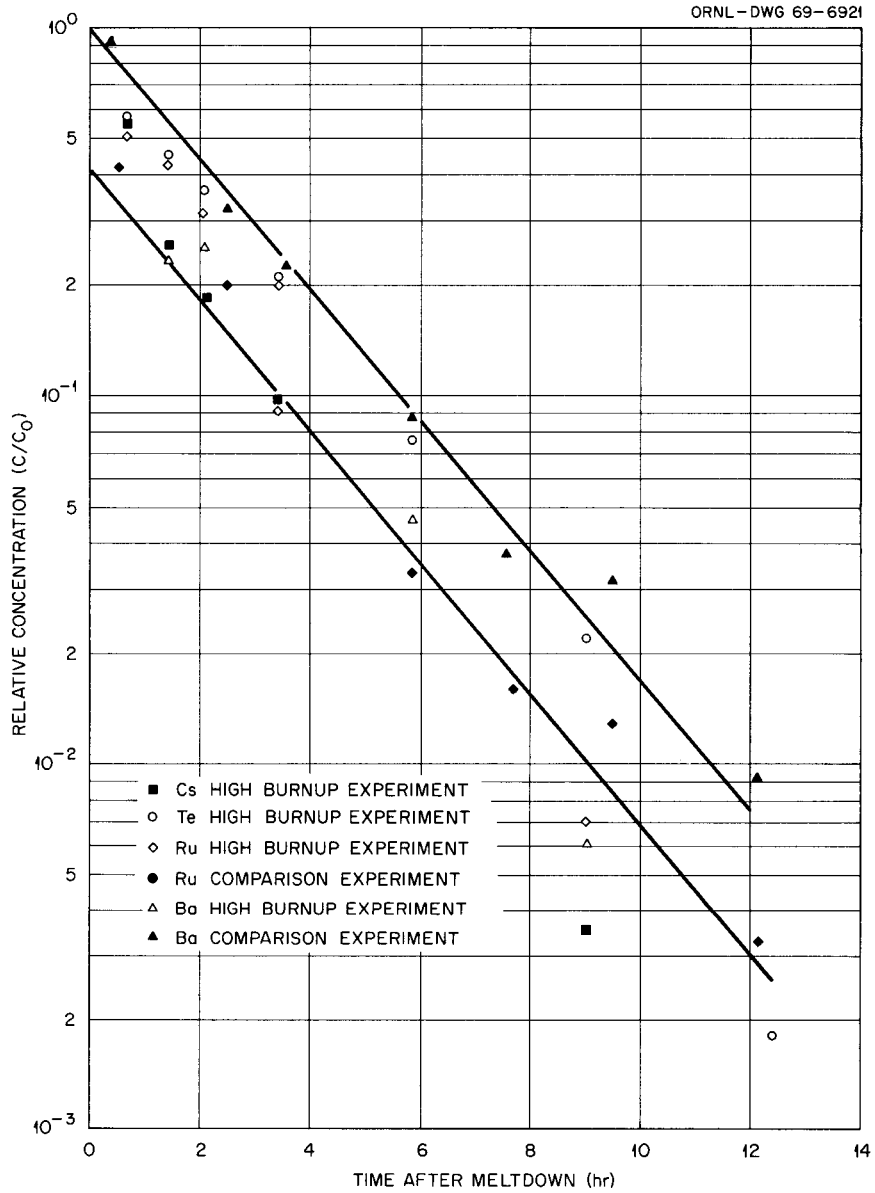


Fig. 4.4.3 Aging Behavior of Particulate Airborne Fission Products.

W_s = steam rate g/sec

ρ_L = density of liquid

K_f = forward reaction rate constant, cm/sec.

We have tried to fit this equation to the data from the comparison experiment only. Again, unfortunately, the high burnup experiment was plagued by heater troubles in the aging vessel and the shape of that curve is not applicable to rigorous interpretation.

Although the mathematical form of the theoretical equation suggest two simultaneously occurring exponential processes, the physics of the situation demands that the phenomenon that lead to the first and second terms are distinct in time. We have fitted our data to two equations. A) the initial period where the decrease in gasborne concentration is gas phase limited:

$$\left(\frac{C_g}{C_o}\right)_{\text{initial}} = f_p e^{-\frac{A}{V} (K_c + K_s)t}$$

where f_p is the fraction of total iodine entering the aging vessel in the molecular form. B) And the final period where the gas-liquid equilibrium has been established and the decrease in gas phase concentration is due to dilution by steam and reaction with the walls.

$$\left(\frac{C_g}{C_o}\right)_{\text{final}} = \frac{K_c HV}{(K_c + K_s)L} e^{-\left(\frac{W_s}{\rho_L L} + \frac{K_f A}{L}\right)t}$$

The final period slope has only one undetermined parameter, K_f . Hilliard¹⁶ suggests a value of 2.5×10^{-6} cm/sec (3×10^{-4} ft/hr) for K_f . Using this value and the known steam rate, liquid volume, density, and surface area, we predict a half-life of 5.4 hours. Experimentally we found 5.3 hours which is fortuitous since in our case it is iodine being fixed on stainless steel, while in the CSE it is iodine on a painted surface. For the initial period again we have only one unspecified parameter, K_c . This parameter, in

principle, can be calculated from the hydrodynamics within the vessel. We predicted a value of 9×10^{-2} cm/sec for K_c and find experimentally a value of 6×10^{-4} cm/sec. This overall initial reduction rate for the gas phase molecular iodine concentration is slower than theoretically anticipated due to a positive contribution from iodine desorbing from the particles and probably also to an incorrect formulation of K_c for our very small tank where the boundary layer is mostly laminar and perhaps fairly thick. Evidence for the desorption of iodine from the particles is evidenced by the particulate curve of Fig. 4.4.2 where there is an initial rapid decrease in concentration leveling off to a slope equal to those shown in Fig. 4.4.3. It appears then that the apparent initial decrease in particulate associated iodine is due to washout by the steam and desorption of some of the iodine.

The value of H , the iodine partition coefficient, that satisfies the intercept in the final portion of molecular iodine curve is 6.6×10^{-4} which is within the range of expected values.

Figures 4.4.4 and 4.4.5 show the iodine concentration in the liquid pool during the aging period. If the formalism is correct, the iodine concentration in the liquid should mirror the decrease in gas phase concentration. Due to the problem in the high burnup experiment the solid curve is not based on any model. However, in Fig. 4.10 the solid line is given by:

$$\frac{C_L}{C_0} = 1 - e^{-\frac{A}{V} (K_c + K_s)t}$$

The fit is very good.

4.5 Evaluation

The results of the in-pile experiments suggest that the mechanisms controlling the transport and deposition of either

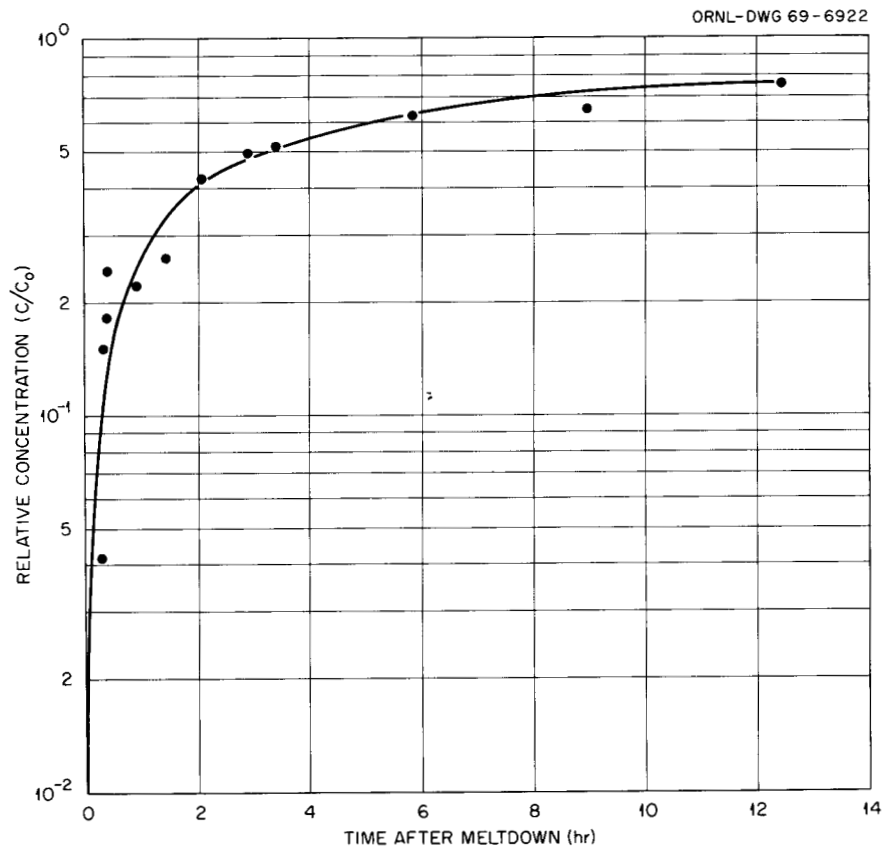


Fig. 4.4.4 Behavior of Condensate Iodine (High Burnup Experiment).

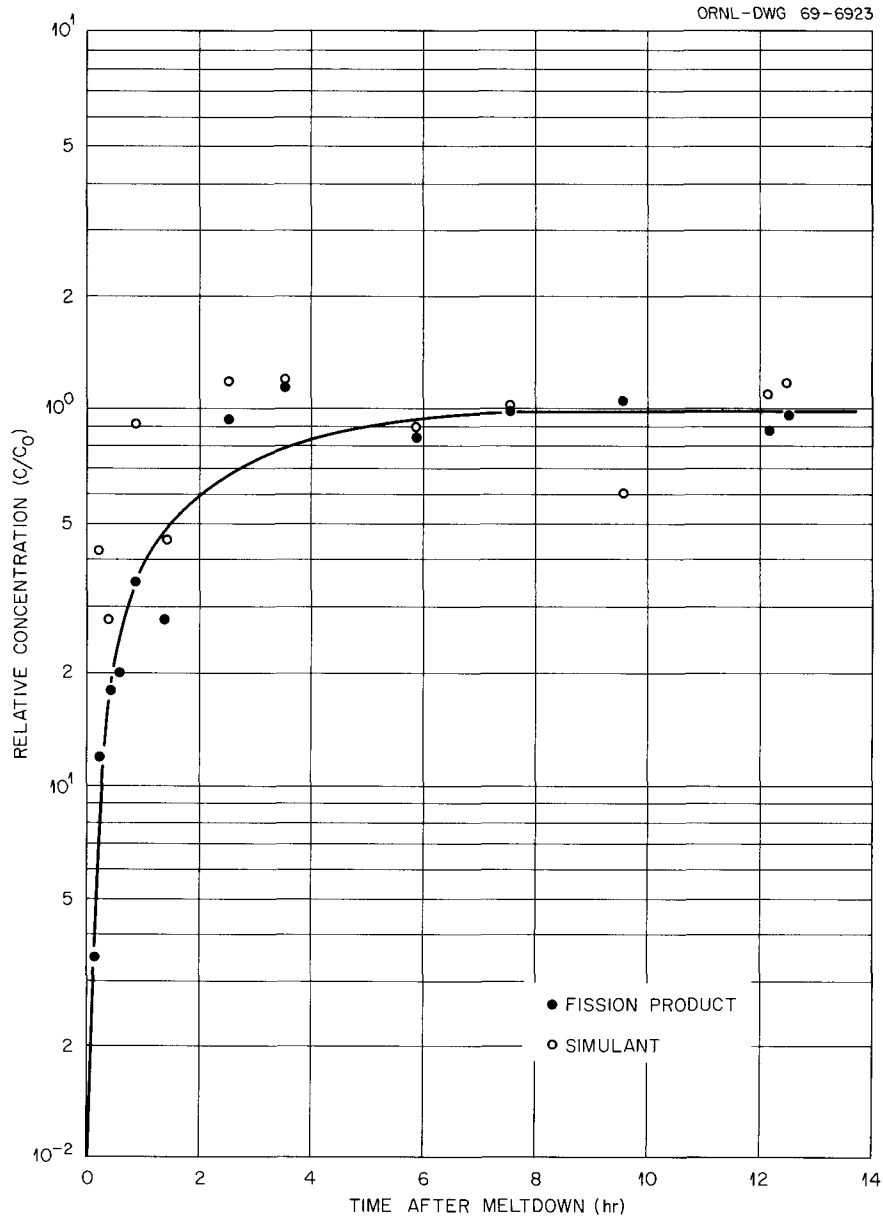


Fig. 4.4.5 Behavior of Condensate Iodine Comparison Experiment and Fission Product Simulant.

real or simulated fission products is governed more by the conditions of the experiment than by the characteristics of the aerosol. The results of these experiments and those at Hanford indicate that while there may be differences between real and simulated fission product aerosols, these do not appear to be significant in the light of the large variations encountered in experiments of the size and complexity as the in-pile meltdown experiments.

5.0 MEASUREMENT OF AEROSOLS WITH PORTABLE SAMPLER

5.1 Introduction

A portable device was designed for sampling in facilities using various methods of fission-product aerosol simulation. The use of this sampler in the various facilities allows a direct comparison of the aerosol form and concentration. The sampler has been used in experiments at ORNL in the Containment Mockup Facility (CMF), Containment Research Installation (CRI), and at Battelle Northwest Laboratory in the Stainless Steel Tank (SAT) associated with the Containment Systems Experiment (CSE). Some of the sampler components have been used in experiments at the Nuclear Safety Pilot Plant (NSPP) at ORNL.

5.2 Description of Sampler

The design of the sampler was completed in January 1967 with devices available at that time. No changes were made in the unit during the sampling program to assure that the results obtained in the various facilities involved were not affected by sampler modification.

The sampling device had to be portable so that transportation was not a major problem and the individual units had to be relatively easy to maintain and operate in the field. With this in mind a sampler with four components was assembled, Figs. 5.2.1 and 5.2.2.

The six-tube May pack sampler was used to provide time-dependent data, and a six-tube particle sampler was used in obtaining representative electron-microscopy samples. The two devices were designed originally for use in the NSPP as off-gas or filter test loop samplers and as such have accumulated a large amount of operational and sampling information.¹⁷ The six-tube May pack unit is shown in Fig. 5.2.3.

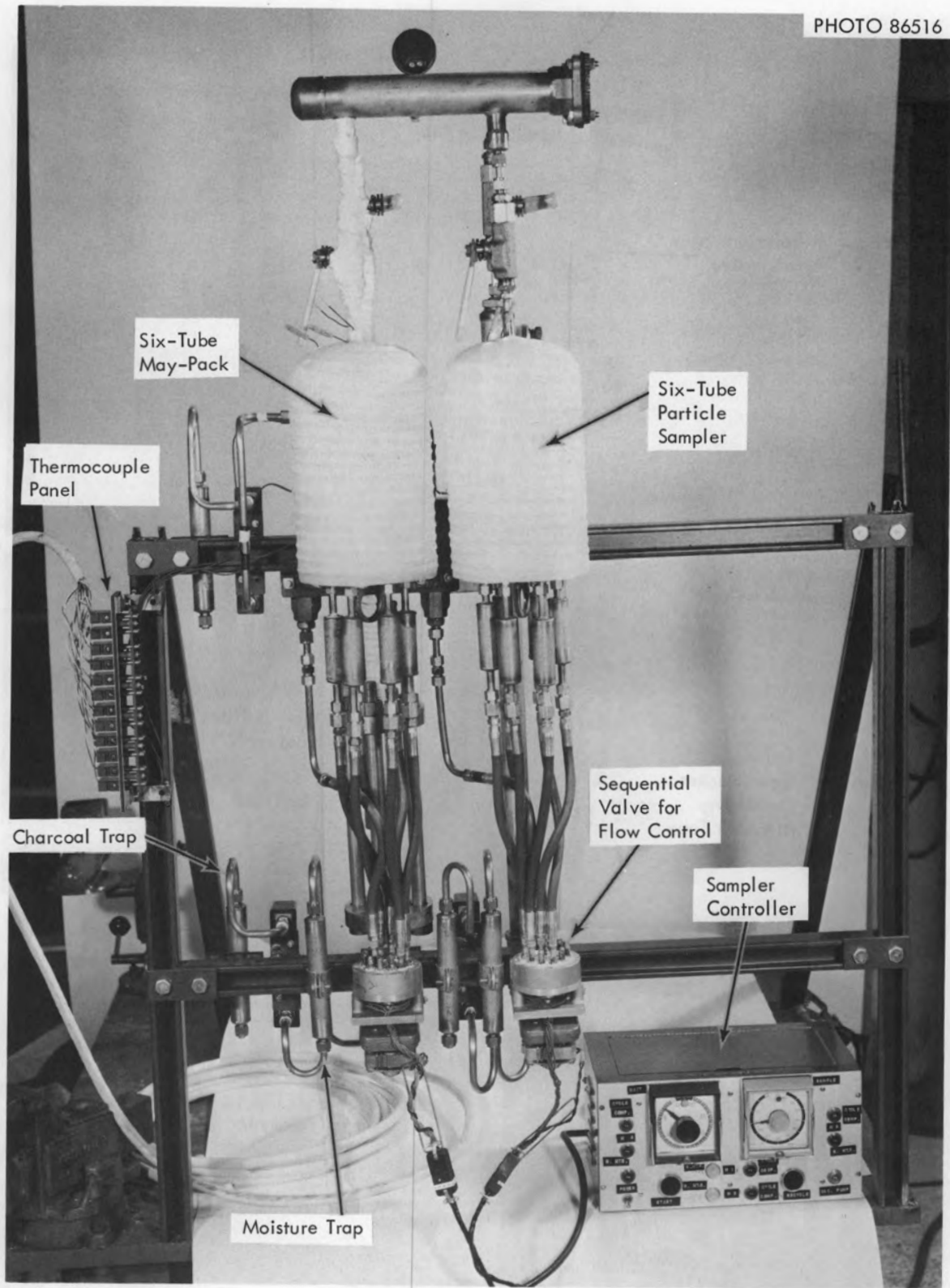


Fig. 5.2.1 Portable Sampler (Front View).

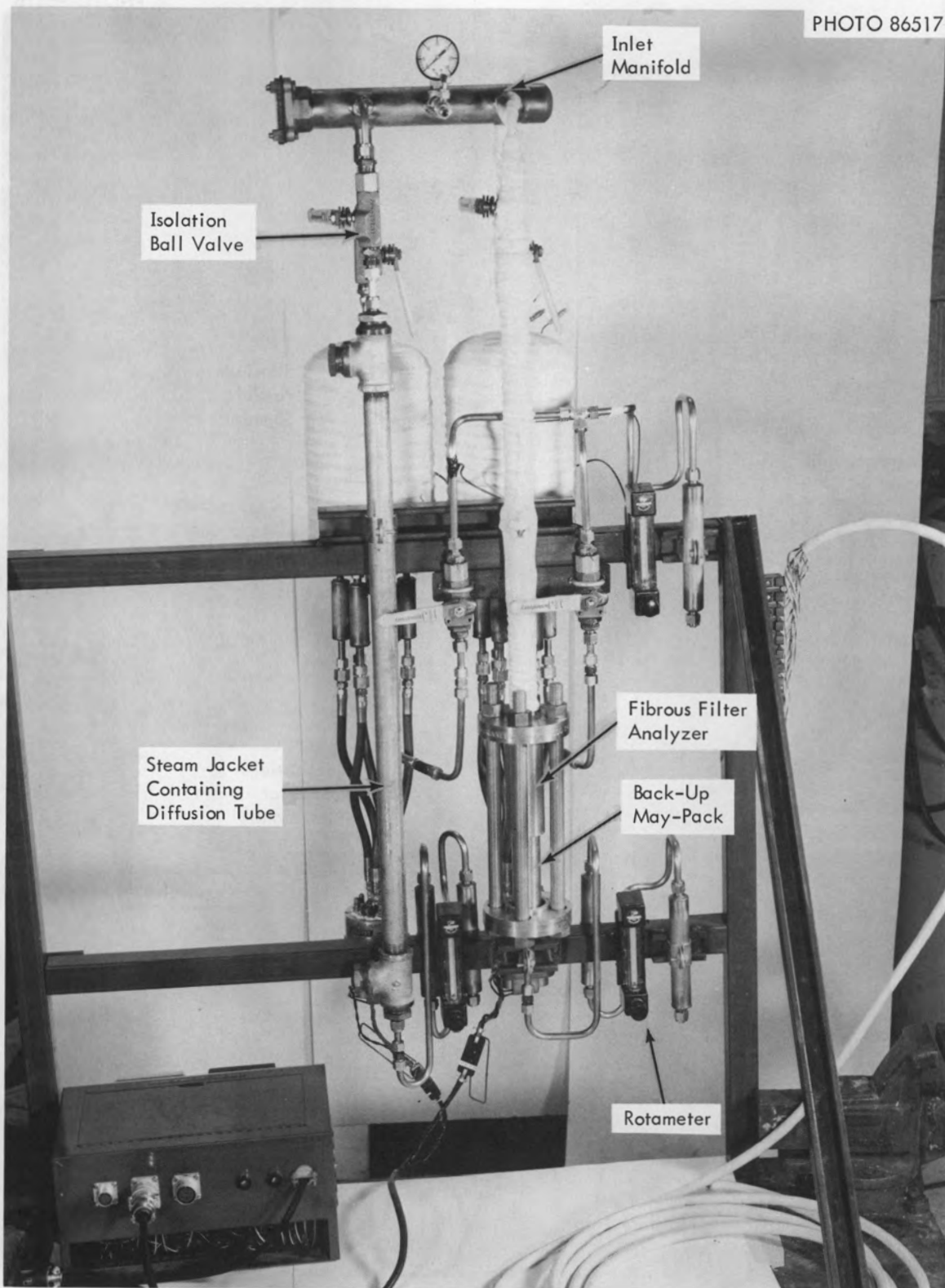


Fig. 5.2.2 Portable Sampler (Back View).

PHOTO 67870

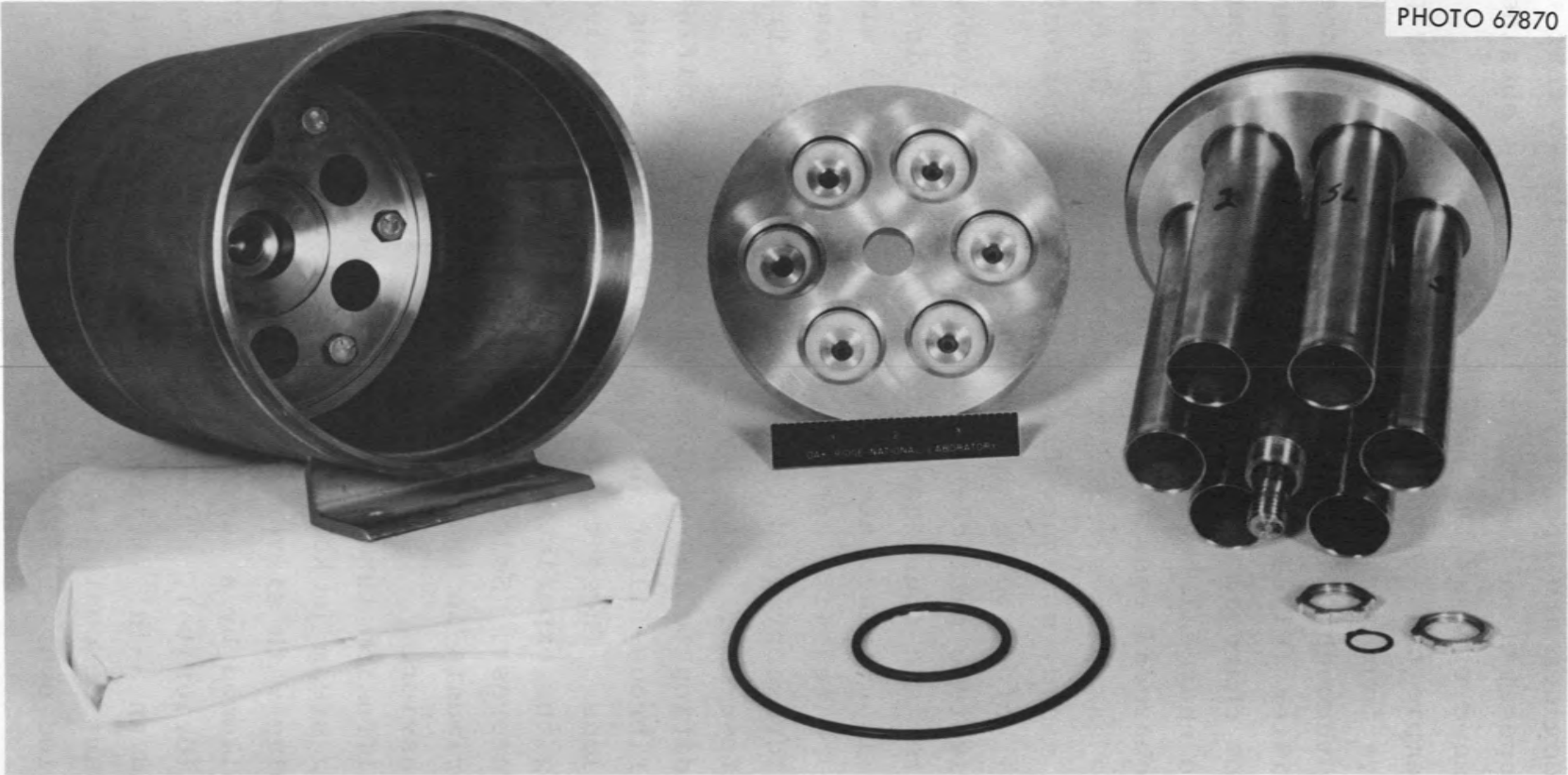


Fig. 5.2.3 Six-Tube May Pack Cluster.

These two devices are operated sequentially so that the material deposited on the particle filters is obtained at about the same time as the May pack sample.

The sample tubes contained in the six-tube May pack sampler have four sets of sampling components. As the sample gas passes through the unit it encounters in sequence: one absolute filter (Flanders F-700), five silver screens (80 mesh), three charcoal loaded fiberglass filters (Whatman ACG/B), two charcoal beds (Barnebey-Cheney MI), and two impregnated charcoal beds (MSA-85851). After exiting the sampler the gas passes through a moisture trap (Drierite), sequential valve, moisture trap, and a final charcoal trap (MSA-85851) before being vented to off-gas.

The six-tube particle sampler tubes are loaded with a single filter and four charcoal beds (MSA-85851) in series. The filter is a triacetate membrane (Gelman GA-6) with the inlet face coated with carbon. This serves as a ready made electron-microscopy grid by simply dissolving the triacetate membrane after use.

In addition to the sequential samplers, a diffusion tube¹⁸ and fibrous-filter analyzer¹⁹ are used as single-sample devices. These two are operated at a preselected time during the experiment when the aerosol form is of greatest interest. Selection of this time is based on previous experiments in the facility that point out general aerosol behavior.

The diffusion tube is a composite of four sections enclosed in a steam jacket. The first 8-in. section is 3/8-in. copper tubing with silver plating on the interior surface. This is followed by a section of tubing containing 20 g of desiccant (Drierite), a 12-in. section of yellow gum rubber tubing, and an 8-in. section of copper tubing with the interior surface coated with finely ground charcoal (MSA-85851 applied over rubber cement).

The fibrous filter analyzer has a two foot inlet manifold of one inch pipe to establish laminar flow before the first filter element. The filters are raw Dacron-polyester staple fibers (99% were 11.3 ± 0.8 microns) which have been carded and punched to give 2.9 cm diameter discs 0.05 cm thick. Twelve of these filters were loaded in the special components used with this sampler and the unit followed by a single tube May pack - with the same loading as the six-tube sampler. The downstream components for both the diffusion tube and fibrous filter analyzer are identical to the six-tube samplers; desiccant, rotameter and charcoal bed.

The temperature of the sampler rig from the manifold connection to the rotameter for each sampler was controlled by resistance heating and monitored with twelve thermocouples.

5.3 Aerosol Measurements at Various Facilities

5.3.1 Containment Mockup Facility (CMF)

The first experiment in which the portable sampler was used was CMF Run 1007 conducted on March 22, 1967. In this run the simulant was designed to represent a 1000 Mwd/T burnup fuel and was released into a steam-air atmosphere. The isotopes included in this run were ^{134}Cs , ^{131}I , ^{129}Te , ^{103}Ru , and ^{140}Ba . The Cs, Te, and Ru were compacted into one small pellet and the ^{140}Ba into a second pellet. The transfer of the isotopes into the CMF tank was accomplished by using boat shaped ribbon heater. A platinum ribbon was used for the Cs-Te-Ru pellet while a helium purged tantalum ribbon was used for the Ba pellet, Fig. 5.3.1.

The vapors from these pellets and the heated iodine sample were swept over molten UO_2 in an induction furnace before entering the CMF tank.

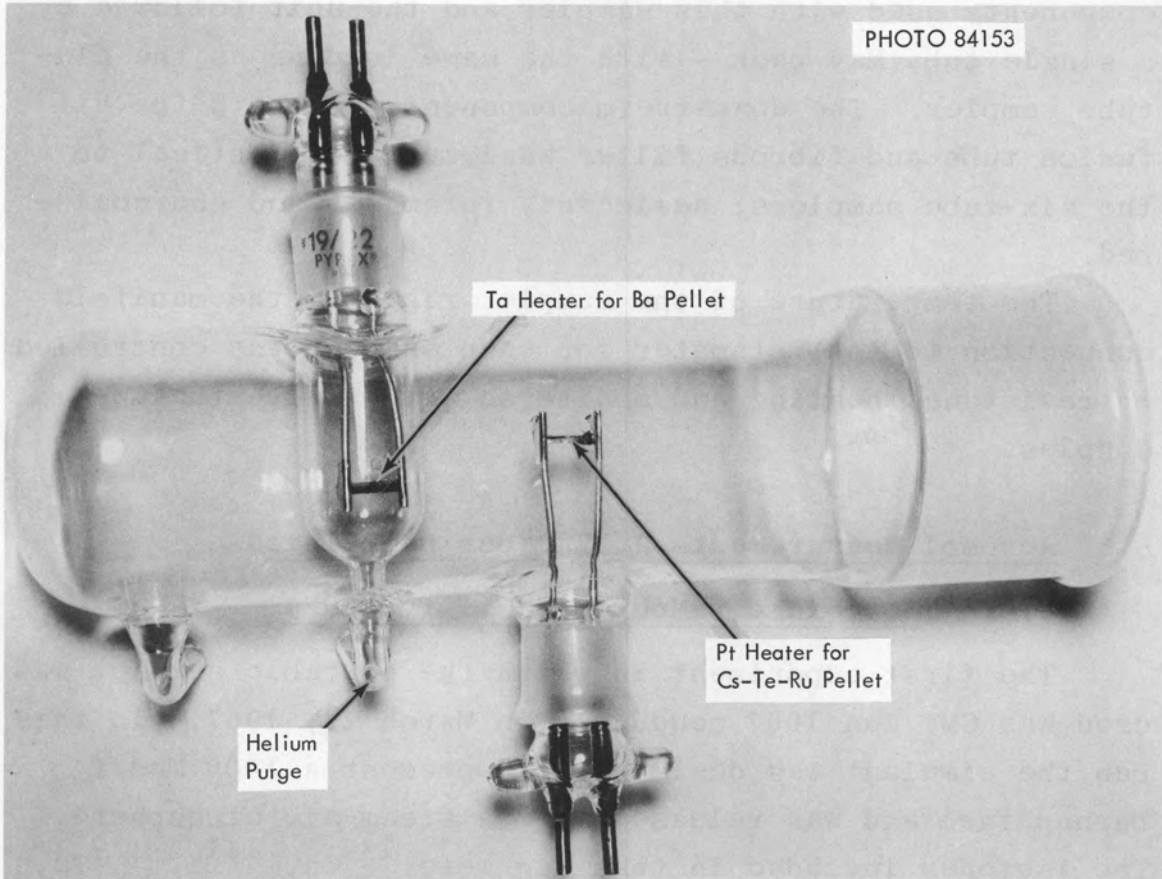


Fig. 5.3.1 Simulant Generator.

The concentration of ^{131}I , ^{134}Cs , and ^{103}Ru during the experiment, as determined by the portable sampler and CMF sampler, are shown in Fig. 5.3.2.

The isotope half-lives as determined by May pack and particle sampler were in very good agreement and averaged 72 min for ^{103}Ru , 95 min for ^{131}I , and 61 min for ^{134}Cs . The values of half-life determined by the CMF samplers were 105 min for ^{103}Ru , 120 min for ^{131}I , and 57 min for ^{134}Cs .

The diffusion tube gave the following diffusion coefficients for the iodine forms trapped:

Silver section - 0.059 cm²/sec

Rubber section - 0.024 cm²/sec

Charcoal section - 0.0936 cm²/sec.

The value for the silver section is less than that expected for molecular iodine, while the charcoal section value is in reasonable agreement with published values.¹⁸ The tracer used in this experiment was ^{131}I .

A value of single fiber efficiency, η_T , of 7.3×10^{-3} for iodine with the calculated velocity of 1.05 cm/sec does not fall within the theoretical or experimentally determined values published previously.¹⁹ The iodine activity probably reflects only a deposition of vapor passing through the unit and is not associated with particulate material. The values of η_T for ^{103}Ru and ^{134}Cs are 3.4×10^{-2} and 3.9×10^{-2} , respectively. These values, for a flow of 1.05 cm/sec, indicate a particle diameter of about 0.3 microns.

Electron microscopy photographs demonstrate the expected pattern of behavior, the first sample has some very large agglomerates while they decrease in size through the run. The photographs indicate the size of agglomerates at the time of the fibrous filter analyzer sample as approximately 0.5 microns.

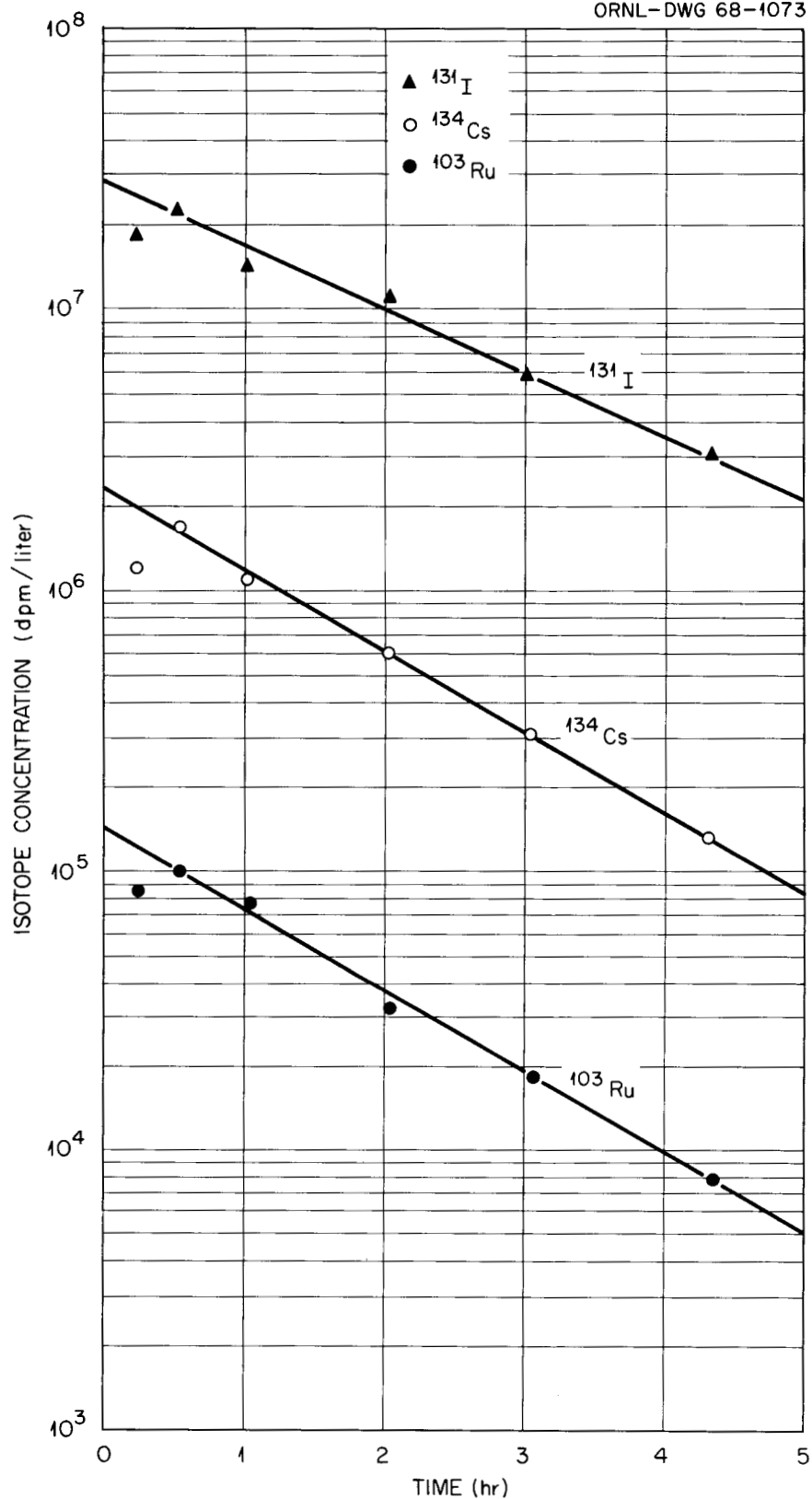


Fig. 5.3.2 Aerosol Isotopic Concentration in Run CMF-1007 as Determined by Portable Sampler and CMF Samplers.

5.3.2 Containment Research Installation (CRI)

The portable sampler was used in CRI experiment 107 on September 28, 1967. The meltdown technique was the same as reported in the CMF experiment, Section 5.3.1. The 7100 Mwd/T burnup fuel simulant contained ^{134}Cs , ^{131}I , ^{103}Ru , ^{129}Te , and ^{85}Sr isotopes.

The ^{131}I and ^{134}Cs isotopes were the only ones where transfer was efficient enough to give measurable concentrations. A comparison of the concentration as determined by both CRI and portable samplers is given in Fig. 5.3.3. The first three samples taken by the portable sampler indicated concentrations much lower than expected. This may in part be explained by the inlet manifold and isolation valving at the inlet to the sampler. These two items probably condensed a major portion of the sample during these first few samples where steam was present in large amounts. The iodine concentration as determined by both samplers indicates a concentration increase in the latter part of the run. The cesium concentration decreases with a 458 min half-life as measured by CRI samplers and 425 min as measured by the portable sampler.

The iodine diffusion coefficients as determined by the three component diffusion tube were $0.072 \text{ cm}^2/\text{sec}$ for the silver section and $0.026 \text{ cm}^2/\text{sec}$ for the charcoal section. No iodine was found on the rubber section. The distribution of the iodine in the diffusion tube was:

Silver section - 27%
Desiccant (Drierite) - 67%
Rubber section - 0.17%
Charcoal section - 5.8%

This would indicate that most of the iodine was particulate in form, being removed by the desiccant bed.

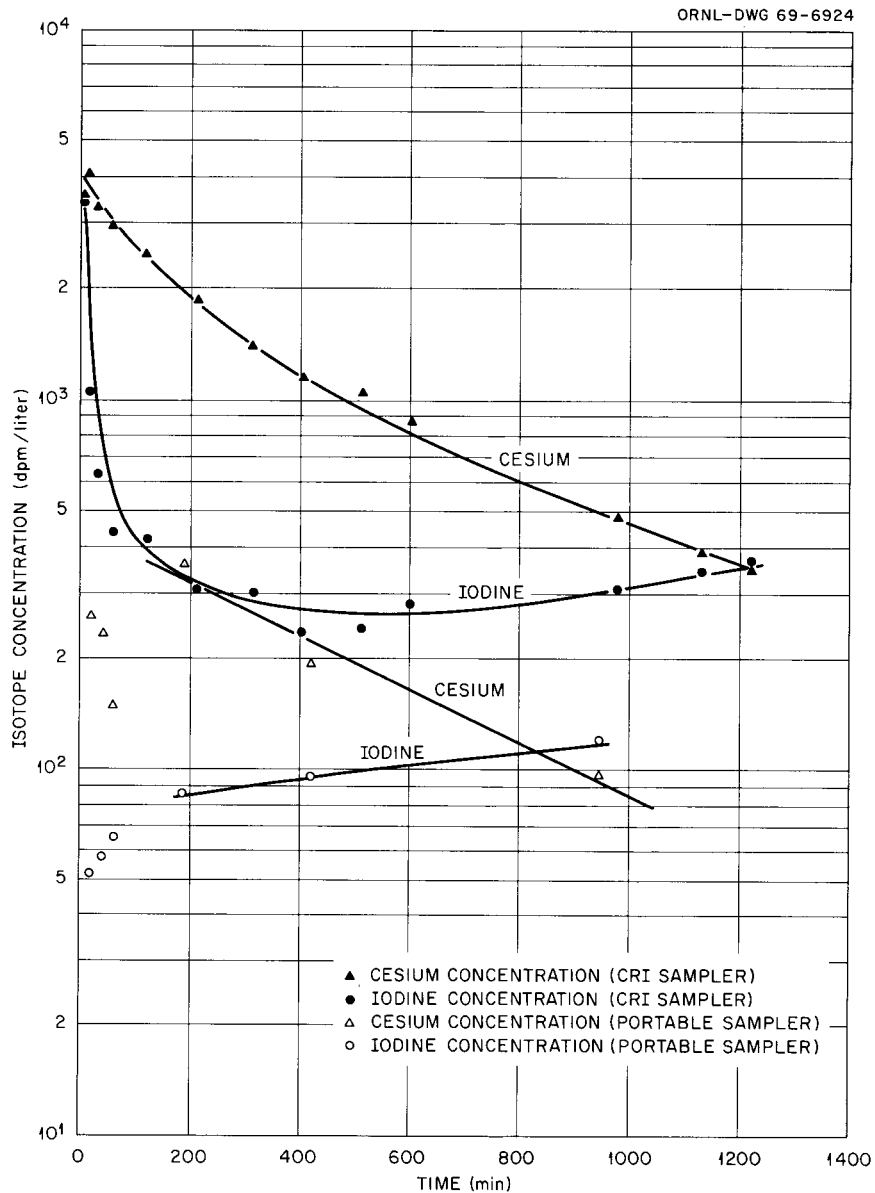


Fig. 5.3.3 CRI-107 Gasborne Concentration at Containment Conditions.

5.3.3 Containment Systems Experiment (CSE)

The experiment at Battelle-Pacific Northwest Laboratory was conducted in the Aerosol Development Facility (ADF). The Stainless Aerosol Tank (SAT) was used for the run, S-85, which was isothermal at 80°C, 1 atmosphere absolute which provided a 50% steam-50% air by volume atmosphere. The aerosol mixture was 1.22 mg iodine traced with 4.3 mCi ^{131}I , 10 mg cesium traced with 5.0 mCi ^{137}Cs , and 7.6 mg ruthenium traced with 9.2 mCi ^{103}Ru . The isotopes were volatilized and passed over an induction heated, zirconium clad, uranium oxide fuel element before entering the SAT.

The data indicate that the general behavior of the aerosol as monitored by the ORNL sampling device is very similar to that monitored by the ADF devices. The ORNL values of concentration are slightly lower which is easily attributable to inlet manifold losses in the portable sampling device. The behavior of the isotopes as a function of time is presented in Figs. 5.3.4-5.3.6.²⁰

The fibrous filter analyzer data yield a particle diameter of 0.36 microns for ^{134}Cs activity and 0.7 microns for ^{103}Ru . The electron microscope photographs from filters exposed at approximately the same time show agglomerates of 0.3 micron size for the portable sampler and 0.6 micron size for a SiO_2 grid used by CSE experimenters. The larger size agglomerates on the SiO_2 grid may be due to the fact that it is a gravity settling type sampler as opposed to the flow technique used by the portable sampler.

5.3.4 Nuclear Safety Pilot Plant (NSPP)

The sampling devices used in the portable sampler have been used in experiments at the Nuclear Safety Pilot Plant. The six-tube samplers were developed initially for use in the NSPP and were used in the experiments reported in Section 2.5; therefore, the information generated in these runs is

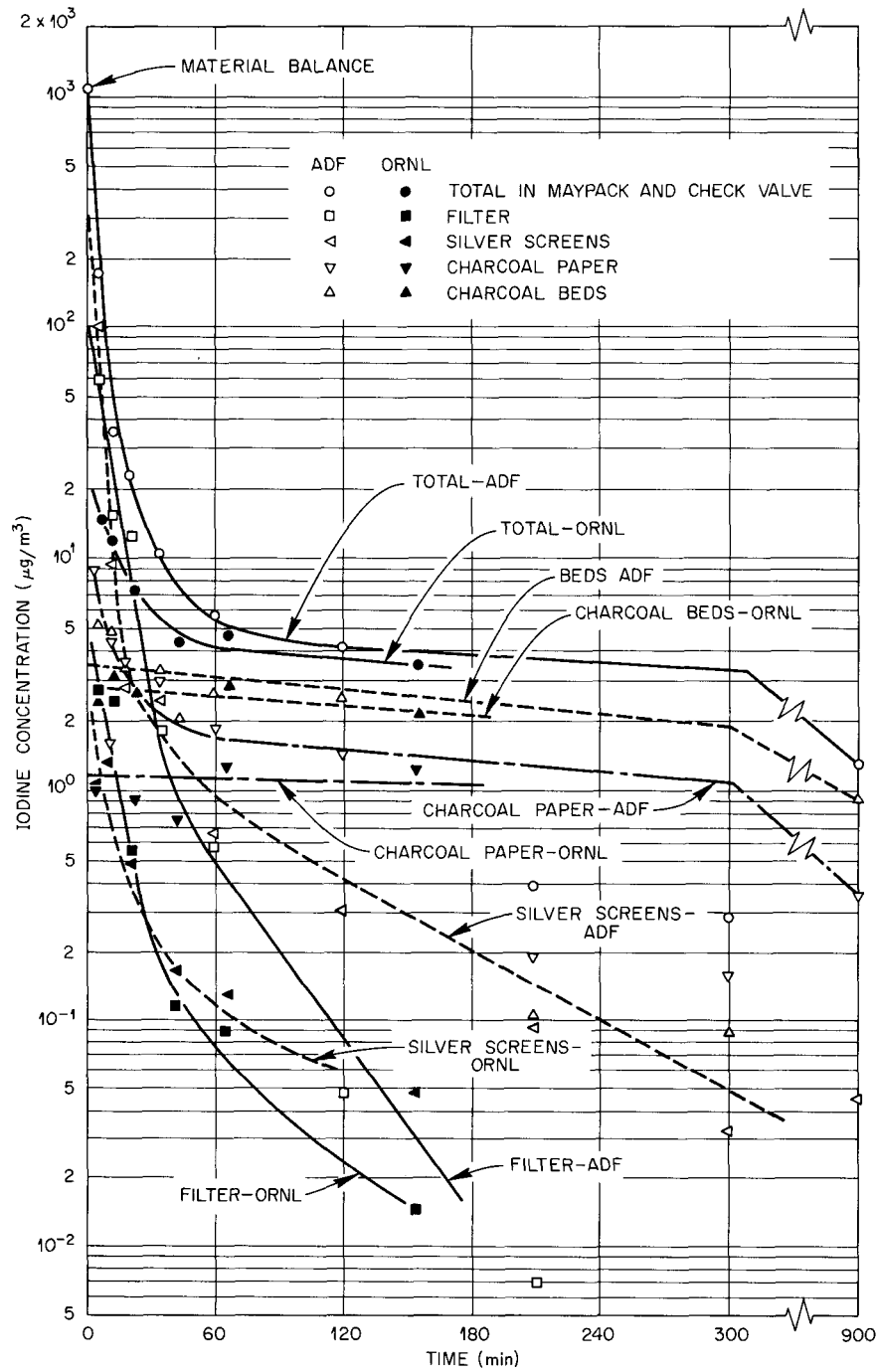


Fig. 5.3.4 Run 85-SAT Gasborne Iodine Concentration at Containment Conditions.

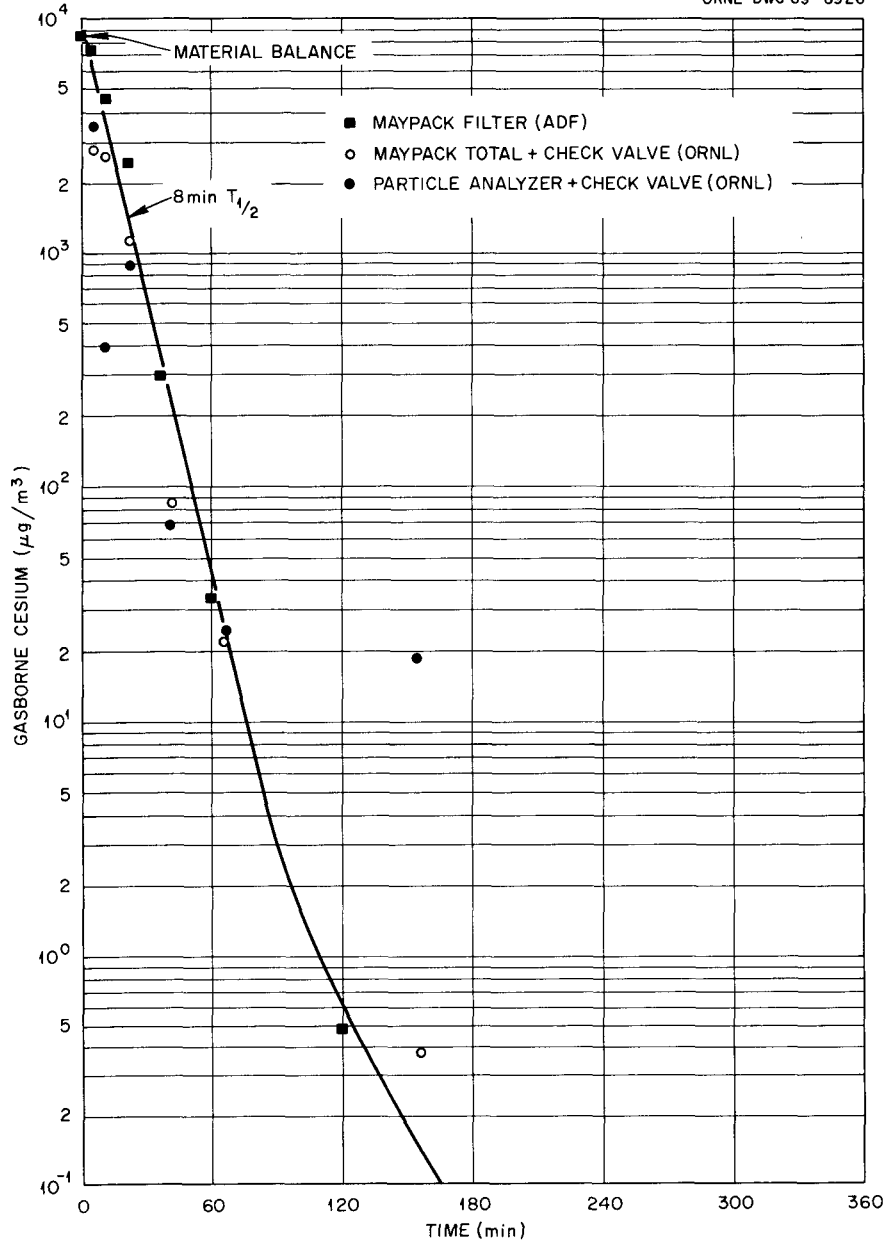


Fig. 5.3.5 Run 85-SAT Gasborne Cesium Concentration at Containment Conditions.

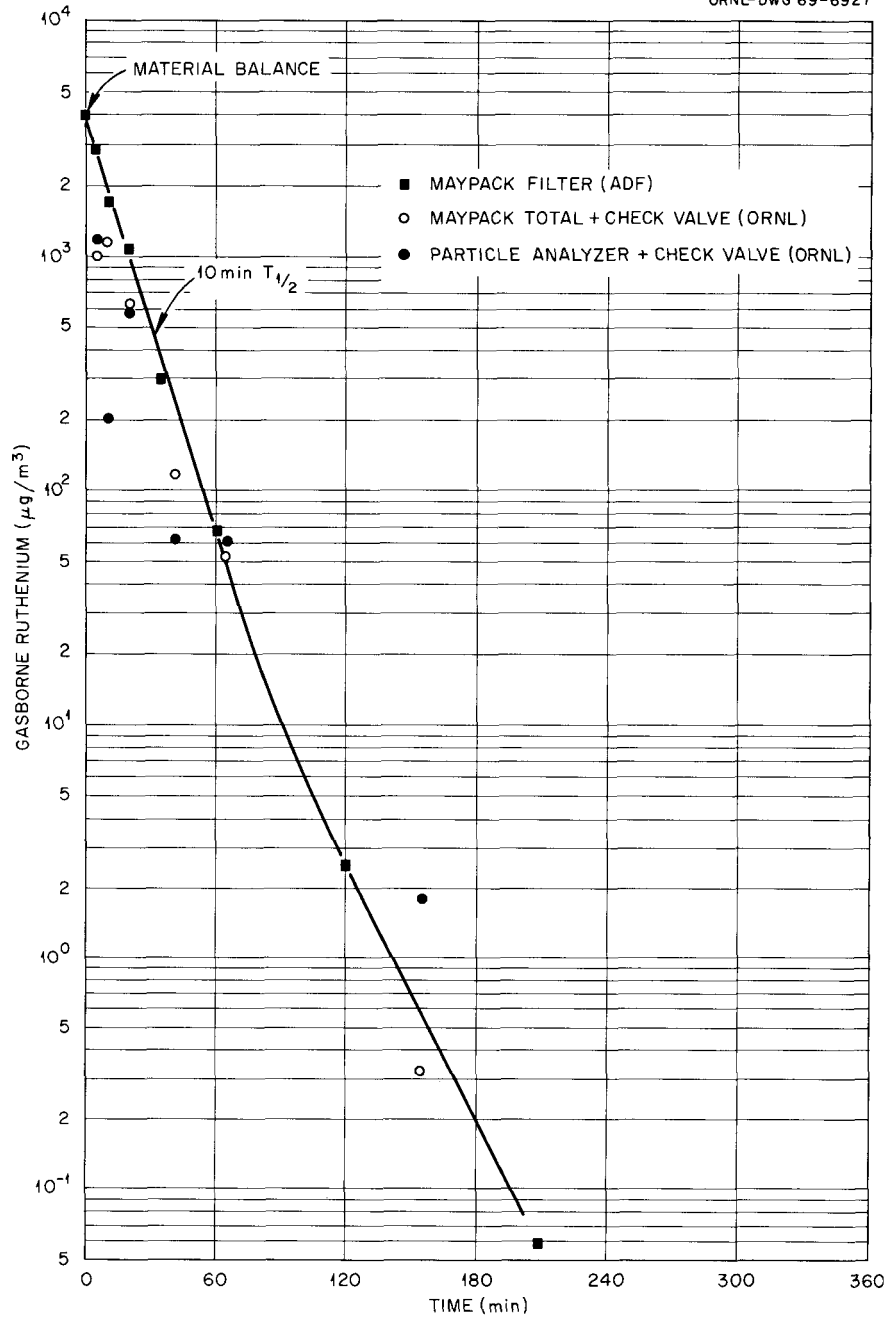


Fig. 5.3.6 Run 85-SAT Gasborne Ruthenium Concentration at Containment Conditions.

directly comparable on a sampler basis to the above reported work.

5.4 Conclusions

The comparison of the different techniques of fission product simulation used by CMF, CRI, CSE and NSPP can be made by direct use of the data of each experimenter. No significant difference that would tend to bias the experimental data has been found between the sampling techniques of the various facilities.

6.0 GENERAL EVALUATION OF THE RESULTS OF SIMULANT VALIDATION EXPERIMENTS

6.1 Criteria of Validation Experiments

As mentioned in Chapter 1, the purpose of the validation studies is to compare the behavior of simulated fission products with that of real fission products to ascertain the applicability of simulants to the Nuclear Safety Program. Such a direct comparison can be made legitimately only if the experimental facility, the operating conditions of the facility, sampling techniques, etc., are the same for both simulated and real fission-product experiments. The groups of experiments described in this report were selected in an effort to meet these criteria.

6.2 Relative Significance of Various Types of Data

The experimental data obtained in these experiments are generally classified as either release and gross distribution of fission products and simulants throughout the system or as aging behavior of fission products and simulants within the containment vessel. Release and gross distribution data from various experiments within a relatively uniform group often exhibit considerable scatter because they are quite sensitive to experimental fluctuations and to the somewhat different conditions which sometimes exist within the furnace. Consequently such scatter often leads to the rather negative conclusion that there seems to be no reason to suspect that simulated and real fission products behave differently rather than to the positive conclusion that simulants either do or do not behave like real fission products.

In contrast, aging behavior appears less sensitive to uncontrolled experimental conditions and is more easily interpretable. This may be due to the fact that after the simulants or fission products enter the containment vessel

and mix with the large mass of gas within the vessel, the resulting massive aerosol moves relatively slowly toward equilibrium. Consequently much of our better data are associated with aging behavior.

Two additional considerations emphasize the importance of aging behavior data for the evaluation of simulant behavior. First, the CSE experiments are primarily studies of various parameters on aging behavior. Second, an inter-comparison between experiments performed in different experimental facilities is desirable in order to insure that the conclusions from the relatively small-scale validation experiments are applicable to the CSE. Such an intercomparison can be attempted for only the aging behavior since in this area the theory and models are more highly developed and the data are better. Consequently, experiments for which only limited aging data are available tend to have a reduced significance as validation studies.

6.3 Limitations of Validation Experiments

Even a cursory examination of the previous chapters shows that each group of experimental data suffers rather severe limitations. Probably the most important reason for these limitations is the fact that the amount of simulated or real fission products on many samples, including most of the aerosol samples, was often either approaching or below the analytical limit of sensitivity. Although this effect was greater for the non-volatile elements it was often significant even for the very volatile iodine.

Another reason for these limitations is that aerosol-sampling devices were being developed and improved during the time that the various series of experiments were performed. Thus an experiment might be run using one type of device only to be compared with an experiment using a different type. Also the sampling techniques of the earlier experiments were quite crude. All too often an experiment

must be compared with one performed under somewhat different conditions because no identical experiment is available. Sometimes this is due to experimental difficulties but sometimes it is due to the fact that support for a significant experiment was not forthcoming, or to an experiment having multiple objectives which are incompatible with each other. Finally, even without the above complications, complex experiments such as these experience uncontrolled and even unknown fluctuations which cause complications when two or more experiments are compared.

6.4 Fuel Compact Method of Simulant Generation

The data for the validation of the fuel compact method of simulant generation are the most limited. The available direct comparison of aerosol aging behavior indicates that, in one simulant run, cesium and strontium behave like real fission products. Although gross release and transport distributions exhibit considerable scatter, simulated and real fission-product data do not show significant differences. For certain experiments performed under different conditions, this agreement of release and transport distributions was qualitatively obtained by considering the different chemical reactions occurring in the furnace. In conclusion, there appears to be no reason to suspect that simulated fission products generated by the melting fuel compacts behave differently than real fission products.

6.5 Vaporized Simulant Method of Simulant Generation: Out-of-Pile Studies

The two groups of experiments which comprise the out-of-pile validation studies of the vaporized simulant method of simulant generation produced data which differ considerably in amount and significance but lead to similar conclusions. The CMF data are again quite limited. The overall distribution of simulated and real fission products in the

containment vessel at the end of the experiments agree within the limits of the scattered data. The aging behavior of simulant cesium is fairly similar to that of the real fission product. Also the aging behavior of simulant cesium and ruthenium is similar to the behavior of the simulant iodine near the end of the aging period. This type of situation has been found to occur for real fission products in the in-pile experiment. These data again lead to the conclusion that we have seen nothing to cause us to suspect the existence of differences between simulant and real fission products.

The CRI data provide by far the most complete direct comparison of simulated and real fission products. The only experimental limitation appears to be the fact that the experiments were run with different aerosol-sampling devices which complicates the interpretation of the aging behavior of particulate and molecular iodine. In addition, the behavior of simulant particulate and molecular iodine at the end of the aging period show increases which cannot be satisfactorily explained by either aerosol sampling or by an unexplained temperature excursion occurring several hours earlier. For the present, therefore, the unexpected positive slopes of these curves should be considered as a type of artifact. When these effects are considered, the aging behavior of the various species of simulated and real fission-product iodine are quite similar. The aging behavior of both simulated and real fission-product iodine is significantly different than that of other elements. This is attributed to initial rapid adsorption of iodine on the stainless steel surfaces. Simulant cesium, tellurium, and ruthenium exhibit very similar aging behavior and the behavior of fission-product cesium and tellurium is also similar. Moreover, these two groups exhibit similar behavior. These fission products and simulants are probably all of the particulate species and therefore behave alike. It is also significant that the behavior of simulant and fission-product iodine in the condensed steam is quite similar.

In conclusion, the CRI data indicate that under the conditions of the experiments and using the available characterization devices, simulants behave like real fission products.

6.6 Vaporized Simulant Method of Simulant Generation: In-Pile Studies

The in-pile experiments have the potential of providing the most complete and significant comparison of simulated and real fission products. Unfortunately the amount of simulants on the aerosol samplers is below the limits of detection so it is impossible to directly compare the aging behavior of simulated and real fission products. However, these studies have provided three types of significant information. First, the experimental conditions of the two in-pile experiments were identical. However, the release and distribution data of fission products and simulants in the same experiment agree much better than do the fission product data of the two identical experiments. Furthermore, the amount of simulant and fission-product iodine found in the steam condensate as a function of aging time agree significantly better than do the fission-product iodine data of the two identical experiments. These data substantiate the tenuous hypothesis drawn from the other experiments that the variation between duplicate experiments is greater than that between simulated and real fission products.

The second type of significant information produced by the in-pile experiments is that fractional amounts of molecular and particulate iodine entering the containment vessel may be different for simulant iodine than for fission-product iodine. Finally, the third type of significant information is that a mathematical model of iodine aerosol behavior developed for the CSE has been used with modest success for real fission-product iodine in the small in-pile installation.

In conclusion, the in-pile studies indicate that the variability between experiments is due more to fluctuations of experimental conditions than to the nature of the aerosol.

7.0 CONCLUSIONS AND RECOMMENDATIONS

The results of the simulant validation program at ORNL suggest that the mechanisms controlling the release, transport, gross distribution, aging, and deposition behavior of simulated or real fission products is governed more by the conditions of the experiment than by the nature of the aerosol. Thus, the variation between duplicate experiments is greater than that between simulated and real fission products, and although differences between simulants and real fission products may exist such differences are rather insignificant. Accordingly, the use of simulated fission products for studies such as those conducted in the CSE appears to produce valid and realistic results which are applicable to the Nuclear Safety Program.

It has been shown that, except for iodine, all fission products and simulants behave similarly because they are all of the particulate species. Therefore, it appears profitable to use only iodine and one other element such as cesium in simulant experiments.

REFERENCES

1. R. K. Hilliard and J. D. McCormack, Fission-Product Simulation in the Containment Systems Experiment, Proceedings of the International Symposium on Fission Product Release and Transport Under Accident Conditions, (CONF-650407), Oak Ridge, Tennessee April 1965.
2. R. K. Hilliard, L. F. Coleman, and J. D. McCormack, Comparisons of the Containment Behavior of a Simulant with Fission Products Released from Irradiated UO_2 , Pacific Northwest Laboratory, BNWL-581, Richland, Washington, March 1968.
3. B. F. Roberts, S. H. Freid, and O. Sisman, Trans. Am. Nucl. Soc. 11, p. 666-67 (1968).
4. R. E. Adams and R. D. Ackley, Removal of Elemental Radioiodine from Flowing Humid Air by Iodized Charcoals, USAEC Report ORNL-TM-2040, Oak Ridge National Laboratory, November 1967.
5. G. M. Watson, R. B. Perez, and M. H. Fontana, Effects of Containment System Size on Fission Product Behavior, USAEC Report ORNL-4033, Oak Ridge National Laboratory, January 1967.
6. W. J. Megaw and F. G. May, Jr., The Behavior of Iodine Released in Reactor Containers, Reactor Sci. Techn. (J. Nucl. Energy Parts A/B) 16, 427 (1962).
7. R. L. Bennett, W. H. Hinds, and R. E. Adams, Development of Iodine Characterization Sampler for Applications in Humid Environments, USAEC Report ORNL-TM-2071, Oak Ridge National Laboratory, May 1968.
8. G. W. Parker et al., Behavior of Fission Products Released From Simulated Fuels in the Containment Mockup Facility, Nucl. Safety Program Semiann. Progr. Rept. June 30, 1965, USAEC Report ORNL-3843, pp. 83-91, Oak Ridge National Laboratory, 1965.
9. G. W. Rogers, Program for Containment System Experiment, HW-83607, Sept. 1964.

10. G. W. Parker, C. J. Barton, and W. J. Martin, Simulation of High Burnup UO_2 Fuel in the Containment Mockup Facility, Nucl. Safety Program Semiann. Progr. Rept. Dec. 31, 1964, USAEC Report ORNL-3776, pp. 70-77, Oak Ridge National Laboratory, 1964.
11. G. W. Parker et al., Fission Product Release from Highly Irradiated UO_2 , Nucl. Safety Program Semiann. Progr. Rept. June 30, 1964, USAEC Report ORNL-3691, pp 6-8, Oak Ridge National Laboratory, 1964.
12. Harold Etherington, Table 5. Fission Product Spectrum From Thermal Fission of Uranium-235 (135 days irradiated), Nuclear Engineering Handbook, Section 11, pp 11-28-31, McGraw-Hill, New York, N. Y., 1958.
13. Howard A. McLain, Potential Metal Water Reactions in Light Water Cooled Power Reactors, ORNL-NSIC-23, pp. 63-75, Oak Ridge National Laboratory, August 1967.
14. G. W. Parker et al., Behavior of I_2 and HI in The Containment Research Installation, Nucl. Safety Program Annual Progress Report for Period Ending Dec. 31, 1966, USAEC Report ORNL-4071, pp 52-65, Oak Ridge National Laboratory, 1966.
15. L. F. Coleman, personal communication.
16. J. G. Knudsen and R. K. Hilliard, Fission Product Transport by Natural Processes in Containment Vessels, BNWL-943, January 1969.
17. L. F. Parsly, Jr., Experience with May Packs in the Nuclear Safety Pilot Plant, USAEC Report ORNL-TM-2044, Oak Ridge National Laboratory, February 1968.
18. R. E. Adams, R. L. Bennett, W. E. Browning, Jr., Characterization of Volatile Forms of Iodine at High Relative Humidity by Composite Diffusion Tubes, USAEC Report ORNL-3985, Oak Ridge National Laboratory, August 1966.
19. M. D. Silverman et al., Characterization of Radioactive Particulate Aerosols by the Fibrous Filter Analyzer, USAEC Report ORNL-4047, Oak Ridge National Laboratory, March 1967.
20. J. D. McCormack, BNWL, personal communication.

DISTRIBUTION

1. R. D. Ackley
2. R. E. Adams
3. T. D. Anderson
4. J. E. Baker
5. C. J. Barton
6. S. E. Beall
7. C. G. Bell
8. M. Bender
9. R. L. Bennett
10. C. R. Benson
11. R. F. Benson
12. R. G. Berggren
13. D. S. Billington
14. F. T. Binford
15. J. P. Blakely
16. R. E. Blanco
17. C. M. Blood
18. A. L. Boch
19. G. E. Boyd
20. R. B. Briggs
21. R. H. Bryan
22. J. R. Buchanan
23. C. A. Burchsted
24. T. J. Burnett
25. D. A. Canonico
26. D. W. Cardwell
27. T. E. Cole
28. Z. Combs
29. J. A. Conlin
30. Wm. B. Cottrell
31. K. E. Cowser
32. E. N. Cramer
33. G. E. Creek
34. D. J. Crouse
35. F. L. Culler, Jr.
36. R. J. Davis
37. W. DeLaguna
38. H. J. de Nordwall
39. W. K. Ergen
40. D. E. Ferguson
41. W. F. Ferguson
42. H.F.E. Feuerstein
43. M. H. Fontana
44. A. P. Fraas
45. S. H. Freid
46. J. H. Frye, Jr.
47. A. B. Fuller
48. W. R. Gall
49. J. S. Gill
50. D. L. Gray
51. B. L. Greenstreet
52. J. C. Griess
53. W. R. Grimes
54. R. C. Gwaltney
55. R. P. Hammond
56. P. N. Haubenreich
57. F. A. Heddleson
58. R. E. Helms
59. W. H. Hinds
60. E. Hoinkus
61. J. M. Holmes
62. D. G. Jacobs
63. W. H. Jordan
64. S. I. Kaplan
65. P. R. Kasten
66. G. W. Keilholtz
67. J. O. Kolb
68. L. F. Looistra
69. R. E. Lampton
70. J. A. Lane
71. C. G. Lawson
72. T. F. Lomenick
73. R. A. Lorenz
74. M. I. Lundin
75. R. N. Lyon
76. H. G. MacPherson
77. R. E. MacPherson
78. A. P. Malinauskas
79. W. J. Martin
80. H. C. McCurdy
81. H. A. McLain
82. J. G. Merkle
83. A. J. Miller
84. E. C. Miller
85. W. H. Montgomery
86. S. E. Moore
87. J. G. Morgan
88. F. H. Neill
89. H. G. O'Brien
90. M. F. Osborne
91. R. C. Olson
92. G. W. Parker
93. R. B. Parker
94. L. F. Parsly, Jr.

95. P. Patriarca
96. A. M. Perry
97. H. B. Piper
98. R. H. Rainey
99. D. M. Richardson
100. P. Rittenhouse
- 101-105. B. F. Roberts
106. G. C. Robinson
107. T. H. Row
108. P. Rubel
109. A. W. Savolainen
110. R. A. Schmidt
111. L. B. Shappert
112. L. J. Shersky
113. R. P. Shields
114. M. D. Silverman
115. O. Sisman
116. M. J. Skinner
117. R. Slusher
118. B. A. Soldano
119. I. Spiewak
120. L. E. Stanford
121. J. T. Stanley
122. W. G. Stockdale
123. W. C. Stoddart
124. D. B. Trauger
125. J. Truitt
126. W. C. Ulrich
127. W. E. Unger
128. C. S. Walker
129. J. L. Wantland
130. W. T. Ward
131. G. M. Watson
132. C. C. Webster
133. M. S. Wechsler
134. A. M. Weinberg
135. G. D. Whitman
136. F. J. Witt
137. F. C. Zapp
138. H. E. Zittel
139. Nuclear Safety Information Center
- 140-141. Central Research Library
- 142-143. Document Reference Section
- 144-153. Laboratory Records Department
154. Laboratory Records Department, ORNL R.C.
- 155-395. Nuclear Safety Program Distribution
- 396-410. Division of Technical Information Extension
411. Laboratory and University Division, AEC, ORO